4. Results and discussion

In order to fulfil the proposed aims and objectives, the present work is carried on three specialized fields:

1. Computational chemistry
2. Synthetic chemistry
3. Biological screening

The results and discussion section are further divided into two sections.

Section I: Design and development of novel anti-TB agents based on the existing DprE1 inhibitors

4.1 Development of pharmacophore model and 3D-QSAR model using a variety of reported scaffolds as DprE1 inhibitors

4.2 Virtual screening for the identification of new moiety by using various filters like pharmacophore model, molecular modelling and Lipinski rule of five

4.3 Hit optimization through molecular docking technique

4.4 Synthesis of designed compounds

4.5 Biological screening of synthesized compounds for anti-TB activity using MABA assay

4.6 Molecular docking, ADMET studies and simulation studies of the synthesized compounds

Section II: Design and development of novel anti-TB agents based on hybrid approach

4.7 Synthesis of the designed compounds

4.8 Biological screening of synthesized compounds for anti-TB activity using MABA assay

4.9 Molecular docking, ADMET studies of the synthesized compounds

Section I

From the literature, it has been evident that there is a diversity of scaffold reported as DprE1 inhibitors. Thus, these reported DprE1 inhibitors were considered to develop a pharmacophore model for DprE1 inhibitory activity.

4.1 Development of pharmacophore model and 3D-QSAR model using a variety of reported scaffolds as DprE1 inhibitors

4.1.1 Selection of dataset

Many scaffolds have been reported in recent years showing DprE1 inhibition. After conducting a thorough literature survey, it was found that 566 compounds from various classes such as benzothiazinones[1–3], azaindoles[4,5], aminoquinolones[6], quinoxalines[7], triazoles[8,9] etc. were reported as DprE1 inhibitors. The first criterion for selection of dataset was a reported IC_{50} value for DprE1 enzyme. Compounds with unclear stereochemistry or biological activity were not considered. So, out of 566 compounds, 300 compounds were selected for which, activity was defined in terms of IC_{50} value. The dataset was generated in such a way that it contains most active, moderately active and least active compounds covering all structural variations. To get robust dataset, compounds having similar structures as well biological activity were omitted from the final selection.

Finally, a set of 150 compounds with IC_{50} value ranging from 100 to 0.003 μM were selected in such a way that the data set provide both structural and biological variations. IC_{50} value of these compounds were converted to pIC_{50} values by taking negative logarithm of IC_{50} values (pIC_{50} = -logIC_{50}). This dataset consisting 150 structures was scrutinized into a model generating set comprising of 140 compounds and an external test set consisting of 10 compounds. The dataset used for the development of pharmacophore model is given in the supplementary data (**Si**).

Pharmacophore model hypothesis was developed using PHASE QSAR module of Schrodinger employing a grid-based 3D-QSAR analysis. Grid points nearest to the atoms in molecules were identified and used to generate 3D descriptors.

4.1.2 Pharmacophore model

The present work aimed to identify the minimium structual features required for DprE1 inhibition. To serve the aim, a definite pharmacophore model was generated using reported DprE1 inhibitors. Active and inactive threshold pIC_{50} were fixed to 6.9 and 5.0 respectively

and applied to the dataset of 140 compounds, giving 41 active, 15 inactive and 84 moderately active compounds. For generation of pharmacophore model, all the 41 active compounds were used. Pharmacophoric sites were created to give six types of structural features such as aromatic ring (R), negative (N), positive (P), hydrophobic (H), H-bond donor (D), and acceptor (A). The software was restricted to find a minimum of 3 and maximum of 5 sites. Based on the active structures of the dataset, several 3-point and 4-point hypothesis were generated. AHRR, AAR, AAH, ARR, HRR and AHR were found to be most probable hypothesis. All the generated hypothesis were evaluated. The survival score ranged from 2.714 to 3.310 (**Table 4.1**).

Table 4.1: Data of the top ranked pharmacophore models

ID	Survival score	Survival inactive	Post hoc score	Site	Vector	Selectivity	Match	Energy
AHRR.28	2.990	1.641	2.991	0.63	0.897	1.359	22	2.254
AHRR.29	2.714	1.782	2.714	0.51	0.850	1.362	22	1.185
AAR.4	3.310	2.432	3.310	0.76	0.901	0.848	21	0.467

The highest ranked survival score for 3-point hypothesis was obtained for AAR.4 i.e. 3.310 whereas 4-point hypothesis AHRR.28 and AHRR.29 were scored as 2.990 and 2.714 respectively as shown in **Table 4.1**. The best model (AHRR.28) containing one hydrogen bond acceptor, one hydrophobic group and two aromatic rings is shown in **Figure 4.1**.
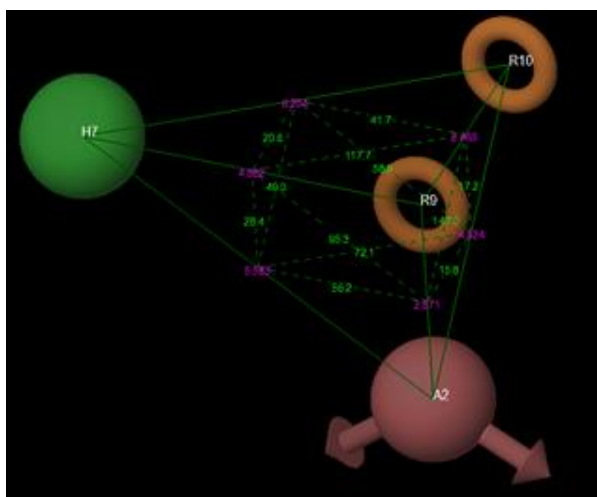

Figure 4.1: Pharmacophore model AHRR.28. Orange coloured torus represents aromatic rings (R9 and R10), green coloured sphere represents hydrophobic group (H7), and light magenta coloured vector represents hydrogen bond acceptor group (A2). Values in purple colour represent distances and in green colour represent the angles between the pharmacophoric features

The angles and distances of AHRR.28 among the pharmacophore are given in **Table 4.2** and **4.3**. The top three ranked pharmacophore models AHRR.28, AAR.4 and AHRR.29

were then used to align the molecules to build atom-based 3D-QSAR analysis. The best model was denoted by various statistical measures. The accuracy of the generated QSAR model was verified by the statistical data such as R^2 and Q^2.

Table 4.2: Angles between the different pharmacophoric features of AHRR.28 model

Site 1	Site 2	Site 3	Angle
H7	A2	R9	56.2
H7	A2	R10	72.1
R9	A2	R10	15.8
A2	H7	R9	28.4
A2	H7	R10	49.0
R9	H7	R10	20.6
A2	R9	H7	95.3
A2	R9	R10	147.0
H7	R9	R10	117.7
A2	R10	H7	58.9
A2	R10	R9	17.2
H7	R10	R9	41.7

Table 4.3: Distance between the different pharmacophoric features of AHRR.28 model

Site 1	Site 2	Distance (Å)
A2	H7	5.583
A2	R9	2.671
A2	R10	4.924
H7	R9	4.662
H7	R10	6.204
R9	R10	2.465

4.1.3 Analysis of 3D-QSAR model

The alignment build from the pharmacophore model was used to develop QSAR model. Dataset was divided randomly into training (118 compound) and test (28 compounds) set such a way that the compounds are divided in 4:1 ratio to give variation in biological activity and structural diversity. A number of models were generated but only top ranked model was considered. 3D-QSAR model obtained by using 4-point hypothesis (AHHR.28) was found to be best model showing $R^2 = 0.8520$, $Q^2 = 0.8660$, PLS factor = 5, F-value =109.7, RMSE=

0.3491, stability = 0.172, SD = 0.477 and Pearson-R = 0.9308. Statistical parameters of QSAR model are shown in the **Table 4.4**. The contour maps obtained for the best 3D-QSAR model is shown in **Figure 4.2**.

Table 4.4: Statistical parameter obtained for the 3D-QSAR model obtained from various alignments

Statistical parameters	AHHR.29	AHRR.28	AHRR.17
R^2	0.8871	0.8520	0.8950
Q^2	0.5950	**0.866**	0.6133
PLS factor	5	5	5
Stability	0.441	0.172	0.257
F-value	133.5	109.7	148.9
RMSE	0.6844	0.3491	0.6923
SD	0.4075	0.477	0.390
Pearson-R	0.7846	**0.9308**	0.8061
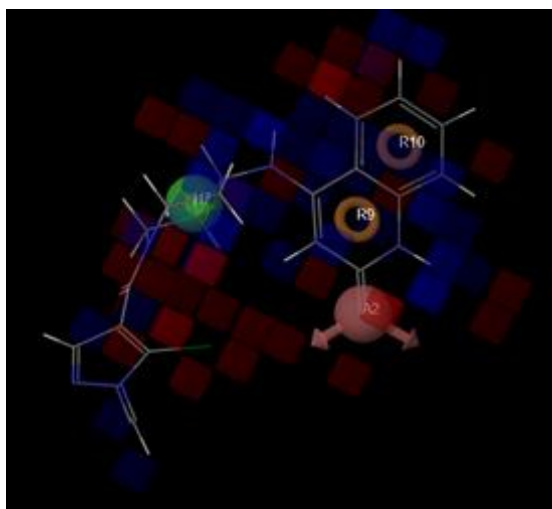
Figure 4.2: 3D-QSAR model visualization (dark blue region showing positive coefficient and red region showing negative coefficient)

4.1.4 Validation of the pharmacophore model using external dataset

Pharmacophore model (AHRR.28) was validated using an external set of ten compounds **V₁-V₁₀** (**Figure 4.3**) which were not included in the pharmacophore model development. The external set was chosen in such a way that it included five active compounds ($pIC_{50}>6$) as well as five inactive compounds ($pIC_{50}<6$). This external set was not considered during the pharmacophore model generation. These compounds were minimized

using the same protocol used for the compounds for model generation. Minimized structures were then matched to the hypothesis in "**search for matches**" panel. Four compounds were picked up of ten compounds. It was worth mentioning that out of the five active compounds, four were picked and none of the inactive compounds were picked (**Table 4.5**). This proves applicability of the developed model. The validation results by mapping the picked compounds over the developed pharmacophore model is shown in **Figure 4.4**.
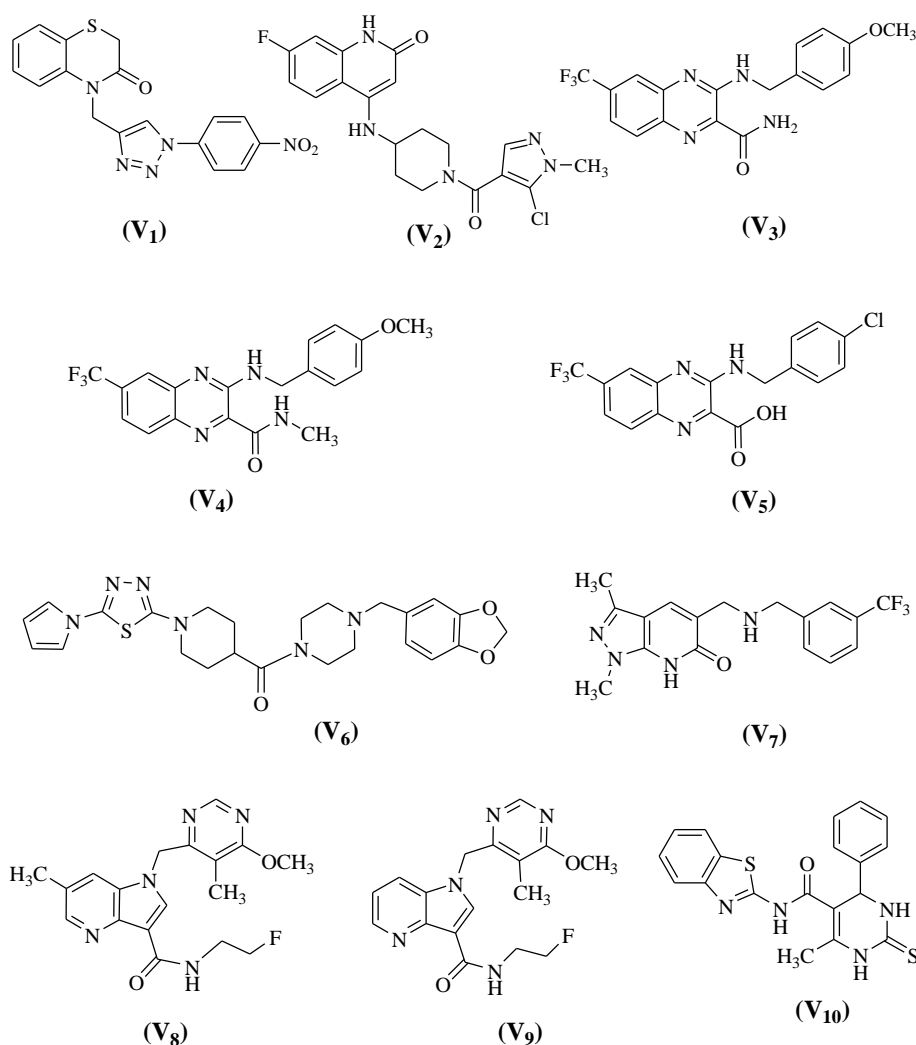

Figure 4.3: Compounds (V_{1-10}) used for the validation of pharmacophore model (AHRR.28)

Table 4.5: Validation results of ten compounds

Comp ID	Observed activity (pIC_{50})	Active/inactive	Picked or Not
V_1	4.183	Inactive	Not
V_2	8.154	Active	**Picked**

V_3	4	Inactive	Not
V_4	4	Inactive	Not
V_5	7.3	Active	Not
V_6	6.39	Active	**Picked**
V_7	4	Inactive	Not
V_8	8.522	Active	**Picked**
V_9	8.00	Active	**Picked**
V_{10}	5.11	Inactive	Not
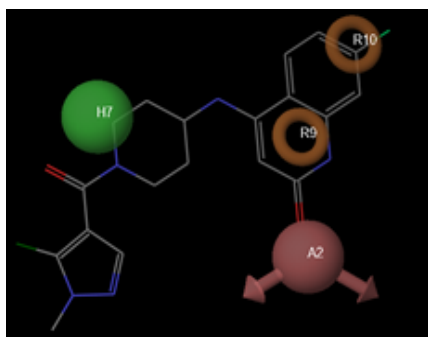
Mapping of compound V_2
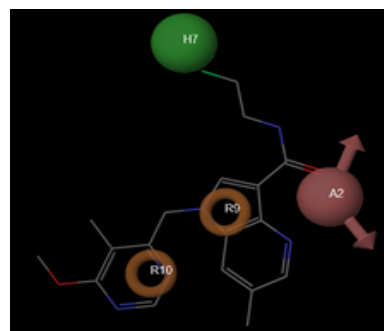
Mapping of compound V_8
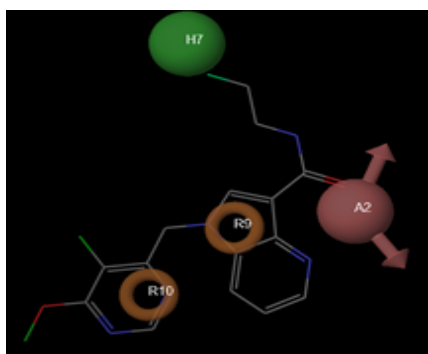
Mapping of V_9
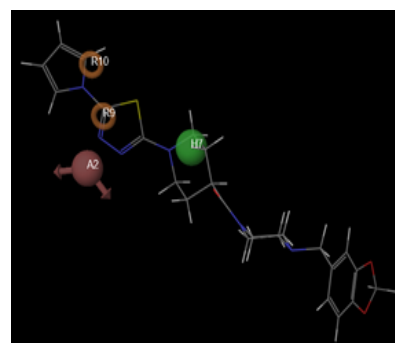
Mapping of V_6

Figure 4.4: Mapping of active structures on pharmacophore model

4.2 Virtual screening for the identification of new moiety by using various filters like pharmacophore model, molecular modelling and Lipinski rule of five

Virtual screening has been proved to be a competent technique for the identification of hits using already available database in public/private domain. Various filters were applied to the Asinex database consisting of 2,12,526 compounds, so as to get initial hits as DprE1 inhibitors. The following filters were used to conduct virtual screening:

4.2.1 First filter: Pharmacophore model

The best pharmacophore model AHRR.28 generated in the study was utilized as the first filter to explore the Asinex database in search of DprE1 inhibitors. The compounds matching all the four pharmacophoric features were picked up. A total of 7099 compounds matched the pharmacophore hypothesis AHRR.28.

4.2.2 Second filter: Molecular docking

Molecular docking was used as second filter. The crystal structure of DprE1 enzyme (4p8n) was used for the docking. Primarily a high throughput virtual screening (HTVS) was used for docking by keeping it flexible. As a result, 7058 compounds were obtained. These compounds were further docked again using the standard precision (SP) method to get 385 hits. Again, these compounds were redocked using extra precision (XP) method to finally get 36 hits.

4.2.3 Third filter: Lipinski rule of five

To assess the drug likeness properties of the compounds obtained in the docking, Lipinski rule of five was applied. Only 08 compounds were following Lipinski rule of five. The virtual screening results are illustrated in **Figure 4.5** and the obtained eight hits (H_{1-8}) are shown in **Figure 4.6**. The resultant hits showed diverse set of chemical scaffolds. This satisfied the aim of carrying out virtual screening i.e., getting newer diverse scaffolds that could act as DprE1 inhibitors.
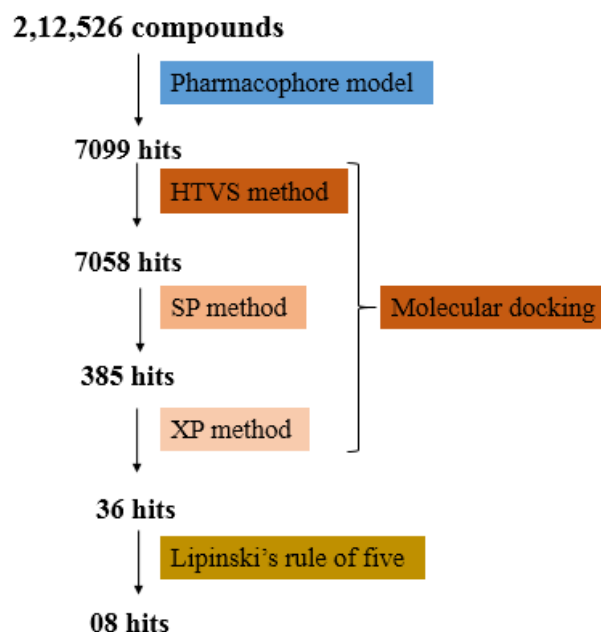

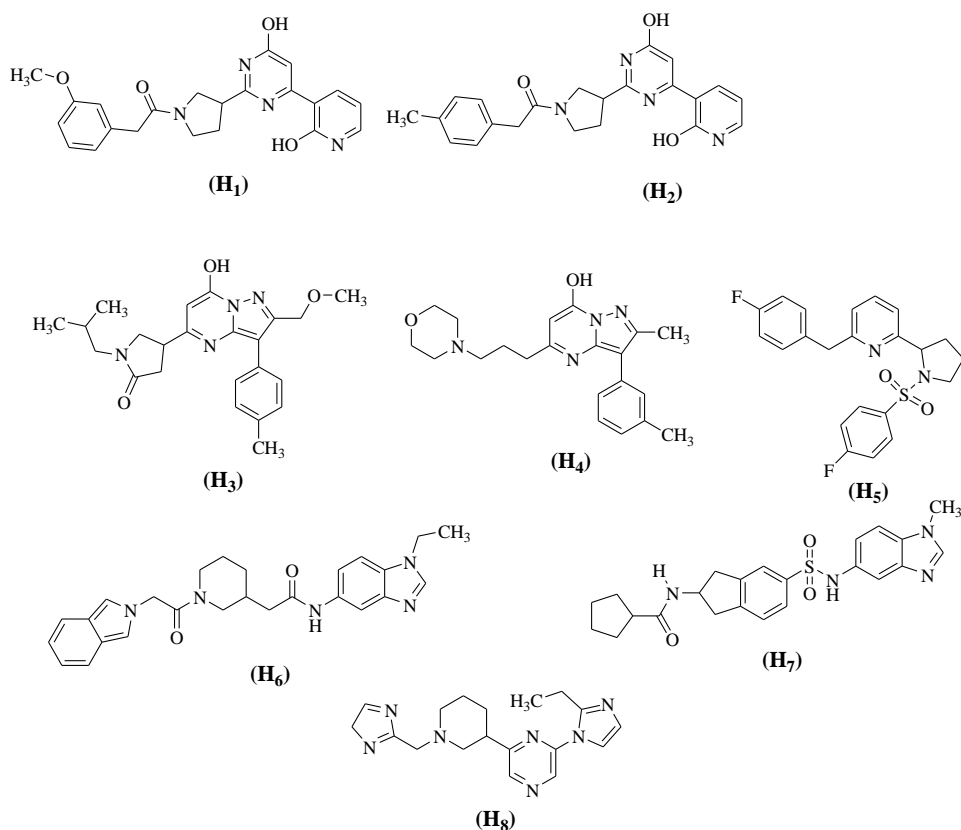**Figure 4.5:** Flow chart of virtual screening

**Figure 4.6:** Hits (**H₁₋₈**) obtained as an output of virtual screening protocol

4.3 Hit optimization through molecular docking techniques

Virtual screening offered highly diverse hits. Some of these hits (**H₃-H₄**) have never been reported as DprE1 inhibitors. These results fulfilled the aim to perform virtual screening in the first place i.e. identification of some new scaffolds as DprE1 inhibitors.

Out of eight hits, two were pyrazolo-pyrimidine derivatives (**H3-H4**). This (pyrazolo-pyrimidine) moiety is not yet reported as DprE1 inhibitor. Considering the literature, importance of pyrazolopyrimidine scaffold for therapeutic applications and synthetic feasibility of pyrazolo-pyrimidine moiety, it was selected for further optimization to obtain target compounds having **Formula III** (**Figure 4.7**). The basic scaffold of the hits was utilized while compounds with various substitutions at different positions were designed to study the structure activity relationship.

Docking studies were carried out for the designed compounds using Formula I, wherein some important interactions within the active site of the enzyme were observed. Compounds were found to interact with CYS 387. Compounds were also seen to form alkyl and pi-alkyl interactions with LYS 134, LEU 363 and TRP 230 amino acid residues.

The physicochemical and pharmacokinetic parameters of the designed compounds were computed. The majority of compounds were predicted to exert drug like properties. Physicochemical properties such as molecular weight, hydrogen bond donors, hydrophobicity, polar surface area etc. were all found to be in the range. It was also predicted that all the compounds would be metabolized by CYP3A4. Most of the compounds were not predicted cross BBB except a few. All the compounds were predicted to show high gastrointestinal absorption.
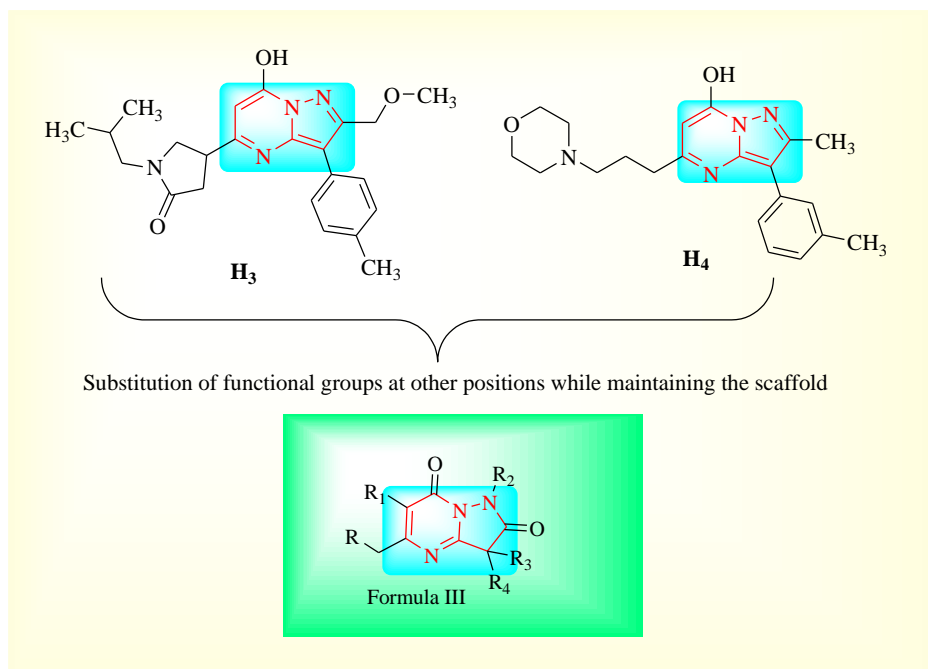
Wherein, R= -Cl, -NH-CH$_2$-C$_6$H$_5$, -NH-CH$_2$-4-C$_6$H$_4$-Cl, -NH-CH$_2$-4-C$_6$H$_4$-F, -NH-CH$_2$-4-C$_6$H$_4$-CH$_3$, -NH-CH$_2$-4-C$_6$H$_4$-OCH$_3$, -NH-CH$_2$-3,4-C$_6$H$_3$-*di*Cl, -NH-C$_6$H$_5$, -NH-2-C$_6$H$_4$-Cl, -NH-4-C$_6$H$_4$-F, -NH-4-C$_6$H$_4$-CH$_3$, -NH-4-C$_6$H$_4$-OCH$_3$, pyridin-4-ylamino, pyrrolidin-1-yl, piperazin-1-yl, morpholino, 4-methylpiperazin-1-yl
R$_1$=Cl/H; R$_2$= Br/H; R$_3$= -C$_6$H, -CH-C$_6$H$_5$, R$_4$= H, -CH-C$_6$H$_5$

Figure 4.7: Designing of pyrazolo[1,5-*a*]pyrimidine-2,7(1*H*,4*H*)-dione compounds based on the hits obtained by virtual screening

4.4 Synthesis of designed compounds

The designed compounds having Formula **III** were synthesized as per scheme **1-3**.

4.4.1 Synthesis of 3-phenylpyrazolo[1,5-*a*]pyrimidine-2,7(1*H*,4*H*)-dione (Formula IIIa) based compounds (106-125)

For the synthesis of the aimed compounds (**Formula IIIa**) the following steps have been utilized as explained in **Scheme 1**.
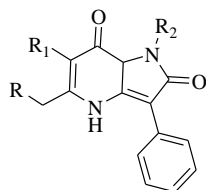
Formula IIIa

3-Amino-4-phenyl-*1H*-pyrazol-5(*4H*)-one (**106**) was synthesized by reacting commercially available ethyl-2-cyano-2-phenylacetate (**105**) with hydrazine hydrate 99%. The synthesized compound was further reacted with various ethyl acetoacetates in presence of glacial acetic acid to yield substituted 3-phenylpyrazolo[1,5-*a*]pyrimidine-2,7(1*H*,4*H*)-dione (**107, 109-110**) by substitution and subsequent cyclization. It was aimed to synthesize three different substituted 3-phenylpyrazolo[1,5-*a*]pyrimidine-2,7(1*H*,4*H*)-dione (**107, 109-110**).

The first class of derivative (**107, 109-110**) was reported as such. The second category of 3-phenylpyrazolo[1,5-*a*]pyrimidine-2,7(1*H*,4*H*)-dione (**107**) was brominated with *N*-bromosuccinimide to give 1-bromo5-methyl-3-phenylpyrazolo[1,5-*a*]pyrimidine-2,7(1*H*,4*H*)-dione (**108**). The third category of compounds was synthesized by substitution reaction of the compound (**110**) with various amines such as benzyl amine, anilines and heterocyclic amine.

This work for the synthesis of 3-phenylpyrazolo[1,5-*a*]pyrimidine-2,7(1*H*,4*H*)-dione (**Formula IIIa**) consisting intermediates and final compounds has been discussed under the following sections:

4.4.1.1 Synthesis of 3-amino-4-phenyl-*1H*-pyrazol-5(*4H*)-one (**106**)

4.4.1.2 Synthesis of 5-methyl-3-phenylpyrazolo[1,5-*a*] pyrimidine-2,7(1*H*,4*H*)-dione (**107**)

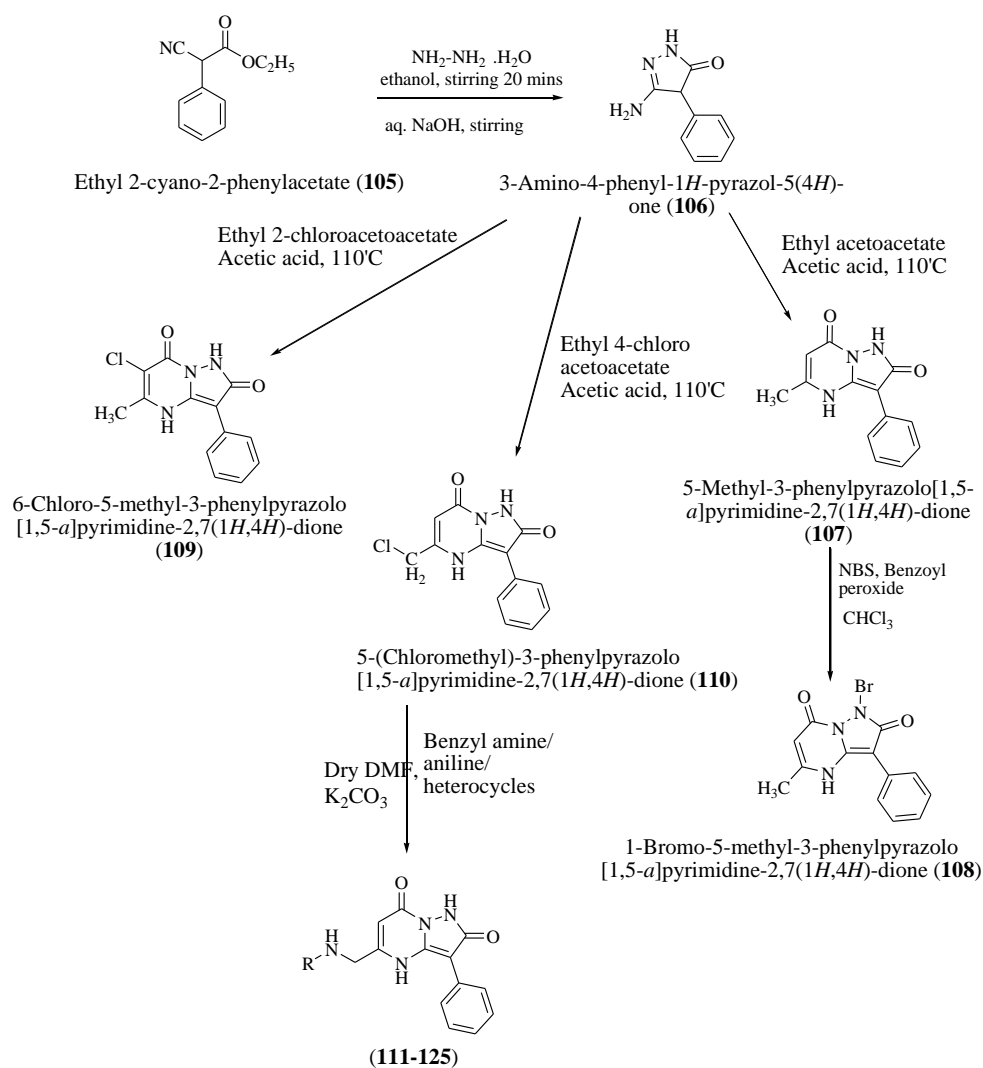4.4.1.3 Synthesis of 1-bromo-5-methyl-3-phenylpyrazolo[1,5-*a*]pyrimidine-2,7(1*H*,4*H*)-dione (**108**)

4.4.1.4 Synthesis of 6-chloro-5-methyl-3-phenylpyrazolo[1,5-*a*]pyrimidine-2,7(1*H*,4*H*)-dione (**109**)

4.4.1.5 Synthesis of 5-(chloromethyl)-3-phenylpyrazolo[1,5-*a*]pyrimidine-2,7(1*H*,4*H*)-dione (**110**)

4.4.1.6 Synthesis of 5-((substitutedbenzylamino)methyl)-3-phenylpyrazolo[1,5-*a*]pyrimidine-2,7(1*H*,4*H*)-dione (**111-116**)

4.4.1.7 Synthesis of 5-((subtitutedphenylamino)methyl)-3-phenylpyrazolo[1,5-*a*]pyrimidine-2,7(1*H*,4*H*)-dione (**117-120**)

4.4.1.8 Synthesis of 5-((subtituted)methyl)-3-phenylpyrazolo[1,5-*a*]pyrimidine-2,7(1*H*,4*H*)-dione (**121-125**)

**Scheme 1**: Synthesis of compounds of 3-phenylpyrazolo[1,5-*a*]pyrimidine-2,7(1*H*,4*H*)-dione (**Formula IIIa**) based compounds

4.4.1.1 Synthesis of 3-amino-4-phenyl-*1H*-pyrazol-5(*4H*)-one (106)

Ethyl 2-cyano-2-phenylacetate (**105**)   3-Amino-4-phenyl-1*H*-pyrazol-5(4*H*)-one (**106**)
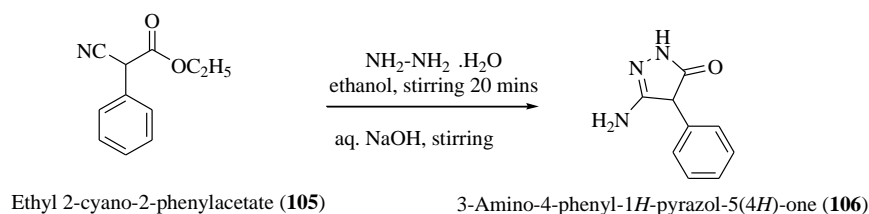
The nucleophilic substitution of hydrazine hydrate on ethyl 2-cyano-2-phenylacetate (**105**) followed by subsequent cyclization yielded 3-amino-4-phenyl-*1H*-pyrazol-5(*4H*)-one (**106**). The IR spectrum of the compound depicted characteristic signals for -NH stretching of amide at 3485 cm^{-1}, whereas two peaks at 3304 cm^{-1} and 3255 cm^{-1} for -NH stretching of primary amine and -C=O stretching at 1647 cm^{-1}. Its mass spectrum showed peaks at m/z 176 [M+1]$^{+}$ and an isotopic peak at 177 [M+2]$^{+}$.

4.4.1.2 Synthesis of 5-methyl-3-phenylpyrazolo[1,5-*a*]pyrimidine-2,7(1*H*,4*H*)-dione (107)

3-Amino-4-phenyl-1*H*-pyrazol-5(4*H*)-one (**106**)   5-Methyl-3-phenylpyrazolo[1,5-*a*]pyrimidine-2,7(1*H*,4*H*)-dione (**107**)
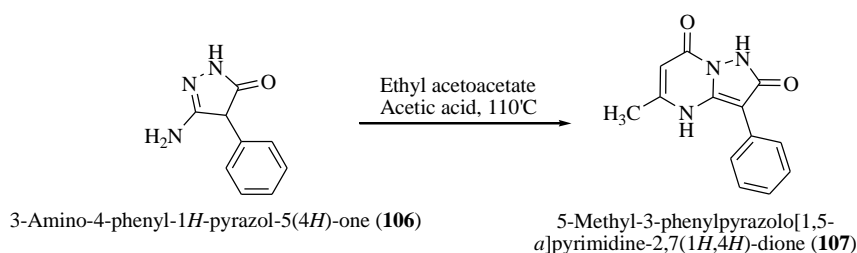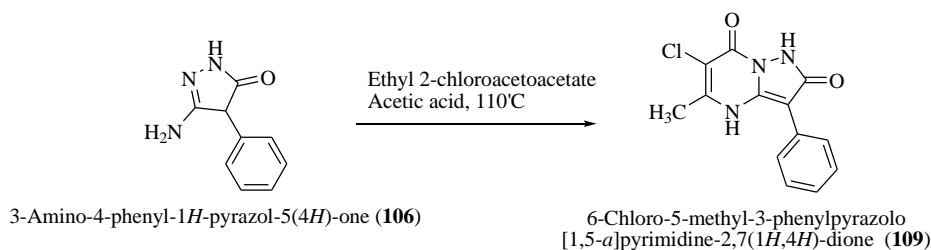
The free amino group was substituted by ethyl acetoacetate followed by intramolecular cyclization to yield the desired compound (**107**). The IR spectrum showed peaks at 1688 cm^{-1} for C=O stretching. The mass spectrum showed quasi molecular ion at m/z 242 [M+1]$^{+}$. The PMR spectrum offered broad peaks at δ 12.04 and 11.52 for the amide and *sec.* amine proton respectively. Two aromatic protons as doublet appeared at δ 7.45-7.43 (d, 2H) and a triplet was obtained for another two aromatic protons at δ 7.36-7.33 (t, 2H, *J* =7.7 Hz). Another triplet for single aromatic proton was seen at δ 7.21-7.18 (t, 1H, *J* =7.3 Hz). A singlet for three methyl protons was seen at δ 2.37 (s, 3H), whereas another singlet was observed at δ 2.19 for one proton (s, 1H).

**4.4.1.3 Synthesis of 1-bromo-5-methyl-3-phenylpyrazolo[1,5-*a*]pyrimidine-2,7(1*H*,4*H*)-dione (108)**

5-Methyl-3-phenylpyrazolo[1,5-
a]pyrimidine-2,7(1*H*,4*H*)-dione (**107**)

1-Bromo-5-methyl-3-phenylpyrazolo
[1,5-*a*]pyrimidine-2,7(1*H*,4*H*)-dione (**108**)
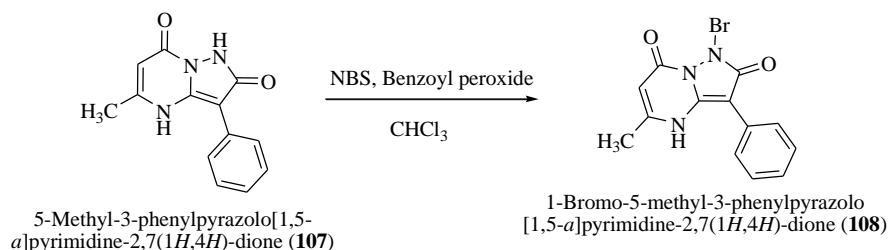
Bromination of compound (**107**) with *N*-bromo succinimide (NBS) offered (**108**). The IR spectrum demonstrated C=O stretching at 1634 cm^{-1}. The mass spectrum showed molecular ion peak at m/z 320.09 [M]$^+$ and isotope peak at 322 [M+2]$^+$. The PMR spectrum of the compound showed a singlet for a single proton 11.58 (s, 1H) and another singlet at 11.28 (s, 1H). Two aromatic protons were observed as doublet of doublets at 7.52-7.50 (dd, 2H, *J* =8.1 and 1.2 Hz). Remaining aromatic protons appeared at 7.43-7.40 (t, 2H) and 7.28-7.24 (t, 1H). A singlet for one proton can be seen at 5.55 (s, 1H), and another singlet for three aliphatic proton was observed at 2.27 (s, 3H).

4.4.1.4 Synthesis of 6-chloro-5-methyl-3-phenylpyrazolo[1,5-*a*]pyrimidine-2,7(1*H*,4*H*)-dione (109)

3-Amino-4-phenyl-1*H*-pyrazol-5(4*H*)-one (**106**)

6-Chloro-5-methyl-3-phenylpyrazolo
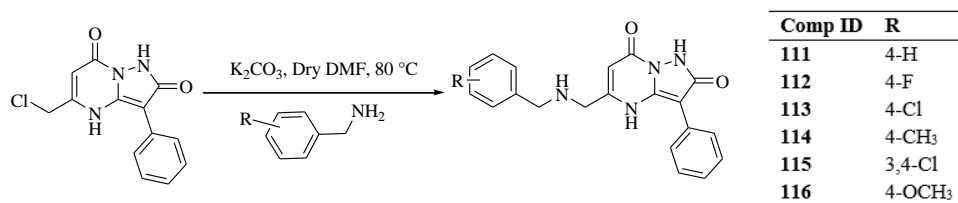[1,5-*a*]pyrimidine-2,7(1*H*,4*H*)-dione (**109**)

The free amino group was substituted by ethyl 2-chloro acetoacetate followed by intramolecular cyclization to yield the desired compound (**109**). The IR spectrum showed peaks at 1697 cm^{-1} for C=O stretching and a strong peak at 758 cm^{-1} for C-Cl. The mass spectrum showed sodiated peak at m/z 297 [M+Na]$^+$. The PMR spectrum offered broad peaks at δ 12.05 and 11.58 for the amide and *sec.* amine proton respectively. Two aromatic protons as doublet appeared at 7.52-7.50 (d, 2H, *J*=7.6) and a triplet was obtained for another two aromatic protons at 7.45-7.41 (t, 2H, *J* =7.6 Hz). Another triplet for single aromatic proton was seen at 7.30-7.27 (t, 1H, *J* =7.2 Hz). A singlet for three methyl protons was seen at 2.43 (s, 3H), whereas another singlet was observed at 1.90 for one proton (s, 1H).

4.4.1.5 Synthesis of 5-(chloromethyl)-3-phenylpyrazolo[1,5-*a*]pyrimidine-2,7(1*H*,4*H*)-dione (110)

3-Amino-4-phenyl-1*H*-pyrazol-5(4*H*)-one (**106**)

5-(Chloromethyl)-3-phenylpyrazolo
[1,5-*a*]pyrimidine-2,7(1*H*,4*H*)-dione (**110**)
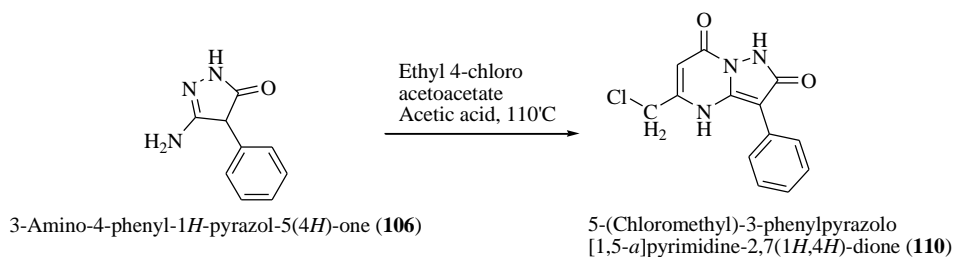
The free amino group was substituted by ethyl 4-chloro acetoacetate followed by intramolecular cyclization to yield the desired compound (**110**). The IR spectrum showed peaks at 1692 cm^{-1} for C=O stretching and a strong peak at 753 cm^{-1} for C-Cl. The mass spectrum offered quasi molecular ion peak at m/z 276 [M+1]$^{+}$. The PMR spectrum offered broad peaks at 12.01 and 11.39 for the amide and *sec.* amine proton respectively. Two aromatic protons as broad singlet at 7.56 (s, 2H) and a triplet was obtained for another two aromatic protons at 7.46-7.43 (t, 2H, *J* =7.6 Hz). Another triplet for single aromatic proton was seen at 7.30-7.27 (t, 1H, *J* =7.4 Hz). A singlet for one proton can be seen at 5.90 (s, 1H), and another singlet for two aliphatic proton was observed at 4.65 (s, 2H).

4.4.1.6 Synthesis of 5-((substitutedbenzylamino)methyl)-3-phenylpyrazolo[1,5-*a*]pyrimidine-2,7(1*H*,4*H*)-dione (111-116)

Comp ID	R
111	4-H
112	4-F
113	4-Cl
114	4-CH₃
115	3,4-Cl
116	4-OCH₃

Nucleophilic substitution of 5-(chloromethyl)3-phenylpyrazolo[1,5-*a*]pyrimidine-2,7(1*H*,4*H*)-dione (**110**) was performed with various benzyl amines in presence of anhydrous potassium carbonate in dry DMF to give the desired products (**111-116**).


(111)   **(112)**   **(113)**
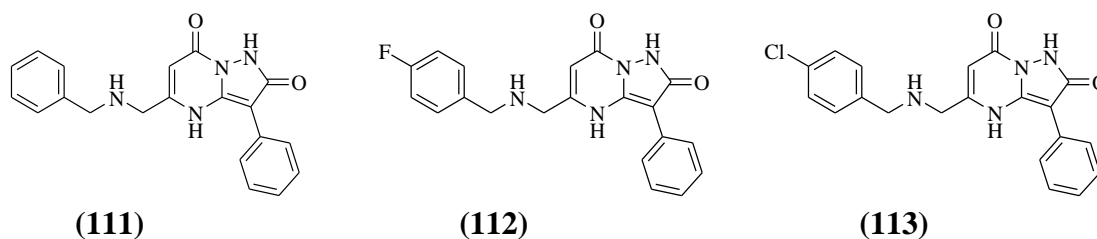
IR spectrum of compound (**111**) showed peaks at 3399 cm^{-1} for -NH stretching and 1645 cm^{-1} for -C=O stretching. The mass spectrum offered quasi molecular ion peak at

m/z 347 [M+1]$^{+.}$ Its PMR spectrum demonstrated a singlet at 8.30 for one proton whereas a doublet was observed 7.57-7.55 (d, 2H) for two aromatic protons. A multiplet was observe for six aromatic protons at 7.47-7.39 (m, 6H). Further two aromatic protons can be seen as triplet at 7.31-7.10 (t, 2H). A singlet was observed at 5.94 (s, 1H). A singlet for two -CH$_2$ was observed at 4.24 (s, 2H). Another singlet for two -CH$_2$ protons appeared at 4.17 (s, 2H).

IR spectrum of compound **(112)** showed peaks at 1640 cm^{-1} for -C=O stretching. The mass spectrum offered quasi molecular ion peak at m/z 365 [M+1]$^{+.}$ Its PMR spectrum demonstrated a board singlet at 9.49 for two -NH proton whereas a doublet was observed at 8.07 (d, *J* = 7.7 Hz, 2H) for two aromatic protons. A multiplet was observe for four aromatic protons at 7.60-7.48 (m, 4H). Further two aromatic protons can be seen as a triplet at 7.37-7.34 (t, *J* = 7.6 Hz, 2H). Another triplet for single aromatic proton appeared at 7.15-7.12 (t, *J* = 7.3 Hz, 1H). A singlet was observed at 5.65 (s, 1H). A singlet for two -CH$_2$ was observed at 4.09 (s, 2H). Another singlet for two -CH$_2$ protons appeared at 3.87 (s, 2H).
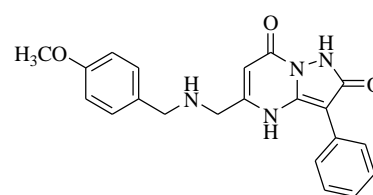
IR spectrum of compound **(113)** showed peaks at 1641 cm^{-1} for -C=O stretching. The mass spectrum offered quasi molecular ion peak at m/z 381 [M+1]$^{+.}$ Its PMR spectrum demonstrated a board singlet at 9.45 for two -NH proton whereas a doublet was observed at 8.02 (d, *J* = 7.8 Hz, 2H) for two aromatic protons. A multiplet was observe for four aromatic protons at 7.54-7.44 (m, 4H). Further two aromatic protons can be seen as a triplet at 7.33-7.30 (t, *J* = 7.6 Hz, 2H). Another triplet for single aromatic proton appeared at 7.11-7.09 (t, *J* = 7.4 Hz, 1H). A singlet was observed at 5.61 (s, 1H). A singlet for two -CH$_2$ was observed at 4.04 (s, 2H). Another singlet for two -CH$_2$ protons appeared at 3.83 (s, 2H).
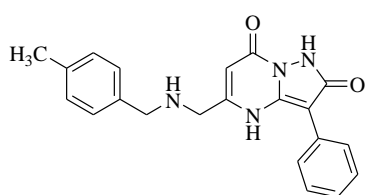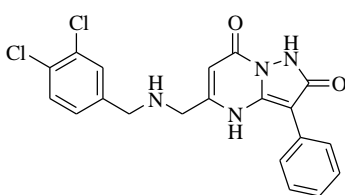
**(114)**   **(115)**   **(116)**

IR spectrum of compound **(114)** offered peaks at 2859 cm^{-1} for aliphatic CH stretching and at 1643 cm^{-1} for -C=O stretching. Its mass spectrum demonstrated peak at m/z 361[M+1]$^{+}$. The PMR of the compounds showed aromatic protons at δ 8.24 (d, 2H) as doublet for two protons, δ 7.40-7.38 (d, 2H), δ 7.35-7.34 (d, 1H), δ 7.28-7.22 (m, 4H) and δ 7.03-7.00 (t, 1H). A singlet appeared at 5.54 (s, 1H). The aliphatic protons were observed at 4.14 (s, 2H), 4.0 (s, 1H), 3.85 (s, 2H), methyl protons appeared as singlet at 2.33 (s, 3H).

IR spectrum of compound **(115)** showed peaks at 3444 cm^{-1} for -NH stretching and 1613 cm^{-1} for -C=O stretching. The mass spectrum offered quasi molecular ion peak at m/z 415 [M]$^{+.}$ Its PMR spectrum demonstrated a board singlet at 9.3 for two -NH proton whereas a doublet was observed at 7.83-7.81 (d, J = 7.2 Hz, 2H) for two aromatic protons. A singlet for one proton appeared at 7.71 (s, 1H), whereas another doublet for single proton at 7.64-7.626 (d, J=8.0, 1H) was observed. A doublet was observed for two aromatic protons at 7.43-7.42 (d, 1H). Further two aromatic protons can be seen as a triplet at 7.36-7.32 (t, J = 7.8 Hz, 2H). Another triplet for single aromatic proton appeared at 7.16-7.13 (t, J = 7.4 Hz, 1H). A singlet was observed at 5.7 (s, 1H). A singlet for two -CH$_2$ was observed at 3.95 (s, 2H). Another singlet for two -CH$_2$ protons appeared at 3.77 (s, 2H).
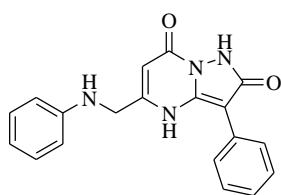
IR spectrum of compound **(116)** showed characteristic at 3433 cm^{-1} for -NH stretching and peaks for C-O stretching can be seen at 1252 cm^{-1}. Its mass spectrum gave quasi molecular ion peak at m/z 377 [M+1]$^{+}$. Its PMR spectrum gave a broad singlet at 9.69 for NH protons. The aromatic protons were observed at 8.32-8.30 (d, J = 8.0 Hz, 2H), 7.51 – 7.49 (m, 2H), 7.33-7.30 (t, J = 7.7 Hz, 2H) each representing two protons, whereas a triplet was observed at 7.08 – 7.02 (m, 3H) representing three protons. A singlet for single proton appeared at 5.59 (s, 1H). Aliphatic protons appeared ad singlets at 4.21 (s, 2H), 3.97 (s, 2H) each representing two protons and methoxy protons appeared at 3.82 (s, 3H) as singlet. ^{13}C-NMR of the compound offered signals for aromatic carbon at 162.56, 159.37, 155.41, 134.42, 131.06, 127.49, 125.20, 125.07, 122.76, 113.86, 93.18, 87.44 whereas aliphatic carbons gave signals at 55.07, 49.84, 48.99.

4.4.1.7 Synthesis of 5-((subtitutedphenylamino)methyl)-3-phenylpyrazolo[1,5-*a*]pyrimidine-2,7(1*H*,4*H*)-dione (117-120)
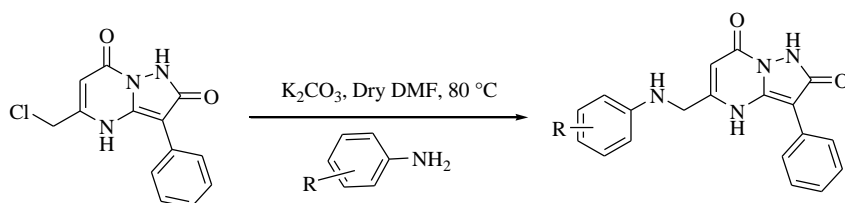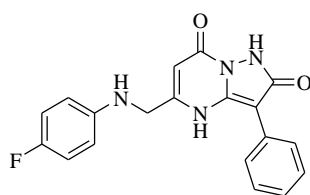

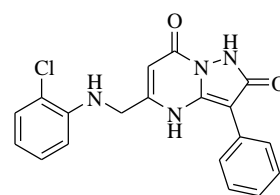| Comp ID	R
117	H
118	4-F
119	2-Cl
120	4-OCH$_3$

Nucleophilic substitution of 5-(chloromethyl)3-phenylpyrazolo[1,5-*a*]pyrimidine-2,7(1*H*,4*H*)-dione was performed with various anilines in presence of anhydrous potassium carbonate in dry DMF to give the desired products (**117-120**).

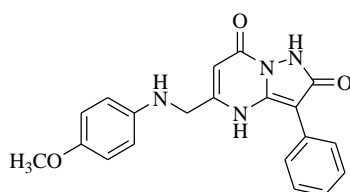**(117)**   **(118)**   **(119)**

IR spectrum of compound **(117)** depicted characteristic peaks for -NH stretching at 3370 cm^{-1} and 1612 cm^{-1} for -C=O stretching. Its mass spectrum offered quasi molecular ion peak at m/z 333 [M+1]$^{+}$. The PMR spectrum offered two peaks appearing as singlet at 11.56 (s, 1H) and 11.32 (s, 1H). The aromatic protons appeared at 7.54-7.52 (s, 2H), 7.46-7.42 (t, 2H), 7.30-7.26 (t, 1H), 7.11-7.07 (t, 2H), 6.62-6.57 (m, 3H) and 6.24 (s, 1H). Another singlet appeared at 5.62 (s, 1H). The aliphatic protons were observed at 4.25 (s, 2H).

IR spectrum of compound **(118)** showed characteristic peaks for -NH stretching at 3443 cm^{-1} and 1613 cm^{-1} for -C=O stretching. Its mass spectrum offered quasi molecular ion peak at m/z 351 [M+1]$^{+}$. The PMR spectrum offered two peaks appearing as singlet at 11.57 (s, 1H) and 11.32 (s, 1H) for -NH protons. The aromatic protons appeared at 7.54 (d, *J* = 6.8 Hz, 2H), 7.45 (t, *J* = 7.8 Hz, 3H), 7.29 (t, *J* = 7.3 Hz, 1H), 6.94 (t, *J* = 8.9 Hz, 2H), 6.65 – 6.57 (m, 2H). Another singlet appeared at 5.63 (s, 1H). The methylene protons were observed at 4.25 – 4.20 (m, 2H). HPLC % purity: 94.99.

IR spectrum of compound **(119)** showed characteristic peaks for -NH stretching at 3376 cm^{-1} and 1616 cm^{-1} for -C=O stretching. Its mass spectrum offered quasi molecular ion peak at m/z 367 [M+1]$^{+}$. The PMR spectrum offered a doublet at 11.46 (d, *J* = 97.6 Hz, 2H) for -NH protons. The aromatic protons appeared at 7.55 (d, *J* = 6.8 Hz, 2H), 7.46 (t, *J* = 7.7 Hz, 2H), 7.30 (t, *J* = 7.3 Hz, 1H), 6.95 (t, *J* = 8.9 Hz, 2H), 6.62 (dd, *J* = 9.0, 4.5 Hz, 2H). Another singlet appeared at 5.64 (s, 1H). The methylene protons were observed at 4.24 (s, 2H).
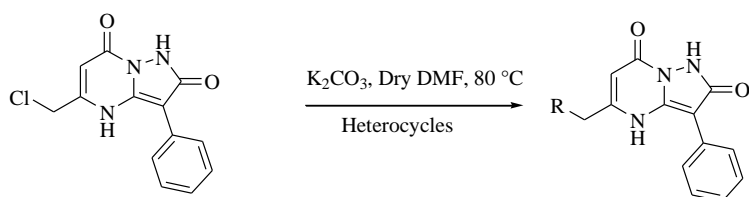

(120)

IR spectrum of compound **(120)** showed characteristic peaks for -NH stretching at 3407 cm^{-1} and 1619 cm^{-1} for -C=O stretching. Its mass spectrum offered quasi molecular ion

peak at m/z 363 [M+1]$^+$. The PMR spectrum offered a doublet at 11.39 (d, *J* = 67.1 Hz, 2H) for -NH protons. The aromatic protons appeared at 7.52 (d, *J* = 7.6 Hz, 3H), 7.45 (t, *J* = 7.7 Hz, 2H), 7.29 (t, *J* = 7.4 Hz, 1H), 6.85 (dd, *J* = 8.1, 1.4 Hz, 1H), 6.74 (td, *J* = 7.6, 1.4 Hz, 1H), 6.60 – 6.52 (m, 2H). Another singlet appeared at 5.63 (s, 1H). The methylene protons were observed at 4.28 (d, *J* = 2.9 Hz, 2H) whereas methyl protons appeared at 3.83 (s, 3H).

4.4.1.8   Synthesis   of   5-((subtituted)methyl)-3-phenylpyrazolo[1,5-*a*]pyrimidine-2,7(1*H*,4*H*)-dione (121-125)
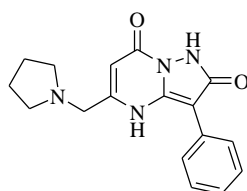
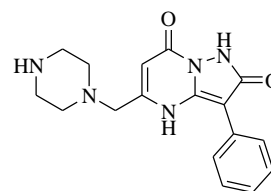| Comp ID	R
121	HN— (4-pyridyl)
122	—N (pyrrolidine)
123	—N NH (piperazine)
124	—N O (morpholine)
125	—N N–CH$_3$ (N-methylpiperazine)

Nucleophilic substitution of 5-(chloromethyl)3-phenylpyrazolo[1,5-*a*]pyrimidine-2,7(1*H*,4*H*)-dione was performed with various *N*-containing heterocycles in presence of anhydrous potassium carbonate in dry DMF to give the desired products (**121-125**).
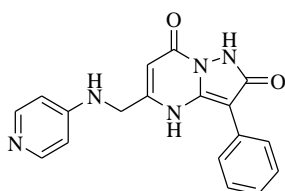
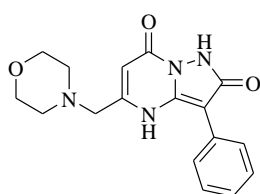**(121)**   **(122)**   **(123)**

IR spectrum of compound (**121**) showed characteristic peaks at 3338 cm^{-1} for -NH stretching and 1659 cm^{-1} for -C=O stretching. The quasi-molecular ion peak appeared at m/z 334 [M+1]$^+$. The PMR spectrum of the compound gave singlet at 10.83 (s, 1H). Aromatic protons appeared at 8.24-8.20 (m, 4H), 8.14-8.10 (s, 2H), 7.24-7.13 (m, 2H), 6.90-6.86 (m, 3H). Another singlet was observed at 5.37 (s, 1H), while aliphatic methylene protons appeared at 5.20 (s, 2H).

IR spectrum of compound (**122**) demonstrated peaks at 3408 for -NH stretching and 1664 cm^{-1} for -C=O cm^{-1} stretching. The quasi-molecular ion peak appeared at m/z 311 [M+1]$^+$. The PMR spectrum of the compound gave singlet at 10.62 (s, 1H) for -NH protons.

Aromatic protons appeared at 8.20-8.19 (d, *J* = 7.8 Hz, 2H), 7.29-7.26 (t, *J* = 7.8, 2H), 7.02-6.99 (t, *J* = 7.3, 1H). Another singlet was observed at 5.54 (s, 1H), while aliphatic methylene protons appeared at 4.07 (s, 2H). Other aliphatic protons appeared at 3.27-3.24 (t, 4H), 1.94-1.92 (m, 4H).

IR spectrum of compound **(123)** demonstrated peaks at 3426 cm^{-1} for -NH stretching and 1645 cm^{-1} for -C=O stretching. The quasi-molecular ion peak appeared at m/z 354 [M+1+28][+] (ethyl adduct)[10]. The PMR spectrum of the compound gave singlet at 11.26 (s, 2H) and another singlet at 8.00 (s, 1H) for -NH protons. Aromatic protons appeared at 7.56 (s, 2H), 7.42 (t, *J* = 7.6 Hz, 2H), 7.25 (t, *J* = 7.5 Hz, 1H). Another singlet was observed at 5.74 (s, 1H), while aliphatic methylene protons appeared at 3.50 (s, 2H). Other aliphatic protons appeared at 3.41 (m, 5H), 2.45 (d, *J* = 5.2 Hz, 3H).

IR spectrum of the compound **(124)** showed peaks at 1678 cm^{-1} for -C=O stretching. The quasi-molecular ion peak appeared at m/z 327 [M+1][+]. The PMR spectrum showed singlet at 11.30 (s, 2H). Aromatic protons appeared at 7.56-7.54 (d, *J* = 7.6 Hz, 2H), 7.45-7.42 (t, *J* = 7.8 Hz, 2H), 7.29 – 7.26 (m, 1H). A singlet appeared at 5.73 (s, 1H). Aliphatic protons appeared at 3.64-3.62 (t, *J* = 4.5 Hz, 4H), 3.48 (s, 2H), 3.18 (s, 1H), 2.51 (m, 4H, *merged with peak of* DMSO-d$_6$).
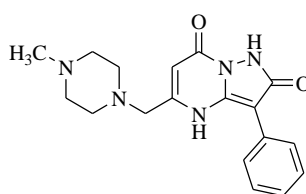
(124)   **(125)**

IR spectrum of compound **(125)** demonstrated peaks at 3444 cm^{-1} for -NH stretching and 1620 cm^{-1} for -C=O stretching. The quasi-molecular ion peak appeared at m/z 340 [M+1][+]. Its PMR spectrum showed peaks at 14.01 and 12.40 for -NH protons. Aromatic protons were observed at 7.54-7.48 (m, 3H) and 7.32-7.29 (m, 2H). A single proton appeared at 5.52 (s, 1H). The -CH2 protons appeared at 3.45 (s, 2H) whereas the piperazine protons were observed at 2.77-2.70 (m, 4H) and 2.69-2.68 (m, 4H). Methyl protons can be seen at 2.24 (s, 3H).

4.4.2 Synthesis of 3,3-dibenzyl-5-methylpyrazolo[1,5-*a*]pyrimidine-2,7(1*H*,3*H*)-dione based compounds (128-141)

The designed compounds having **formula III-b** were synthesized by implementing scheme 2.
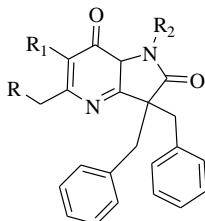
Formula III-b

The work relate to the intermediates and the designed compounds has been explained under the main headings:

4.4.2.1 Synthesis of methyl 2-benzyl-2-cyano-3-phenylpropanoate **(128)**

4.4.2.2 Synthesis of 3-amino-4,4-dibenzyl-1*H*-pyrazol-5(4*H*)-one **(129)**

4.4.2.3 Synthesis of 3,3-dibenzyl-5-methylpyrazolo[1,5-*a*]pyrimidine-2,7(1*H*,3*H*)-dione **(130)**

4.4.2.4 Synthesis of 3,3-dibenzyl-1-bromo-5-methylpyrazolo[1,5-*a*]pyrimidine-2,7(1*H*,3*H*)-dione (**131**)

4.4.2.5 Synthesis of 3,3-dibenzyl-6-chloro-5-methylpyrazolo[1,5-*a*]pyrimidine-2,7(1*H*,3*H*)-dione (**132**)

4.4.2.6 Synthesis of 3,3-dibenzyl-5-(chloromethyl)pyrazolo[1,5-*a*]pyrimidine-2,7(1*H*,3*H*)-dione (**133**)

4.4.2.7 Synthesis of 5-((substitutedamino)methyl)-3,3-dibenzylpyrazolo[1,5-*a*]pyrimidine-2,7(1*H*,3*H*)-dione (**134-141**)
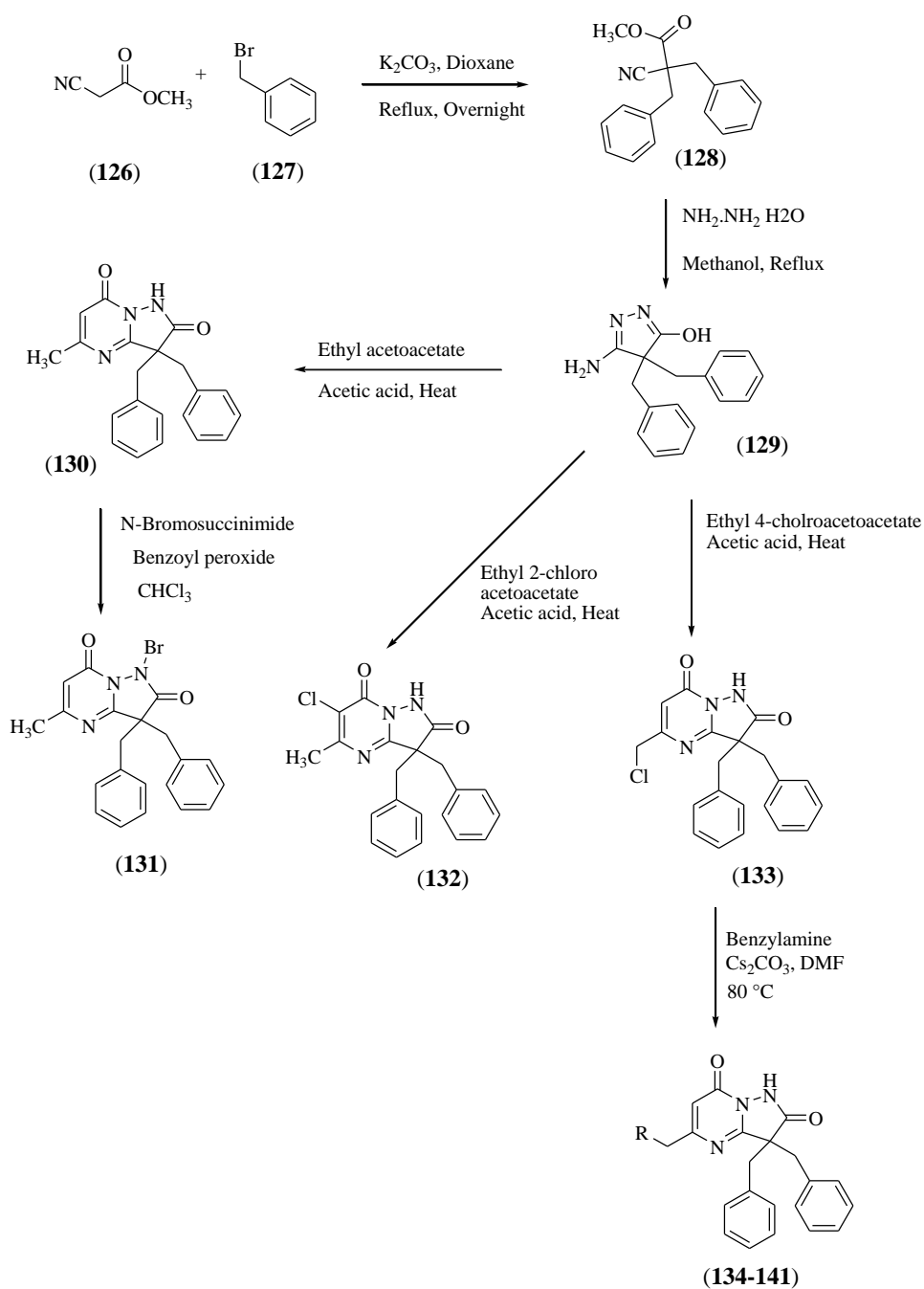
Scheme 2: Synthesis of disubstituted pyrazolo-pyrimidine derivatives (**Formula IIIb**)

4.4.2.1 Synthesis of methyl 2-benzyl-2-cyano-3-phenylpropanoate (128)

Substitution of methyl cyanoacetate (**126**) with benzyl bromide (**127**) in dioxane yielded compound (**128**). IR spectrum of compound (**128**) gave peaks at 2264 cm^{-1} for -CN, and C=O peak of ester was obtained at 1743 cm^{-1}.

4.4.2.2 Synthesis of 3-amino-4,4-dibenzyl-1*H*-pyrazol-5(4*H*)-one (129)

Methyl 2-benzyl-2-cyano-3-phenylpropanoate (**128**)

3-Amino-4,4-dibenzyl-1*H*-pyrazol-5(4*H*)-one (**129**)

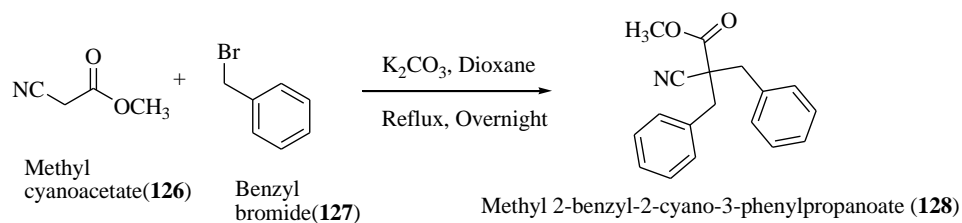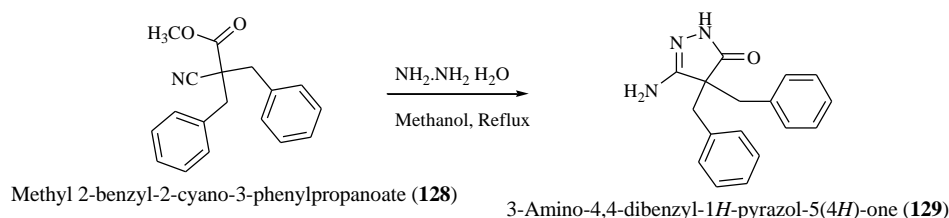Substitution of methyl-2-benzyl-2-cyano-3-phenylpropanoate (**129**) with hydrazine hydrate in methanol gave the product (**129**). IR spectrum of the compound (**129**) gave peak at 3434 cm^{-1} for -NH and 1632 cm^{-1} for -C=O. Its mass spectrum gave peak at m/z 280 [M+1]$^{+}$. The PMR spectrum showed singlet for one proton at δ 9.39 (s, 1H), ten aromatic protons appeared as multiplet at δ 7.20-7.14 (m, 10H). a singlet was observed at 6.183 (s, 1H). Four aliphatic -CH$_2$ protons appeared as dd at 3.07-2.90 (dd, 4H).

4.4.2.3 Synthesis of 3,3-dibenzyl-5-methylpyrazolo[1,5-*a*]pyrimidine-2,7(1*H*,3*H*)-dione (130)

3-Amino-4,4-dibenzyl-1*H*-pyrazol-5(4*H*)-one (**129**)

3,3-Dibenzyl-5-methylpyrazolo[1,5-*a*]pyrimidine-2,7(1*H*,3*H*)-dione (**130**)
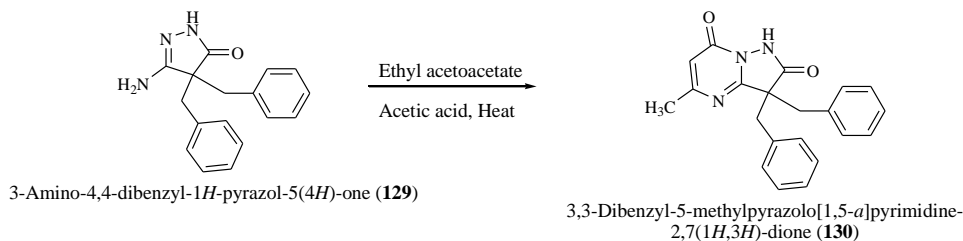
Substitution and subsequent cyclization of compound (**129**) with ethyl acetoacetate gave the desire compound (**130**). IR spectrum of compound (**130**) offered peaks at 1683 cm^{-1} for -C=O. Its mass spectrum gave peak at m/z 346 [M+1]$^{+}$ and 347 [M+2]. Its PMR offered peaks at δ 12.80 (s, 1H) for -NH protons. The aromatic protons appeared at δ 7.28-7.19 (m, 6H). Another peak for aromatic proton appeared at 7.04-7.02 (m, 4H). A singlet was observed at 6.15 (s, 1H). Four aliphatic -CH$_2$ protons appeared as multiplet at 3.3 (m, 4H, *merged with peak of* H$_2$O). Three methyl protons appeared at 2.41 (s, 3H). The ^{13}C NMR gave aromatic peaks at 170.31, 161.99, 151.68, 114.47, 129.21, 128.99, 128.14, 127.99, 127.08, 109.77, whereas the aliphatic peaks were obtained at 58.65, 41.51 and 21.24.

4.4.2.4   Synthesis   of   3,3-dibenzyl-1-bromo-5-methylpyrazolo[1,5-*a*]pyrimidine-2,7(1*H*,3*H*)-dione (131)

3,3-Dibenzyl-5-methylpyrazolo[1,5-*a*]pyrimidine-2,7(1*H*,3*H*)-dione (**130**)

3,3-Dibenzyl-1-bromo-5-methylpyrazolo[1,5-*a*]pyrimidine-2,7(1*H*,3*H*)-dione (**131**)
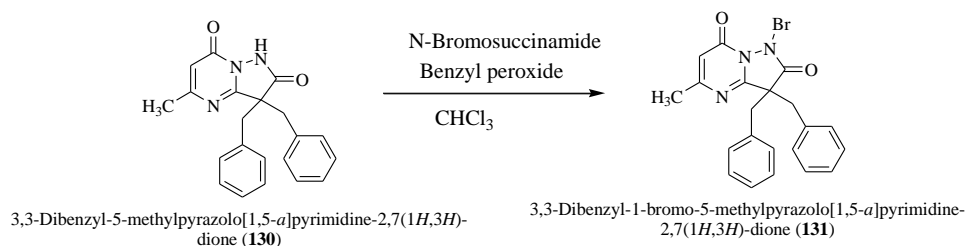
Bromination of (**130**) with *N*-bromo succinimide (NBS) yielded compound (**131**) The IR spectrum of compound (**131**) offered peaks at 1704 cm⁻¹ for -C=O. Its mass spectrum gave peak at m/z 424 [M]⁺ and 426 [M+2]⁺. Its PMR offered peaks at δ 12.99 (s, 1H). The aromatic protons appeared at δ 7.96-6.97 (m, 10H). A singlet was observed at 6.12 (s, 1H). Four aliphatic -CH₂ protons appeared as multiplet at 3.29 (m, 4H, *merged with peak of* H₂O). Three methyl protons appeared at 2.36 (s, 3H).

**4.4.2.5   Synthesis   of   3,3-dibenzyl-6-chloro-5-methylpyrazolo[1,5-*a*]pyrimidine-2,7(1*H*,3*H*)-dione (132)**

3-Amino-4,4-dibenzyl-1*H*-pyrazol-5(4*H*)-one (**129**)

3,3-Dibenzyl-6-chloro-5-methylpyrazolo[1,5-*a*]pyrimidine-2,7(1*H*,3*H*)-dione (**132**)
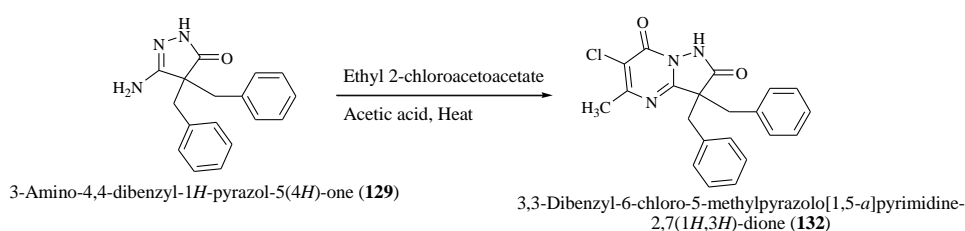
IR spectrum of the compound (**132**) gave peak at 1740 cm⁻¹ and 1689 cm⁻¹ for -C=O of ketone and amide respectively. Its mass spectrum gave peak at m/z 380 [M]⁺ and 382 [M+2]⁺. Its PMR spectrum offered peaks at δ 13.16 (s, 1H) for -NH/OH proton (disappeared in D₂O exchange). The aromatic protons appeared at 7.36-7.30 (m, 2H) and at 7.24-7.14 (m, 8H). The aliphatic -CH₂ protons appeared at 3.37-3.21 (m, 4H) and methyl protons were seen at 2.53 (s, 3H).

4.4.2.6 Synthesis of 3,3-dibenzyl-5-(chloromethyl)pyrazolo[1,5-*a*]pyrimidine-2,7(1*H*,3*H*)-dione (133)

3-Amino-4,4-dibenzyl-1*H*-pyrazol-5(4*H*)-one (**129**)

3,3-dibenzyl-5-(chloromethyl)pyrazolo[1,5-*a*]pyrimidine-2,7(1*H*,3*H*)-dione (**133**)
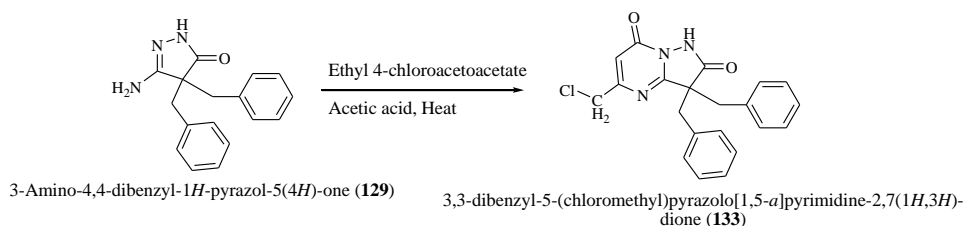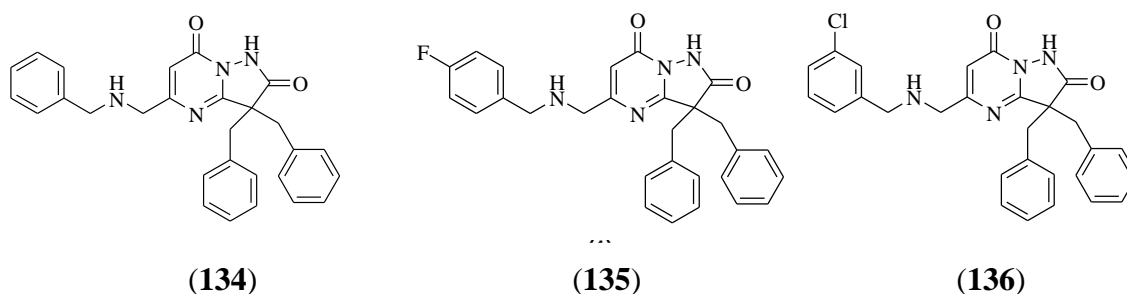
IR spectrum of the compound (**132**) gave peak at 1731 cm^{-1} and 1684 cm^{-1} for -C=O of ketone and amide respectively. Its mass spectrum gave peak at m/z 380 [M]$^+$. Its PMR offered peaks at δ 8.68 (s, 1H). The aromatic peaks were obtained at 7.43-7.30 (m, 4H) and 7.29-7.25 (m, 6H). Another peak was obtained at 6.38 (s, 1H). Aliphatic protons were obtained at 4.62 (s, 1H), 3.52-3.50 (dd, 2H) and 3.02-3.00 (dd, 2H).

4.4.2.7   Synthesis   of   5-((substitutedamino)methyl)-3,3-dibenzylpyrazolo[1,5-a]pyrimidine-2,7(1*H*,3*H*)-dione (134-141)

3,3-dibenzyl-5-(chloromethyl)pyrazolo[1,5-*a*]pyrimidine-2,7(1*H*,3*H*)-dione (**133**)

(**134-141**)
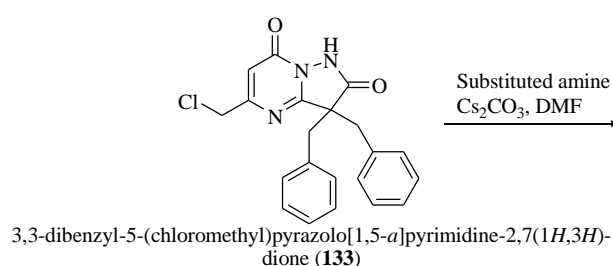
| Comp ID	R
134	4-H
135	4-F
136	3-Cl
138	(2-pyridylamino)
138	4-CH$_3$
139	3,4-*di*Cl
140	4-OCH$_3$
141	(morpholine)

Nucleophilic   substitution   of   3,3-dibenzyl-5-(chloromethyl)pyrazolo[1,5-*a*]pyrimidine-2,7(1*H*,3*H*)-dione (**133**) was performed with various benzyl amines in presence of anhydrous potassium carbonate in dry DMF to give the desired products (**134-141**).

(**134**)   (**135**)   (**136**)

IR spectrum of compound (**134**) gave peaks at 3439 cm^{-1} for -NH and 1639 cm^{-1} for -C=O. The mass spectrum gave peak at m/z 451 [M+1]$^+$. Its PMR spectrum offered peaks at 7.73-7.67 (m, 2H), 7.38-7.31 (m, 3H) and 7.05-7.01 (m, 11H), 5.86 (s, 1H). The aliphatic protons were observed at 4.17-4.11 (m, 2H), 3.80 (s, 1H, -NH), 3.70 (s, 1H), 3.57 (s, 1H), 3.14-3.11 (m, 2H) and 3.07-3.04 (m, 2H).

IR spectrum of compound (**135**) gave peaks at 1637 cm^{-1} for -C=O. The mass spectrum gave peak at m/z 471 [M+3]$^+$. Its PMR spectrum offered peaks for aromatic protons at 7.78 (m, 3H), 7.44-7.21 (m, 4H) and 7.04-6.99 (m, 8H). A singlet can be seen at 5.70 (s, 1H). The aliphatic -CH$_2$ protons appeared at 3.87 (s, 2H), 3.06-3.02 (dd, 4H), 2.21 (s, 2H).

IR spectrum of compound (**136**) gave peaks at 1614 cm⁻¹ for -C=O. The mass spectrum gave peak at m/z 482 [M-2]⁺. Its PMR spectrum offered peaks for aromatic protons at 8.68 (s, 1H), 7.43-7.30 (m, 4H), 7.29-7.18 (m, 10H). A singlet can be seen at 6.26 (s, 1H). The aliphatic -CH₂ protons appeared at 4.07 (s, 2H), 3.98 (s, 2H), 3.52-3.50 (dd, 2H), 3.10-3.00(dd, 2H), 2.459 (s, 2H).
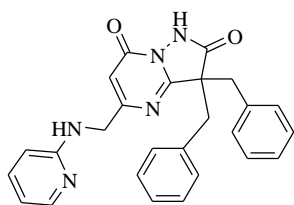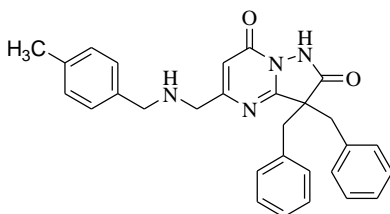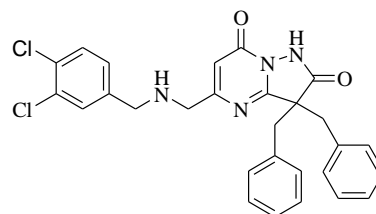
(137)   **(138)**   **(139)**

IR spectrum of compound (**137**) gave peaks at 1648 cm⁻¹ for -C=O. The mass spectrum gave peak at m/z 436.19 [M]⁺. Its PMR spectrum offered peaks for aromatic protons at 8.68 (s, 1H), 8.07-8.05 (m, 1H), 7.43-7.30 (m, 5H), 7.29-7.25 (m, 6H), 6.92-6.90 (m, 1H), 6.40 (dd, 1H), 6.31 (s, 1H), 6.24 (s, 1H). Aliphatic protons appeared at 4.69 (s, 2H), 3.52-3.50 (dd, 2H) and 3.02-3.00 (dd, 2H).

IR spectrum of compound (**138**) gave peaks at 1687 cm⁻¹ for -C=O. The mass spectrum gave peak at m/z 467.77 [M+3]⁺. Its PMR spectrum offered peaks for aromatic protons at 8.68 (s, 1H), 8.07-8.05 (m, 1H), 7.43-7.30 (m, 5H), 7.29-7.25 (m, 6H), 6.92-6.90 (m, 1H), 6.40 (dd, 1H), 6.31 (s, 1H), 6.24 (s, 1H). Aliphatic protons appeared at 4.69 (s, 2H), 3.52-3.50 (dd, 2H) and 3.02-3.00 (dd, 2H).

IR spectrum of compound (**139**) gave peaks at 1587 cm⁻¹ for -C=O. The mass spectrum gave peak at m/z 521.19 [M+2]⁺. Its PMR spectrum offered peaks for aromatic protons at 8.68 (s, 1H), 7.43-7.30 (m, 4H), 7.29-7.25 (m, 6H), 7.16-7.14 (s, 2H), 7.04-7.02 (d, 2H), 6.26 (s, 1H). Aliphatic protons appeared at 4.07 (s, 2H), 3.98 (s, 2H), 3.52-3.50 (dd, 2H) and 3.02-3.00 (dd, 2H). Methyl protons appeared at 2.38 (s, 3H).
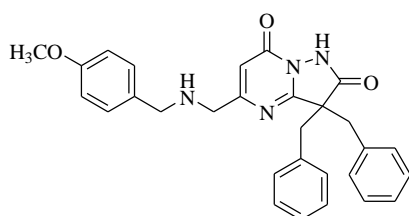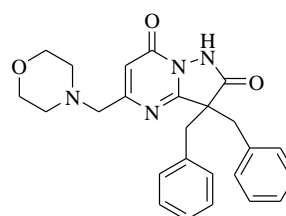
(140)   **(141)**

IR spectrum of compound (**140**) gave peaks at 3424 for -NH. The mass spectrum gave peak at m/z 481 [M+1]$^+$. Its PMR spectrum offered peaks at 7.71-7.69 (m, 2H), 7.37-7.31 (m, 2H) and 7.07-7.02 (m, 9H) and 6.96-6.93 (m, 2H). Another singlet can be seen at 6.02 (s, 1H). Aliphatic protons were observed at 4.14-4.13 (m, 3H). The methoxy protons appeared at 3.76 (s, 3H). The aliphatic protons were observed at 3.65 (s, 2H) and 3.19-3.10 (m, 4H).

IR spectrum of compound (**141**) gave peaks at 3432 for -NH and 1683 for -C=O. The mass spectrum gave peak at m/z 431 [M+1]$^+$. Its PMR spectrum gave peak at δ 8.65 (s, 1H). The aromatic protons appeared at 7.43-7.39 (m, 4H) and 7.30-7.25 (m, 6H). A singlet was observed at 6.30 (s, 1H). Aliphatic protons appeared at 3.77 (s, 2 H). Aliphatic protons of morpholino group appeared at 3.56-3.50 (m, 6H) and 3.02-3.00 (d, 2H). Benzylic -CH$_2$ protons appeared at 2.93-2.91 (m, 4H).

4.4.3 Synthesis of 3-benzyl-7-hydroxy-5-methylpyrazolo[1,5-*a*]pyrimidin-2(1*H*)-one based compounds (142-152)
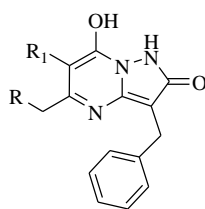
Formula III-c

The designed compounds with **Formula III-c** were synthesized by implementing scheme 3.

The work relate to the intermediates and the designed compounds has been explained under the main headings:

4.4.3.1 Synthesis of methyl-2-cyano-3-phenylpropanoate (**142**)

4.4.3.2 Synthesis of 5-amino-4-benzyl-1,2-dihydropyrazol-3-one (**143**)

4.4.3.3 Synthesis of 3-benzyl-5-methylpyrazolo[1,5-*a*]pyrimidine-2,7(1*H*,4*H*)-dione (**144**)

4.4.3.4 Synthesis of 3-benzyl-6-chloro-5-methylpyrazolo[1,5-*a*]pyrimidine-2,7(1*H*,4*H*)-dione (**145**)

4.4.3.5 Synthesis of 3-benzyl-5-(chloromethyl)pyrazolo[1,5-*a*]pyrimidine-2,7(1*H*,4*H*)-dione (**146**)

4.4.3.6 Synthesis of 5-((substituted)methyl)-3-benzylpyrazolo[1,5-*a*]pyrimidine-2,7(1*H*,4*H*)-dione (**147-152**)
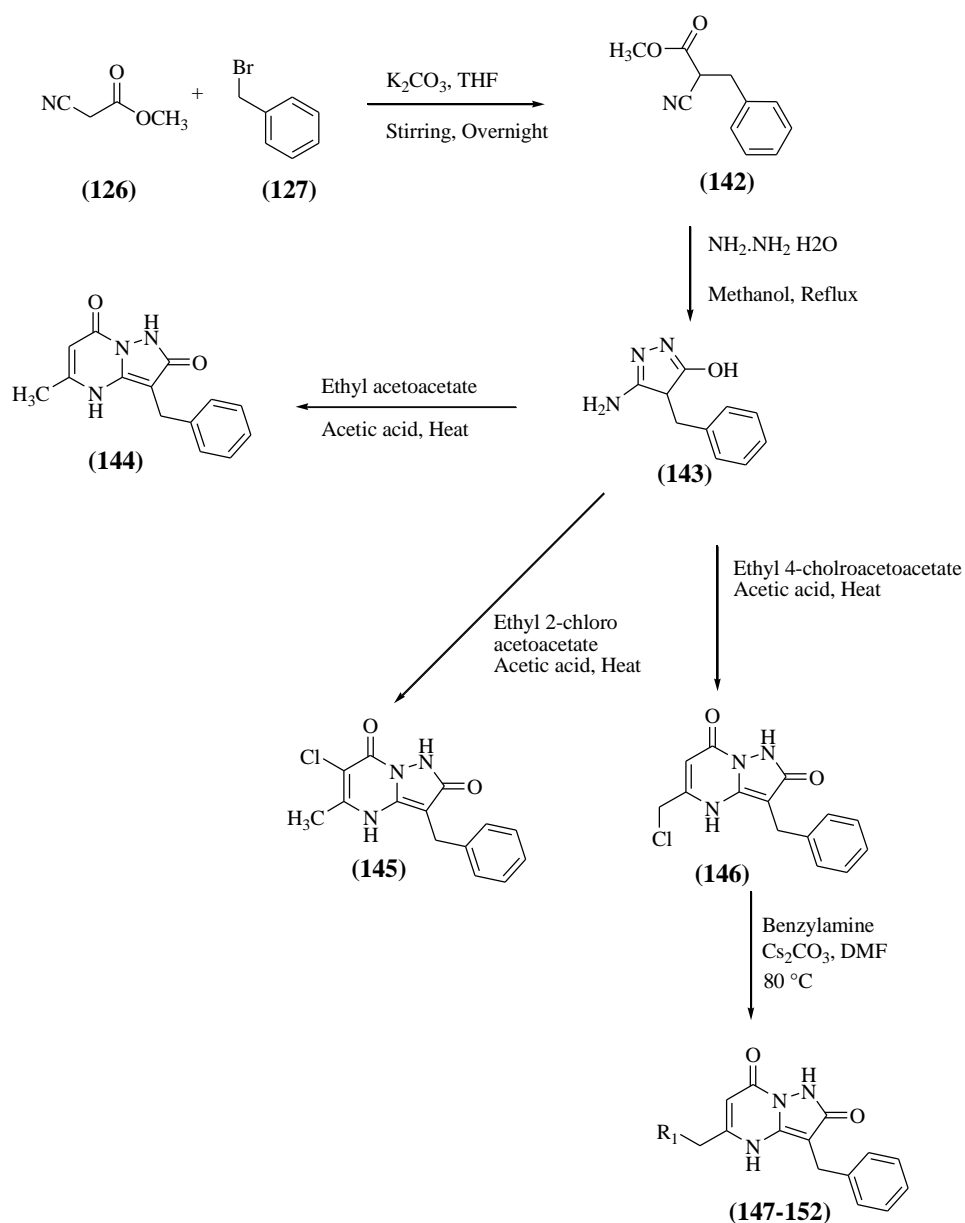
Scheme 3: Synthesis of 3-benzyl-7-hydroxy-5-methylpyrazolo[1,5-*a*]pyrimidin-2(1*H*)-one derivatives

4.4.3.1 Synthesis of methyl-2-cyano-3-phenylpropanoate (142)
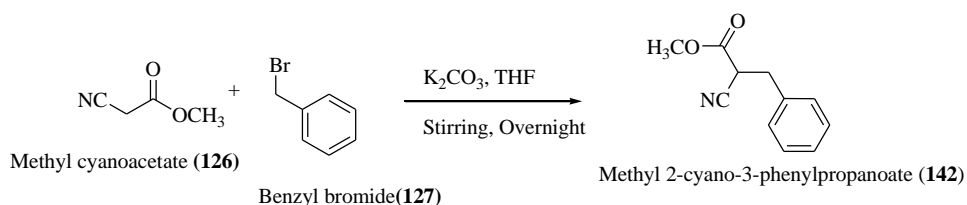
IR of the compound (**142**) gave peaks at 2252 cm^{-1} and 1748 cm^{-1} for -CN and -C=O respectively.

4.4.3.2 Synthesis of 5-amino-4-benzyl-1,2-dihydropyrazol-3-one (143)

Methyl 2-cyano-3-phenylpropanoate (**142**)

5-Amino-4-benzyl-4*H*-pyrazol-3-ol (**143**)
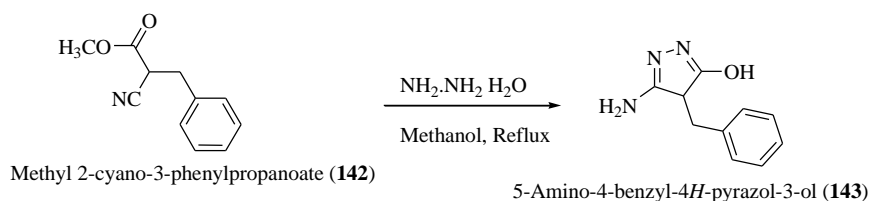
IR spectrum of the compound (**143**) gave peaks at 3169 cm^{-1} and 1676 cm^{-1} for -NH and -C=O respectively. Its PMR showed peaks at δ 11.36 (s, 1H), 9.56 (s, 1H) for -NH/OH protons. The aromatic protons were seen at 7.26-7.19 (m, 5H), 7.13 (m, 1H) whereas aliphatic protons were observed at 3.58 (s, 2H).

4.4.3.3   Synthesis   of   3-benzyl-5-methylpyrazolo[1,5-*a*]pyrimidine-2,7(1*H*,4*H*)-dione (144)

5-Amino-4-benzyl-4*H*-pyrazol-3-ol (**143**)

3-Benzyl-5-methylpyrazolo[1,5-*a*]pyrimidine
-2,7(1*H*,4*H*)-dione (**144**)
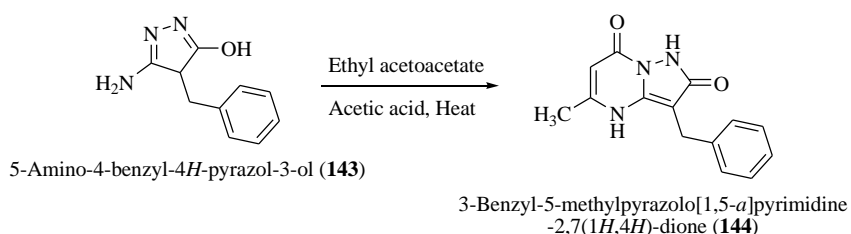
IR spectrum of the compound (**144**) depicted peaks at 3354 cm^{-1} and 1622 cm^{-1} for -NH and -C=O respectively. Its PMR spectrum offered peaks at 12.69 (s, 1H) and 9.53 (s, 1H) for -NH/-OH protons. The aromatic protons appeared at 7.29-7.20 (m, 5H) and 5.18 (s, 1H). The aliphatic protons appeared at 3.36 (s, 2H) and 2.10 (s, 3H). Its mass spectrum gave isotope peaks at m/z 256[M+1]$^+$ and 254 [M-2]$^+$.

4.4.3.4 Synthesis of 3-benzyl-6-chloro-5-methylpyrazolo[1,5-*a*]pyrimidine-2,7(1*H*,4*H*)-dione (145)

5-Amino-4-benzyl-4*H*-pyrazol-3-ol (**143**)

3-Benzyl-6-chloro-5-methylpyrazolo[1,5-*a*]
pyrimidine-2,7(1*H*,4*H*)-dione (**145**)
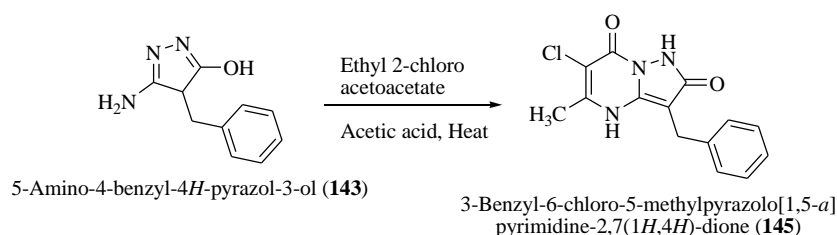
IR spectrum of the compound (**145**) gave peaks at 3234 cm^{-1} and 1640 cm^{-1} for -NH and -C=O respectively. Its PMR offered peaks at 13.30 (s, 1H) and 7.91 (s, 1H) for NH/OH protons. The aromatic protons appeared at 7.29-7.20 (m, 5H). The aliphatic protons appeared at 3.75 (s, 2H) and 2.37 (s, 3H).

4.4.3.5 Synthesis of 3-benzyl-5-(chloromethyl)pyrazolo[1,5-*a*]pyrimidine-2,7(1*H*,4*H*)-dione (146)

5-Amino-4-benzyl-4*H*-pyrazol-3-ol (**143**)   3-Benzyl-5-(chloromethyl)pyrazolo[1,5-*a*] pyrimidine-2,7(1*H*,4*H*)-dione (**146**)
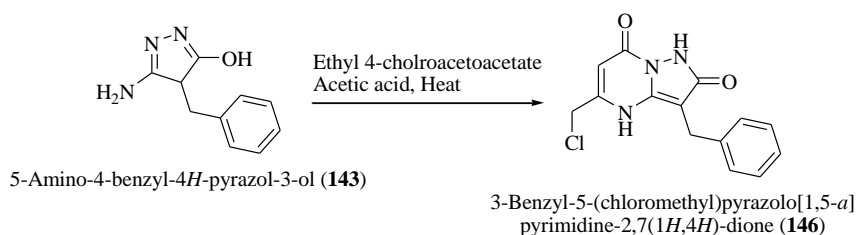
IR spectrum of the compound (**146**) gave peaks at 3224 cm^{-1} and 1619 cm^{-1} for -NH and -C=O respectively. Its PMR offered peaks at 13.30 (s, 1H) and 8.57 (s, 1H) for NH/OH protons. The aromatic protons appeared at 7.29-7.20 (m, 5H) and 6.12 (s, 1H). The aliphatic protons aprearred at 4.63 (s, 2H) and 3.75 (s, 2H). Its mass spectrum gave molecular ion peak at 288 [M-1]$^{+}$.

4.4.3.6 Synthesis of 5-((substituted)methyl)-3-benzylpyrazolo[1,5-*a*]pyrimidine-2,7(1*H*,4*H*)-dione (147-151)

3-Benzyl-5-(chloromethyl)pyrazolo[1,5-*a*] pyrimidine-2,7(1*H*,4*H*)-dione (**146**)

(147-152)

Comp ID	R
147	4-H
148	4-F
149	4-Cl
150	3,4-*di*Cl
151	(pyridin-2-yl)
152	4-CH$_3$
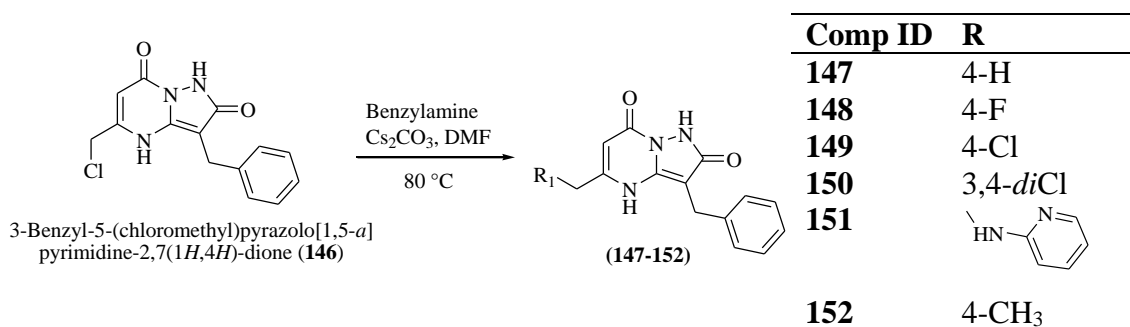
Nucleophilic substitution of 3-benzyl-5-(chloromethyl)pyrazolo[1,5-*a*]pyrimidine-2,7(1*H*,4*H*)-dione (**146**) was performed with various benzyl amines in presence of anhydrous potassium carbonate in dry DMF to give the desired products (**147-152**)

(**147**)   (**148**)   (**149**)
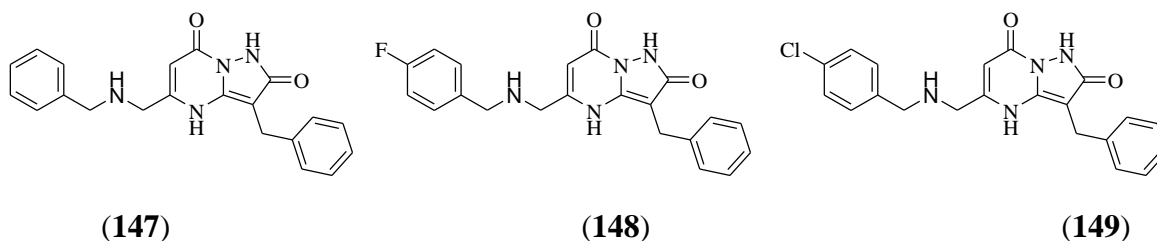
IR spectrum of the compound (**147**) gave peak at 1685 cm^{-1} for C=O. Its PMR offered peaks at δ 9.53 (s, 1H, -OH). The aromatic peaks were obtained at 7.35-7.20 (m, 10H). A singlet was observed at 5.48 (s, 1H). The aliphatic peaks were observed at δ 3.98 (s, 2H), 3.68 (s, 2H), 3.53 (s, 1H), and 3.36 (s, 2H).

IR spectrum of the compound (**148**) gave peak at 1690 cm^{-1} for C=O. Its PMR offered peaks at δ 9.65 (s, 1H, -OH). The aromatic peaks were obtained at 7.41-7.32 (m, 9H). A singlet was observed at 5.60 (s, 1H). The aliphatic peaks were observed at δ 4.15 (s, 2H), 3.80 (s, 2H), 3.65 (s, 1H), and 3.48 (s, 2H).

IR spectrum of the compound (**149**) gave peak at 1655 cm^{-1} for C=O. Its PMR offered peaks at δ 9.53 (s, 1H, -OH). The aromatic peaks were obtained at 7.29-7.20 (m, 9H). A singlet was observed at 5.48 (s, 1H). The aliphatic peaks were observed at δ 4.03 (s, 2H), 3.68 (s, 2H), 3.53 (s, 1H), and 3.36 (s, 2H). Its mass spectrum gave isotope peak at 397 [M+2]$^{+}$.
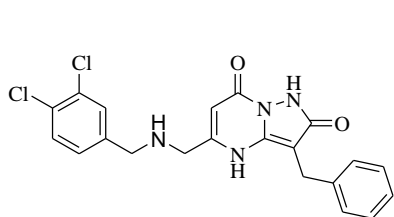
(**150**)   (**151**)   (**152**)

IR spectrum of the compound (**150**) gave peak at 1679 cm^{-1} for C=O. Its PMR offered peaks at δ 9.53 (s, 1H, -OH). The aromatic peaks were obtained at 7.36-7.34 (m, 2H) and 7.29-7.15 (m, 6H). A singlet was observed at 5.48 (s, 1H). The aliphatic peaks were observed at δ 4.08 (s, 2H), 3.78 (s, 1H), 3.68 (s, 2H), 3.36 (s, 2H). Its mass spectrum gave [M-2]$^{+}$ at 427.

IR spectrum of the compound (**151**) gave peak at 1689 cm^{-1} for C=O. Its PMR offered peaks at δ 9.53 (s, 1H, -OH). The aromatic peaks were obtained at δ 8.07-8.05 (d, 2H), 7.29-7.20 (m, 5H). A singlet was observed at 6.73 (s, 1H). Further a doublet was obtained at δ 6.45-6.43 (d, 2H). A singlet appeared at 5.53 (s, 1H). The aliphatic peaks were observed at δ 4.26 (s, 2H), 3.36 (s, 2H).

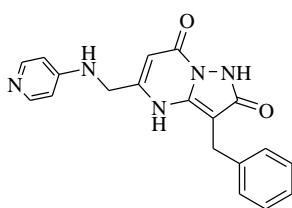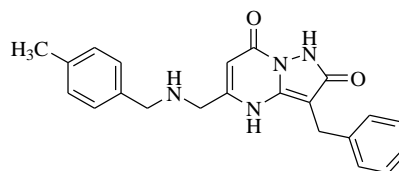IR spectrum of the compound (**152**) gave peak at 1686 cm^{-1} for C=O. Its PMR offered peaks at δ 13.30 (s, 1H, -OH). The aromatic peaks were obtained at 7.29-7.14 (m, 8H) and 7.04-7.02 (m, 2H). A singlet was observed at 6.00 (s, 1H). The aliphatic peaks were observed at δ 4.07 (s, 2H), 3.99 (s, 2H), 3.75 (s, 2H), and 2.38 (s, 3H). Its mass spectrum gave molecular ion peak at 374 [M]$^{+}$.

4.5 Biological screening

4.5.1 Biological screening of synthesized compounds as anti-TB agents using MABA assay

The prepared compounds were evaluated for their percentage inhibition against *Mycobacterium bovis* (BCG). Results are shown in **Table 4.6** and **Figure 4.8**. Overall, seven compounds (**109, 118, 130, 132, 144, 145 and 146**) out of 38 compounds exhibited inhibition of the bacteria. It was found that compound **118** and **132** was exhibiting 90.87% inhibition, comparable to that of standard drugs. Compounds **130, 144, 145,** and **109** having chlorine in the 6th and 5th position respectively are showing inhibition, thus it can be agreed that presence of chlorine atom is favorable for inhibitory activity.

Table 4.6: Anti-tubercular activity of the synthesized compounds

Comp ID	% Inhibition	Comp ID	% Inhibition	Comp ID	% Inhibition
108	NI	122	NI	140	NI
109	55.1	123	NI	141	NI
110	3	124	NI	144	55.1
111	NI	125	NI	145	60.21
112	NI	130	80.1	146	42
113	NI	131	NI	147	NI
114	NI	132	90.87	148	NI
115	NI	133	NI	149	NI
116	NI	134	NI	150	NI
117	NI	135	NI	151	NI
118	90.87	136	NI	152	NI
119	NI	137	NI	Isoniazid	93.46
120	NI	138	NI	Rifampicin	96.09
121	NI	139	NI	Blank	0.06

NI: No inhibition at 10µg/mL.

Inspired from the results of the primary screening, compound (**118**) was taken up for further studies and it was found that compound (**118**) was exhibiting an MIC value of ≤1.5µg/ml.
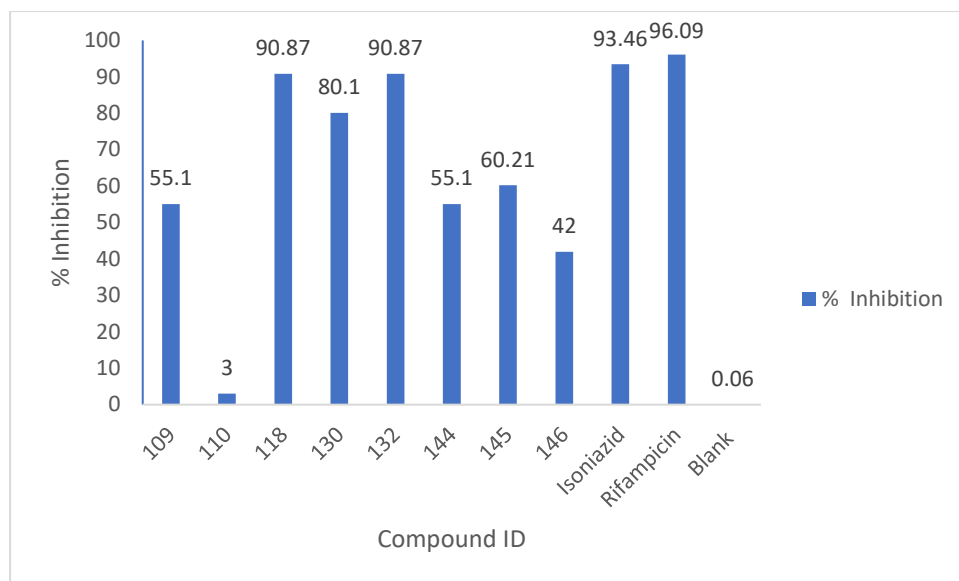
Figure 4.8: Percentage inhibition of *Mycobacterium bovis* (BCG) by the synthesized compounds using MABA assay.

4.5.2 Cell viability assay

As compound (**118**) was found to be significantly active, its safety aspect was assessed by performing cell viability assay using human lung adenocarcinoma cell line A549. This cell viability assay was based on resazurin dye. Results indicated that the compound (**118**) does not show any significant reduction in cell viability at 1.5 µg/ml and 3.125 µg/ml at any point of time. However significant reduction in cell viability was observed at the concentration of 6.25 µg/ml after 6th day of treatment. The results are demonstrated in **Figure 4.9**.

4.6 Molecular docking, ADMET studies and simulation studies of the synthesized compounds

Computational studies such as molecular docking, ADME predictions, molecular simulations provide an insight to the behaviour of the molecule with the enzyme within the body. These studies also help in deducing the mode of the action as well as figuring out the pharmacokinetics of the compounds.
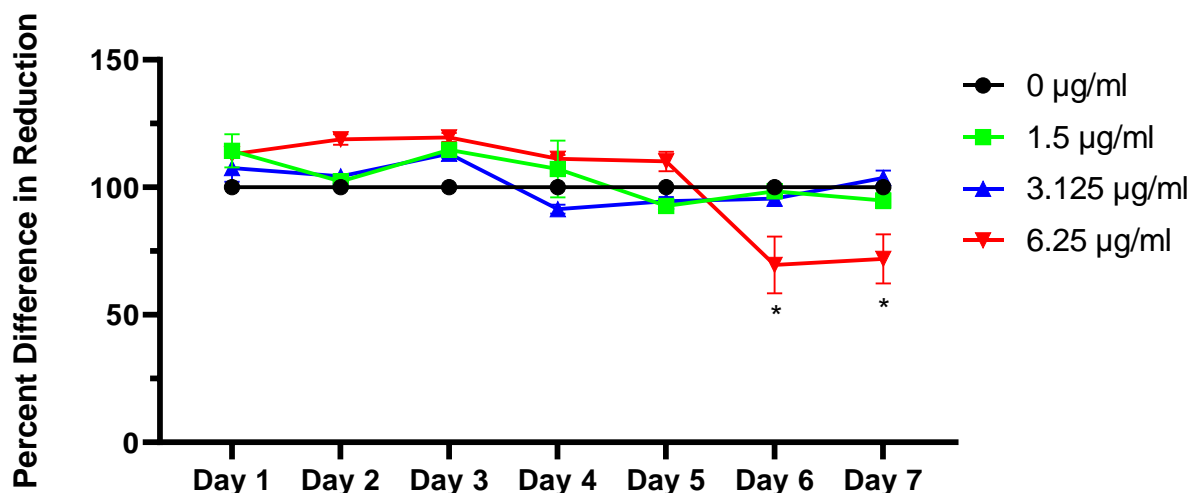
Figure 4.9: Impact of compound (**118**) concentrations -1.5µg/ml, 3.125µg/ml and 6.25 µg/ml on cell viability in A549 cell line. Percent difference in reduction of Resazurin in A549 cells upon treatment with compound at 1.5µg/ml, 3.125µg/ml and 6.25 µg/ml final concentration. The graph represents percent reduction in resazurin compared to untreated positive control at each day. Each concentration was evaluated in triplicates and Error bars depict the standard error of the mean. T-test was used to calculate statistical significance. $*p \leq 0.05$, n=3

4.6.1 Molecular docking study

Molecular docking helps in understanding the interactions of the designed molecule with the target enzyme. So, to understand the interactions and corelation to the biological activity, molecular docking studies were performed for the synthesized compounds using PDB ID: 4P8N with co crystal structure QN118. Upon studying the results (**Table 4.7**), it was noted that the compounds exhibit some critical interactions with the active site of the molecule. The binding affinity of the compounds is given in **Table 4.7**.

The docking results of compound (**110**) into the active site of enzyme indicated types of interactions. The binding affinity of the compound was found to be -7.8 Kcal/mol which was found to quite less than the standard compound. Interaction studies revealed that the compound was majorly binding to the enzyme via Pi-alkyl interaction between the aromatic/heterocycle of the compound with various amino acids such as Tryptophan, proline, arginine, cysteine etc. Further the compound was forming conventional hydrogen bonding with amino acid residue TYR A:415 and Pi-sigma with ILE A:131 (**Figure 4.10**).

Table 4.7: The binding affinity of the synthesized compounds

Comp ID	Binding affinity (Kcal/ mol)	Comp ID	Binding affinity (Kcal/ mol)	Comp ID	Binding affinity (Kcal/ mol)
108	-8.4	**121**	-8.9	**138**	-7.9
109	-8.1	**122**	-8.5	**139**	-8.3
110	-7.8	**123**	-8.7	**140**	-8.2
111	-9.0	**124**	-8.8	**141**	-8.6
112	-9.6	**125**	-9.2	**144**	-8.9
113	-9.3	**130**	-8.9	**145**	-8.6
114	-9.7	**131**	-7.9	**146**	-8.5
115	-8.9	**132**	-8.1	**147**	-7.8
116	-9.1	**133**	-8.2	**148**	-8.3
117	-9.2	**134**	-7.9	**149**	-8.2
118	-9.5	**135**	-8.4	**150**	-8.6
119	-9.3	**136**	-7.8	**151**	-7.8
120	-9.2	**137**	-8.2	**152**	-7.9
QN118 **(Standard)**	-9.5				
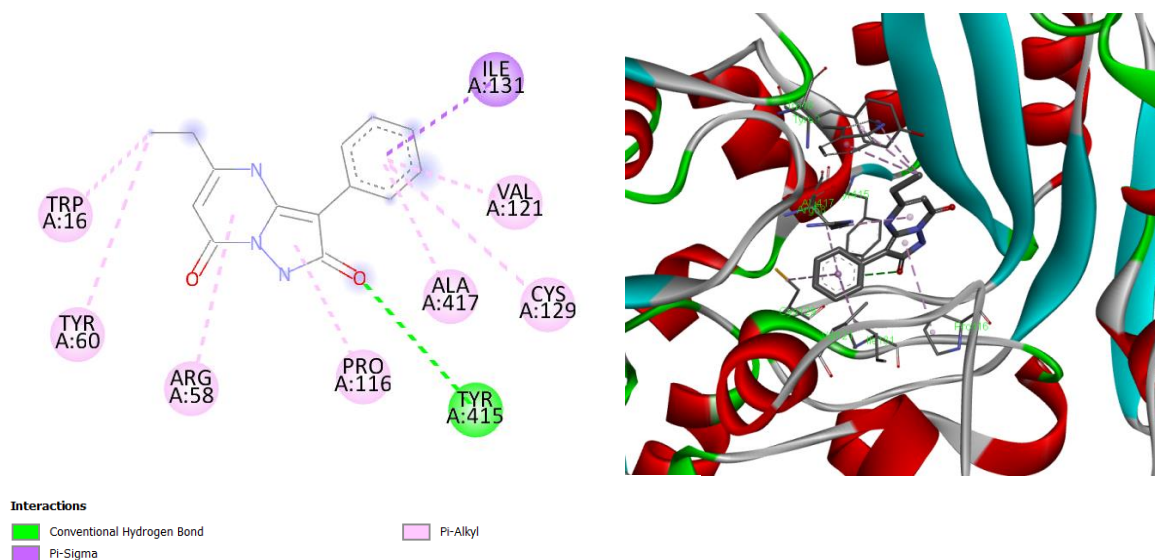
Figure 4.10: The 2D and 3D interaction of the compound (**110**)

Further, it was found that the compound (**114**) was found to be interacting via conventional hydrogen bonding with CYS 387. The compound is also seen to form alkyl and pi-alkyl interactions with LYS 134, LEU 363 and TRP 230 amino acid residues (**Figure 4.11**).
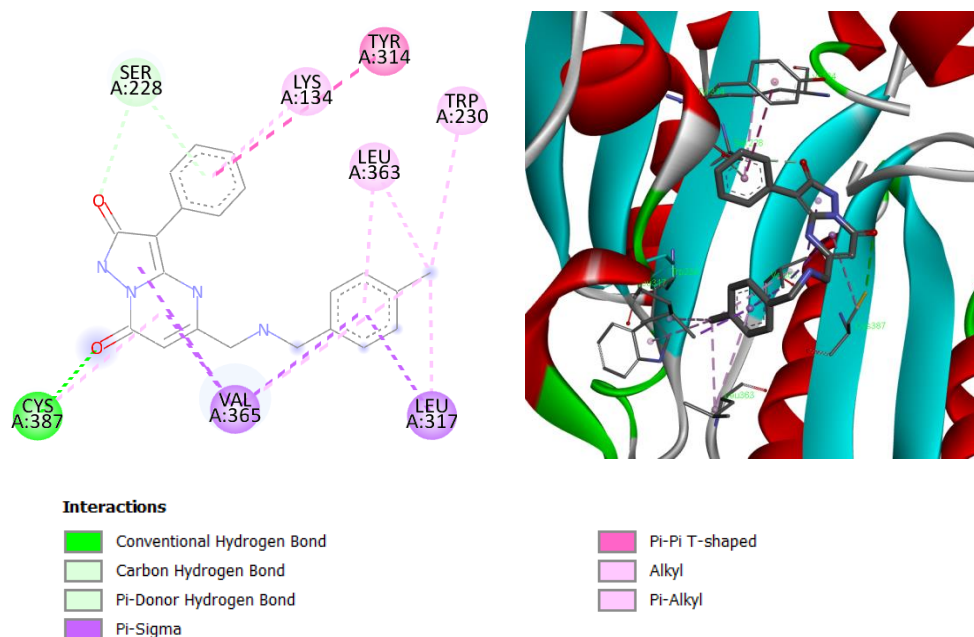
Figure 4.11: The 2D and 3D interactions of the compound (**114**)

The docking studies of standard QN118 compound depicted one conventional H-bonding with ASN 385, two halogen bonding (fluorine) interaction with ARG 58 and ALA 417, a Pi-Donor hydrogen bond with GLY 117, a Pi cation with LYS 418, two C-H bonding with SER 228 and SER 59, four alkyl interaction with VAL 365, LYS 367, ARG 58 and five alkyl interaction with VAL 365, PRO 116, VAL 121, ILE 131 and ALA 417 (**Figure 4.12**).
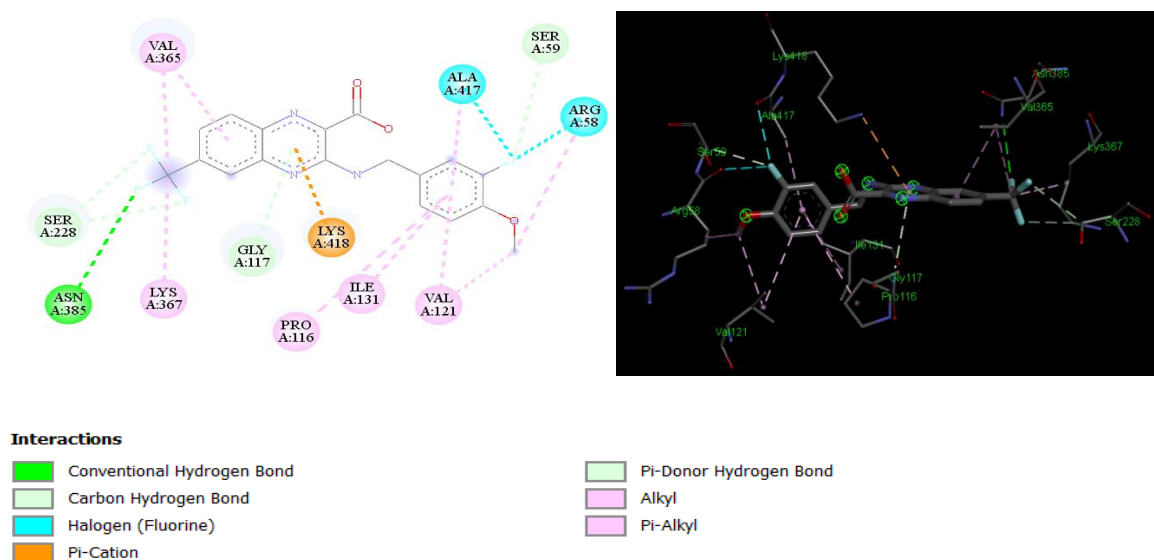
Figure 4.12: The 2D and 3D interactions of standard QN118

4.6.2 Pharmacokinetics prediction

To evaluate the requirements of the drug-likeliness, the properties of the synthesized compounds were evaluated for their *in-silico* parameters by using SWISSADME.

To evaluate the drug-likeness and lead like properties of the designed compounds, their ADMET properties were predicted which certainly plays important role to push forward any drug candidate into the drug pipeline. The ADMET prediction results indicated that these pyrazolo-pyrimidine derivatives have the favourable physicochemical properties and all the compound follow Lipinski's rule of five. the results are shown in **Table 4.8**.

Table 4.8: Predicted pharmacokinetic parameters of the compounds

| Comp No.	MW	HBA	HBD	TPSA	iLogp	Clogp	Log S	GIA	BBB	CYP	LP
108	320.14	2	1	59.27	2.38	2.33	-3.70	High	Yes	Yes; 1	Yes
109	275.69	2	2	70.13	2.00	2.41	-3.35	High	Yes	Yes; 1	Yes
110	275.69	2	2	70.13	1.86	2.06	-2.76	High	Yes	Yes; 1	Yes
111	346.38	3	3	82.16	2.74	2.60	-3.32	High	No	No	Yes
112	364.37	4	3	82.16	2.82	2.90	-3.47	High	No	No	Yes
113	380.83	3	3	82.16	2.92	3.11	-3.90	High	No	Yes	Yes
114	360.41	3	3	82.16	2.89	2.91	-3.61	High	No	No	Yes
115	415.27	3	3	82.16	2.84	3.58	-4.49	High	No	No	Yes
116	376.41	4	3	91.36	2.91	2.58	-3.38	High	No	No	Yes
117	332.36	2	3	82.16	2.46	2.65	-3.71	High	No	No	Yes
118	350.35	3	3	82.16	2.59	2.97	-3.86	High	No	No	Yes
119	366.80	2	3	82.16	2.75	3.19	-4.29	High	No	No	Yes
120	362.38	3	3	91.39	2.74	2.65	-3.76	High	No	No	Yes
121	333.34	3	3	95.05	2.00	1.91	-3.04	High	No	No	Yes
122	310.35	3	2	73.37	2.55	2.01	-2.77	High	No	No	Yes
123	325.37	4	3	85.40	2.36	1.12	-2.12	High	No	No	Yes
124	326.35	4	2	82.60	2.54	1.44	-2.31	High	No	No	Yes
125	339.39	4	2	76.61	2.80	1.40	-2.49	High	No	No	Yes
130	345	3	1	63.99	2.77	2.95	-4.13	HIGH	YES	C19, C9	Yes
131	424	3	0	55.20	3.33	3.52	-5.21	High	YES	C9 C19	Yes
132	379	3	1	63.99	2.93	3.50	-4.89	High	YES	3A4	Yes

	MW	HBA	HBD	TPSA	iLOGP	ClogP	Log S	GIA	BBB	CYP	LP
133	379	3	1	63.99	2.76	3.15	-4.27	High	YES	C19 C9	Yes
134	450	4	2	76.02	3.28	3.58	-4.87	High	YES	C	Yes
135	468	5	2	76.02	3.61	3.94	-5.0	High	YES	All	Yes
136	484	4	2	76.02	3.53	4.11	-5.43	high	yes	all	Yes
137	437	4	2	88.91	2.84	2.96	-4.56	High	NO	All	Yes
138	464	4	2	76.02	3.32	3.87	-5.14	high	yes	4	Yes
139	519	4	2	76.02	3.91	4.66	-6.03	High	YES	C19 C9	No
140	480	5	2	85.25	3.87	3.64	-4.91	High	NO	All	Yes
141	430	5	1	76.46	2.92	2.40	-3.86	High	NO	All	Yes
144	255	2	2	70.13	1.94	1.95	-2.8	High	No	1A2	Yes
145	289	2	2	70.13	2.06	2.51	-3.5	High	Yes	1A2	Yes
146	289	2	2	70.13	1.93	2.16	-2.9	High	Yes	1A2	Yes
147	360	3	3	82.16	2.35	2.60	-3.5	High	No	C19	Yes
148	378	4	3	82.16	2.69	2.96	-3.6	High	No	no	Yes
149	394	3	3	82.16	2.920	3.20	-4.0	High	No	3A4	Yes
150	429	3	3	82.16	3.06	3.71	-4.6	High	No	3A4	Yes
151	347	3	3	95.05	2.11	2.02	-3.2	High	No	No	Yes
152	374	3	3	82.16	2.73	2.96	-3.8	High	No	No	Yes

MW: Molecular weight (g/mol); HBA: H-bond acceptors; HBD: H-bond donors; TPSA: Topological polar surface area; iLOGP; Lipophilicity (Log $P_{o/w}$); ClogP Lipophilicity (Consensus Log $P_{o/w}$); Log S: Water solubility (ESOL); GIA: Gastrointestinal absorption; BBB: Blood-brain-barrier permeation; CYP: Cytochrome P450 enzyme inhibition; LP: Lipinski rule compliance

Table 4.9: Toxicity prediction of compounds (**108-152**)

Comp ID	Prediction by Dereck	Prediction by Sarah	Comp ID	Prediction by Dereck	Prediction by Sarah
108	Inactive	Negative	**132**	Inactive	Out of domain
109	Inactive	Negative	**133**	**Plausible**	Out of domain
110	**Plausible**	**Positive**	**134**	Inactive	Out of domain
111	Inactive	Negative	**135**	Inactive	Out of domain
112	Inactive	**Equivocal**	**136**	Inactive	Out of domain
113	Inactive	Negative	**137**	Inactive	Out of domain
114	Inactive	Negative	**138**	Inactive	Out of domain
115	Inactive	Negative	**139**	Inactive	Out of domain

116	Inactive	Negative	140	Inactive	Out of domain
117	Inactive	**Equivocal**	141	Inactive	Out of domain
118	Inactive	**Positive**	144	Inactive	Negative
119	Inactive	Negative	145	Inactive	Negative
120	Inactive	**Positive**	146	**Plausible**	**Positive**
121	Inactive	**Equivocal**	147	Inactive	Negative
122	Inactive	Negative	148	Inactive	Negative
123	Inactive	Negative	149	Inactive	Negative
124	Inactive	Negative	150	Inactive	Negative
125	Inactive	Negative	151	Inactive	Negative
130	Inactive	Out of domain	152	Inactive	Negative
131	Inactive	Out of domain			

Genotoxic profile of the compounds was predicted by Nexus software[11] which helps in determining if any particular motif of the compound structure is causing mutagenicity and the results are shown in **Table 4.9**. The Derek results indicating "Inactive" implies that the compounds are predicted to be non-mutagenic. Plausible results indicate that there is a possibility of compounds being mutagenic and the weight of evidence supports the proposition.

Sarah results indicating "positive" implies the compound is predicted to be positive in a bacterial reverse mutation assay (Ames test). Whereas, negative results indicate that the compounds are predicted to be negative in a bacterial reverse mutation assay (Ames test). Equivocal results imply that a strong argument cannot be made based on the training set for either activity or inactivity in Ames test. Out of domain results indicate that the prediction is not possible because at least one atom present in a fragment of the compounds is not represented in the training set used to build the model.

It is noteworthy that compounds having chlorine atom (**110** and **146**) are predicted to be mutagenic.

4.6.3 Molecular simulations studies of compound (118)

The molecular simulation studies of compound (**118**) show the stability of complex in a time period of 1ns. For the simulation studies different parameters of molecular dynamics has been taken into consideration which includes the RMSD analysis, RMSF analysis and radius

of gyration (R_g). From the RMSD analysis it was observed that the complex attains stability for a very short span of time and the RMSD keep on fluctuating during the given time period window. The deviation occurs in between RMSD 3.0- 4.2 nm for a time period 0.84ns. In last 0.2ns the deviation of complex occurs in between 2.0-3.0 nm.
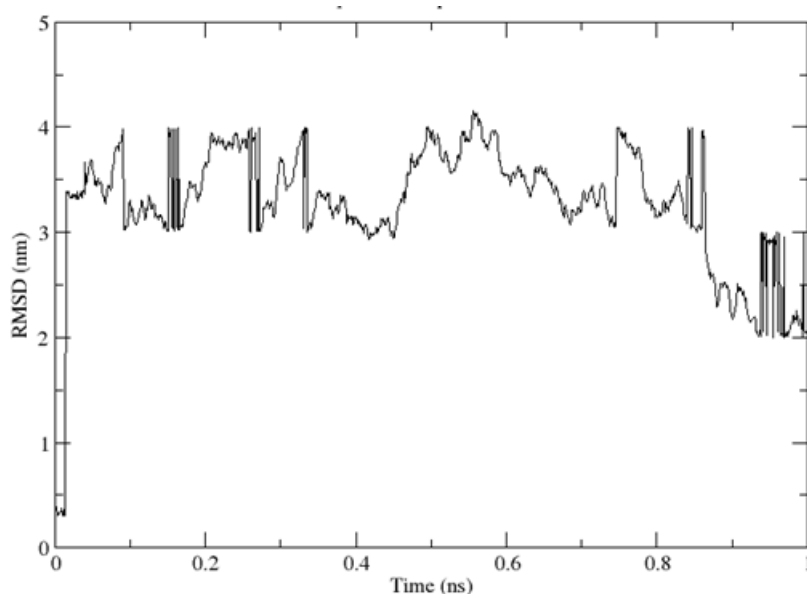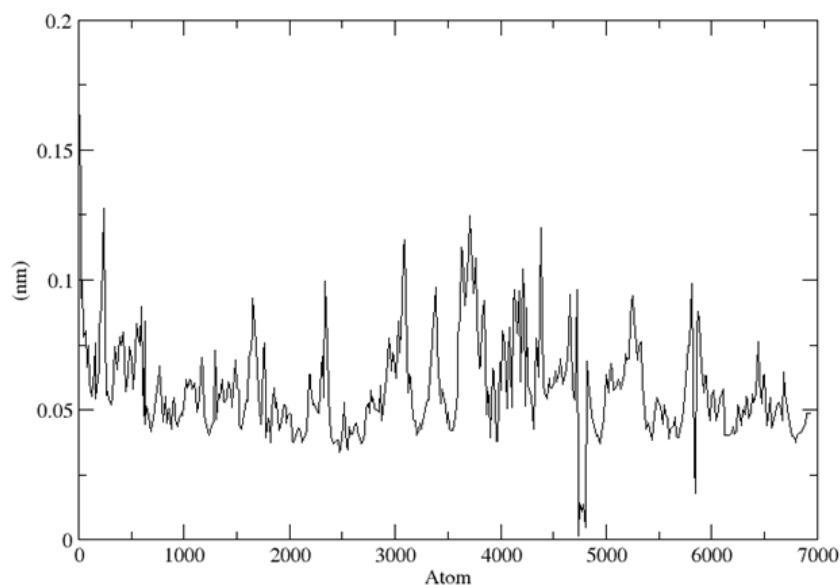

Figure 4.13: RMSD of complex (**118**)

Figure 4.14: RMS of complex (**118**)

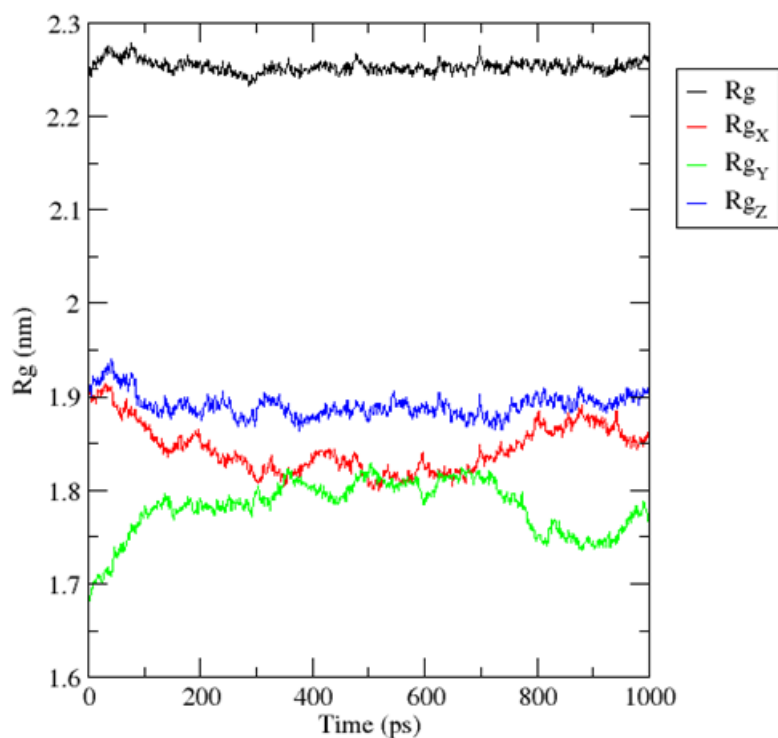**c)Radius of gyration (total and around axes)**

Figure 4.15: Radius of gyration of complex (**118)**

Additionally, the RMSF studies revealed that the atoms in the complex shows steep fluctuations in the given time period with a low stability profile. The atoms show stability within the plot but only for short intervals. The Root mean square fluctuations observed in between 0.038-0.132 nm. The radius of gyration studies determined for this complex indicates towards the instability and shows no significant deviations between 100-1000ps and the R_g remains in the range 0.25-0.27nm (**Figures 4.13-4.15**).

SECTION II

The compounds designed by implementing the hybrid approach of fusing pyrazolone and chalcones are described here. The work done here is illustrated under the heading of

4.7 Synthesis of the designed compounds (**211-249** and **250-261**)

4.8 Biological screening of synthesized compounds as anti-TB agents by MABA assay

4.9 Molecular docking, ADMET studies of the synthesized compounds

4.7 Synthesis of the designed compounds (**211-249** and **250-261**)

The synthesis of compounds designed by condensing pyrazolone derivatives with substituted chalcones were performed under the following headings:

4.7.1 Synthesis of 3-(3-oxo-1,3-diphenylpropylamino)-4,4-dibenzyl-1*H*-pyrazol-5(4*H*)-one derivatives (**211-249**)

4.7.2 Synthesis of 3,3-dibenzyl-3,3a-dihydro-5,7-diphenylpyrazolo[1,5-*a*]pyrimidin-2(1*H*)-one derivatives (**250-261**)

The intermediates used of for synthesis of desired compounds (**211-249**) and (**250-261**) are same. But the synthesis procedure of final compounds is different and the products obtained are different. Both these synthesises are based on Michael-aza addition reaction.

4.7.1 Synthesis of 3-(3-oxo-1,3-diphenylpropylamino)-4,4-dibenzyl-1*H*-pyrazol-5(4*H*)-one derivatives (211-249)

To prepare substituted chalcone derivatives (**174-207**), commercially available substituted benzaldehydes were reacted with substituted acetophenones in presence of a strong base. These substituted chalcones (**174-207**) were fused with 3-amino-4,4-dibenzyl-1*H*-pyrazol-5(4*H*)-one (**129**) in presence of weak base such as anhydrous potassium carbonate in DMF to yield the desired compounds (**211-249**). The reaction proceeds via Michael-aza addition of NH$_2$ of the pyrazolone on the double bond of the chalcone to offer final compounds (**211-249**).

The intermediates (**174-207**) and targeted final (**211-249**) compounds has been discussed under the following headings:

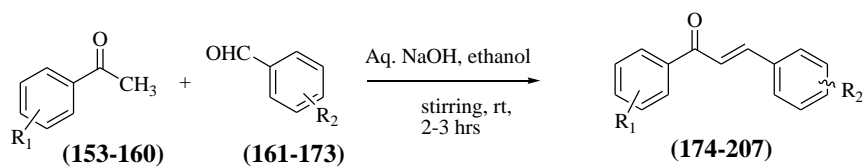4.7.1.1 Synthesis of substituted chalcones (**174-207**)

4.7.1.2 Synthesis of 3-amino-4,4-dibenzyl-1*H*-pyrazol-5(4*H*)-one **(129)** and 3-amino-4,4-*bis*(4-methylbenzyl)-1*H*-pyrazol-5(4*H*)-one (**210**)

4.7.1.3 Synthesis of 3-(3-oxo-1,3-diphenylpropylamino)-4,4-dibenzyl-1*H*-pyrazol-5(4*H*)-one derivatives **(211-249)**

**4.7.1.1 Synthesis of substituted chalcones (174-207)**

Various substituted benzaldehydes were condensed with a variety of acetophenones in ethanolic KOH solution to yield desired substituted chalcones. The reaction proceeds via Claisen-Schmidt condensation. The chalcone intermediates were synthesized by using **Scheme 4**. IR spectra of the chalcones **(174-207)** showed characteristic peaks for -C=O in the range of 1689-1650 cm^{-1} (**Table 4.10**).

The pyrazolone derivatives were synthesized by using scheme 2 mentioned in section 4.4.2.1 and 4.4.2.2

Scheme 4: Synthesis of chalcone derivatives

**Table 4.10**: Spectral data of substituted chalcones **(174-207)**

(174-207)
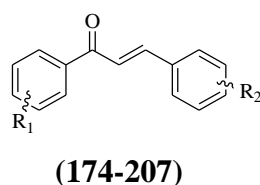
Comp.	R$_1$	R$_2$	IR peaks (cm^{-1})
174	H	H	3051, 1661, 1604, 1445, 1209, 991, 749
175	H	4-Cl	3053, 2923, 2850, 1659, 1602, 1332, 1215, 870, 762
176	H	4-CH$_3$	3050, 3020, 2859, 1654, 1596, 1216, 981, 813
177	H	4-F	3065, 2801, 1659, 1597, 1216, 835
178	H	4-Br	3057, 2992, 1657, 1601, 1485, 1329, 1218, 821, 689
179	H	4-NO$_2$	3073, 2929, 2840, 2441, 1660, 1602, 1218, 893
180	H	4-OCH$_3$	3058, 3008, 2933, 2844, 1654, 1598, 1509, 1304, 1015, 820
181	H	3-Cl	3060, 1657, 1602, 1305, 1213, 771, 670

182	H	3-F	3058, 1663, 1604, 1480, 1443, 1142, 850
183	H	3-Br	3061, 2835, 1689, 1602, 1216
184	H	3-NO_2	3070, 2867, 1662, 1607, 1529, 1349, 1221, 780
185	H	3-OCH_3	3061, 2955, 2830, 1654, 1599, 1209, 1044, 766
186	H	2-NO_2	3058, 2920, 2857, 1662, 1622, 1396, 1071, 690
187	2-Br	H	3023, 2917, 1652, 1601, 1400, 1325, 1176, 809
188	4-Cl	3-Cl	3023, 2918, 1663, 1604, 1310, 980, 789
189	4-CH_3	3-Cl	3026, 2920, 1664, 1604, 1415, 1082, 981, 790
190	4-Cl	3-NO_2	3065, 3034, 1667, 1609, 1527, 1289, 1090, 738
191	4-Cl	3-OCH_3	2928, 2843, 1658, 1598, 1211, 1092, 825, 790
192	4-Br	H	3057, 2916, 1654, 1601, 1394, 1106, 826, 792
193	4-CH_3	4-Br	3023, 2917, 1652, 1601, 1400, 1325, 1176, 809
194	4-Cl	4-Br	3084, 2945, 1659, 1598, 1402, 1218, 1090, 738
195	4-Cl	H	3079, 2985, 1660, 1556, 1413. 1030, 780
196	4-CH_3	4-Cl	3026, 2920, 1664, 1604, 1415, 1311, 1031, 790
197	4-Cl	4-Cl	3085, 1653, 1593, 1327, 1213, 1091, 817
198	4-Cl	4-OCH_3	3000, 2970, 2934, 2840, 1654, 1592, 1508, 1302, 1114, 817
199	4-NO_2	H	3053, 2841, 1659, 1596, 1512, 1329, 1204, 847, 740
200	4-Cl	4-NO_2	3109, 2856, 1662, 1603, 1534, 1347, 1178, 794
201	4-CH_3	4-CH_3	3023, 2916, 2860, 1651, 1596, 1327, 1176, 813, 729
202	4-CH_3	H	3031, 2921, 1654, 1599, 1210, 1113, 977, 759
203	4-CH_3	4-F	3036, 2919, 2843, 1657, 1601, 1505, 1414, 1218, 819
204	4-F	4-Cl	3074, 1666, 1602, 1265, 874, 811
205	3-Cl	H	3023, 2986, 1632, 1280, 1001, 756.
206	4-CH_3	3-F	2917, 1685, 1600, 1504, 1222, 1031, 838
207	4-F	3-F	3181, 3072, 1660, 1599

4.7.1.2 Synthesis of 3-amino-4,4-dibenzyl-1*H*-pyrazol-5(4*H*)-one (129) and 3-amino-4,4-*bis*(4-methylbenzyl)-1*H*-pyrazol-5(4*H*)-one (210)

Synthesis of intermediate (**128**) and (**129**) is mentioned in the section 4.4.2.1 and 4.4.2.2.

4.7.1.2.1 Synthesis of methyl-2,2-bis(4-methylbenzyl)-2-cyano-ethanoate (209)

Methyl 2-
cyanoacetate (**126**)   1-(Bromomethyl)-4-
methylbenzene (**208**)   Methyl-2,2-bis(4-methylbenzyl)-2-
cyano-ethanoate (**209**)
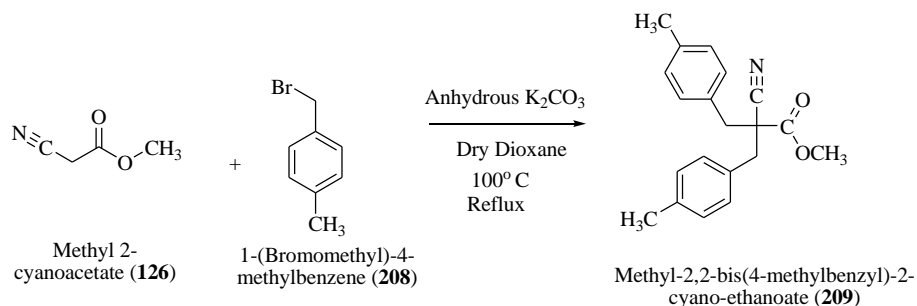
Substitution of methyl cyanoacetate (**126**) with 1-(bromomethyl)-4-methylbenzene (**208**) in dioxane yielded compound (**209**). IR spectrum of compound (**209**) gave peaks at 2245 cm^{-1} for -CN, and C=O peak of ester was obtained at 1744 cm^{-1}.

4.7.1.2.2 Synthesis of 3-amino-4,4-*bis*(4-methylbenzyl)-1*H*-pyrazol-5(4*H*)-one (210)

Methyl-2,2-bis(4-methylbenzyl)-
2-cyano-ethanoate (**209**)   3-Amino-4,4-bis(4-methylbenzyl)-
1*H*-pyrazol-5(4*H*)-one (**210**)
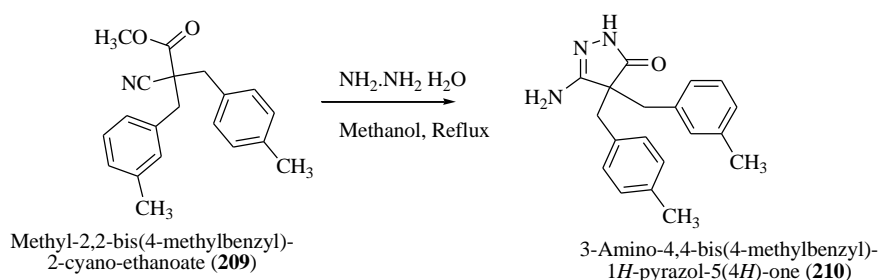
Substitution of methyl-2,2-*bis*(4-methylbenzyl)-2-cyano-ethanoate (**209**) with hydrazine hydrate in methanol gave the product (**210**). IR spectrum of the compound (**210**) gave peak at 3426 cm^{-1} for -NH and 1632 cm^{-1} for -C=O. Its mass spectrum gave peak at m/z 308 [M+1]$^{+}$.

4.7.1.3 Synthesis of 3-(3-oxo-1,3-diphenylpropylamino)-4,4-dibenzyl-1*H*-pyrazol-5(4*H*)-one derivatives (211-249)

Michael-aza addition of with 3-amino-4,4-dibenzyl-1*H*-pyrazol-5(4*H*)-one (**129**) or 3-amino-4,4-bis(4-methylbenzyl)-1*H*-pyrazol-5(4*H*)-one (**210**) to substituted chalcones (**174-207**) in presence of anhydrous potassium carbonate in dry DMF offered the desired final compounds (**211-249**). IR spectra of final compounds demonstrated peak for carbonyl of amide as well as ketone group. There is an evident -NH stretching in the range of 3500-3300 cm^{-1}.

Scheme 5: Synthesis of compounds (**211-249**)
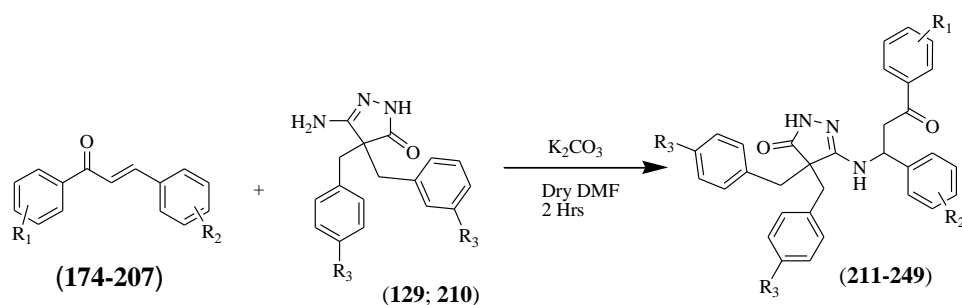
| Comp.	R$_1$	R$_2$	R$_3$	Comp.	R$_1$	R$_2$	R$_3$	Comp.	R$_1$	R$_2$	R$_3$
211	H	H	H	224	2-Br	H	H	237	4-Cl	4-NO$_2$	H
212	H	4-Cl	H	225	4-Cl	3-Cl	H	238	4-CH$_3$	4-CH$_3$	H
213	H	4-CH$_3$	H	226	4-CH$_3$	3-Cl	H	239	4-CH$_3$	H	H
214	H	4-F	H	227	4-Cl	3-NO$_2$	H	240	4-CH$_3$	4-F	H
215	H	4-Br	H	228	4-Cl	3-OCH$_3$	H	241	4-F	4-Cl	H
216	H	4-NO$_2$	H	229	4-Br	H	H	242	3-Cl	H	H
217	H	4-OCH$_3$	H	230	4- CH$_3$	4- Br	H	243	4-CH$_3$	3-F	H
218	H	3-Cl	H	231	4-Cl	4-Br	H	244	4-F	3-F	H
219	H	3-F	H	232	4-Cl	H	H	245	H	H	4-CH$_3$
220	H	3-Br	H	233	4-CH$_3$	4-Cl	H	246	H	4-Cl	4-CH$_3$
221	H	3-NO$_2$	H	234	4-Cl	4-Cl	H	247	H	4-F	4-CH$_3$
222	H	3-OCH$_3$	H	235	4-Cl	4-OCH$_3$	H	248	H	4-CH$_3$	4-CH$_3$
223	H	2-NO$_2$	H	236	4-NO$_2$	H	H	249	H	4-NO$_2$	4-CH$_3$

IR spectrum of the compound (**211**) showed -NH stretching 3438 cm^{-1} and peaks for C=O were obtained at 1682 and 1643 for amide C=O and ketone. The PMR spectrum demonstrated signals for aromatic protons at δ7.79 (dd, *J* = 8.4, 1.3 Hz, 2H), 7.74 – 7.62 (m, 1H), 7.58 (dd, *J* = 8.3, 7.2 Hz, 2H), 7.24 (m, 5H), 7.19 – 7.14 (m, 4H), 7.13 – 7.08 (m, 1H), 7.04 (dd, *J* = 8.2, 6.7 Hz, 2H), 6.96 (tt, *J* = 7.3, 1.3 Hz, 1H), 6.55 (dd, *J* = 9.7, 2.7 Hz, 3H). The signals for aliphatic protons were observed at δ 5.58 (dd, J = 8.7, 3.8 Hz, 1H), 3.38 (dd, J = 18.4, 8.7 Hz, 1H), 3.18 (dd, J = 25.0, 13.1 Hz, 2H), 3.07 (dd, J = 18.6, 13.1 Hz, 2H), 2.31 (ddd, J = 22.2, 18.4, 4.0 Hz, 1H). ^{13}C-NMR spectrum of the compound exhibited aromatic signals at δ 196.33, 170.20, 159.44, 139.42, 135.80, 135.50, 133.29, 129.68, 129.50, 128.70, 128.59, 127.74, 127.57, 126.28 and aliphatic peaks at 58.09, 49.30, 41.59, 40.80, 37.97. The mass spectrum showed quasi molecular peak at m/z 487 [M]$^+$ and an isotope peak at 488 [M+1]$^+$.
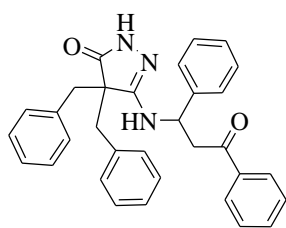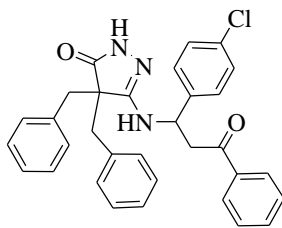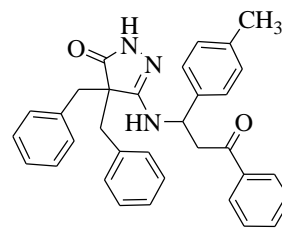
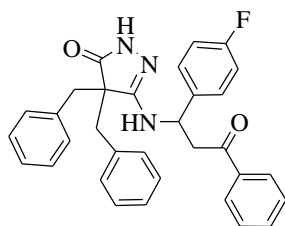(211)   (212)   (213)
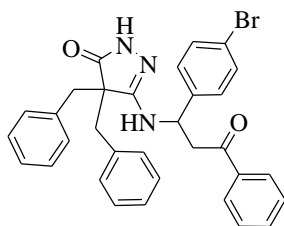
IR spectrum of the compound (212) showed -NH stretching 3437 cm^{-1} and peaks for C=O were obtained at 1686 and 1644 for amide C=O and ketone. The PMR spectrum demonstrated signals for aromatic protons at δ 7.73-7.71 (d, 2H), 7.67-7.63 (t, 1H), 7.54-7.51 (t, 2H), 7.21-7.18 (m, 4H), 7.17-7.14 (t, 4H), 7.13-7.09 (t, 2H), 7.07-7.01 (d, 2H), 6.93-6.90 (t, 1H), 6.53-6.50 (m, 3H), The signals for aliphatic protons were observed at δ 5.48-5.45 (m, 1H) for one proton, 3.34-3.31 (m, 1H) for single proton, 3.15-3.08 (dd, 2H) and 3.02-2.98 (dd, 2H) for -CH$_2$ protons, and δ 2.34-2.29 (dd, 1H) for one proton. The mass spectrum showed quasi molecular peak at m/z 523[M+1]$^+$ and an isotope peak at 525 [M+2]$^+$.
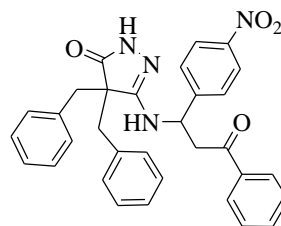
IR spectrum of the compound (213) showed -NH stretching 3462 cm^{-1} and peaks for C=O were obtained at 1689 and 1641 for amide C=O and ketone. The PMR spectrum demonstrated signals for aromatic protons at δ 7.82 – 7.75 (m, 2H), 7.78 – 7.69 (m, 1H), 7.63 – 7.56 (m, 2H), 7.30 – 7.13 (m, 14H), 7.02 – 6.95 (m, 2H), 6.85 (d, *J* = 8.1 Hz, 3H), 6.56 (s, 3H), 6.45 – 6.39 (m, 3H). The signals for aliphatic protons were observed at δ 5.53 (dd, *J* = 8.9, 3.7 Hz, 1H), 3.38 (d, *J* = 3.8 Hz, 1H), 3.39 – 3.31 (m, 1H), 3.23 – 3.16 (m, 2H), 3.07 (dd, *J* = 20.5, 13.1 Hz, 2H), 2.22 (s, 3H), 2.19 (d, *J* = 3.7 Hz, 1H). The mass spectrum showed quasi molecular peak at m/z 502 [M+1]$^+$ and an isotope peak at 503 [M+2]$^+$.

(214)   (215)   (216)
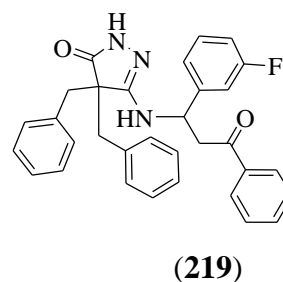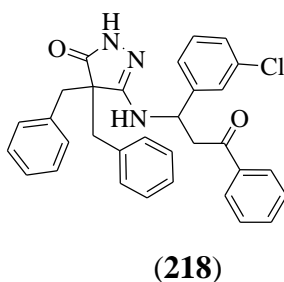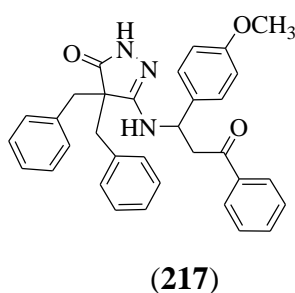
IR spectrum of the compound (214) showed -NH stretching 3404 cm^{-1} and peaks for C=O were obtained at 1686 and 1644 for amide C=O and ketone. The PMR spectrum demonstrated signals for aromatic protons at δ 7.77 – 7.71 (m, 2H), 7.70 – 7.63 (m, 1H), 7.57 – 7.51 (m, 2H), 7.21 – 7.18 (m, 2H), 7.15 (d, *J* = 1.8 Hz, 3H), 7.14 – 7.09 (m, 3H), 6.97 – 6.90 (m, 1H), 6.81 (t, *J* = 8.9 Hz, 2H), 6.57 – 6.50 (m, 4H). The signals for aliphatic protons

were observed at δ 5.49 (dd, J = 8.8, 3.9 Hz, 1H), 3.32 (d, J = 8.6 Hz, 1H), 3.12 (dd, J = 23.8, 13.1 Hz, 2H), 3.01 (dd, J = 13.2, 10.7 Hz, 2H), 2.29 (dd, J = 18.4, 3.9 Hz, 1H). The mass spectrum showed quasi molecular peak at m/z 506 $[M+1]^+$.

IR spectrum of the compound (**215**) showed -NH stretching 3442 cm^{-1} and peaks for C=O were obtained at 1685 and 1641 for amide C=O and ketone. The PMR spectrum demonstrated signals for aromatic protons at δ 7.82 – 7.76 (m, 2H), 7.76 – 7.69 (m, 1H), 7.63 – 7.56 (m, 2H), 7.23 (dd, *J* = 7.8, 6.0 Hz, 4H), 7.21 – 7.19 (m, 4H), 7.15 (d, *J* = 7.8 Hz, 1H), 7.02 – 6.95 (m, 1H), 6.62 (d, *J* = 3.5 Hz, 2H), 6.52 (s, 1H), 6.50 (s, 1H). The signals for aliphatic protons were observed at δ 5.51 (dd, J = 8.5, 4.0 Hz, 1H), 3.39 – 3.34 (m, 1H), 3.18 (dd, J = 23.5, 13.1 Hz, 2H), 3.06 (dd, J = 13.1, 8.6 Hz, 2H), 2.36 (dd, J = 18.5, 4.0 Hz, 1H). The mass spectrum showed quasi molecular peak at m/z 566 $[M]^+$ and an isotope peak at 568 $[M+2]^+$.

IR spectrum of the compound (**216**) showed -NH stretching 3433 cm^{-1} and peaks for C=O were obtained at 1686 and 1643 for amide C=O and ketone. The PMR spectrum demonstrated signals for aromatic protons at δ 7.90 (d, *J* = 8.8 Hz, 2H), 7.83 – 7.78 (m, 2H), 7.76 – 7.69 (m, 1H), 7.60 (t, *J* = 7.8 Hz, 2H), 7.27 – 7.22 (m, 2H), 7.21 (d, *J* = 1.0 Hz, 3H), 7.16 (t, *J* = 7.7 Hz, 2H), 7.03 – 6.96 (m, 1H), 6.83 (d, *J* = 8.8 Hz, 2H), 6.69 (s, 2H). The signals for aliphatic protons were observed at δ 5.64 (dd, *J* = 8.1, 4.3 Hz, 1H), 3.46 (dd, *J* = 18.7, 8.2 Hz, 1H), 3.19 (dd, *J* = 25.5, 13.1 Hz, 2H), 3.08 (dd, *J* = 13.0, 1.6 Hz, 2H), 2.52 (dd, *J* = 18.7, 4.3 Hz, 1H). The mass spectrum showed quasi molecular peak at m/z 533 $[M+1]^+$ and an isotope peak at 534 $[M+2]^+$.

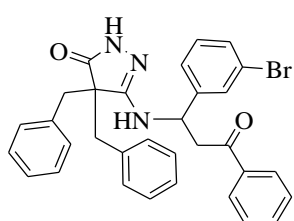(**217**)   (**218**)   (**219**)

IR spectrum of the compound (**217**) showed -NH stretching 3442 cm^{-1} and peaks for C=O were obtained at 1684 and 1643 for amide C=O and ketone. The PMR spectrum demonstrated signals for aromatic protons at δ 7.91-7.89 (d, 2H), 7.81-7.79 (d, 2H), 7.74-7.71 (t, 1H), 7.61-7.58 (t, 2H). Further aromatic peaks were obtained at 7.25-7.14 (m, 8H), 7.01-6.97 (t, 1H), 6.83-6.81 (d, 2H) and 6.68 (s, 2H). The signals for aliphatic protons were

observed at δ 5.63-5.62 (dd, 1H) for one proton, 3.48-3.42 (m, 1H) for single proton, methoxy protons were observed at 3.37 (s, 3H, *merged with H₂O peak*). 3.18-3.15 (dd, 2H) and 3.09-3.06 (dd, 2H) for -CH₂ protons, and δ 2.49-2.50 (dd, 1H) for one proton. The mass spectrum showed quasi molecular peak at m/z 517 [M+1]⁺ and an isotope peak at 518 [M+1]⁺.

IR spectrum of the compound (**218**) showed -NH stretching 3439 cm⁻¹ and peaks for C=O were obtained at 1681 and 1640 for amide C=O and ketone. The PMR spectrum demonstrated signals for aromatic protons at δ 7.75 (d, *J* = 8.2 Hz, 2H), 7.61 (d, *J* = 8.2 Hz, 2H), 7.19 (dd, *J* = 15.3, 7.4 Hz, 5H), 7.15 – 7.08 (m, 4H), 7.07 – 6.97 (m, 3H), 6.94 (t, *J* = 7.4 Hz, 1H), 6.51 (d, *J* = 6.8 Hz, 3H). The signals for aliphatic protons were observed at δ 5.52 (dd, *J* = 8.4, 4.1 Hz, 1H), 3.35 – 3.28 (m, 1H), 3.18-3.10 (dd, 2H), 3.05-3.02 (dd, 2H), 2.30 (dd, *J* = 18.5, 4.2 Hz, 1H)
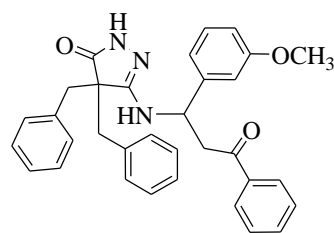
IR spectrum of the compound (**219**) showed -NH stretching 3420 cm⁻¹ and peaks for C=O were obtained at 1689 and 1643 for amide C=O and ketone. The PMR spectrum demonstrated signals for aromatic protons at δ 7.77 – 7.72 (m, 2H), 7.70 – 7.63 (m, 1H), 7.54 (t, *J* = 7.8 Hz, 2H), 7.21 – 7.17 (m, 2H), 7.16 – 7.13 (m, 2H), 7.11 (d, *J* = 7.4 Hz, 4H), 7.04 (dd, *J* = 8.0, 6.2 Hz, 1H), 6.91 (m, *J* = 6.9, 2.0 Hz, 2H), 6.57 (s, 2H), 6.42 (dt, *J* = 10.3, 2.2 Hz, 1H), 6.38 (d, *J* = 7.8 Hz, 1H). The signals for aliphatic protons were observed at δ 5.52 (dd, *J* = 8.4, 4.1 Hz, 1H), 4.04 (m, 1H), 3.35 – 3.31 (m, 1H), 3.12 (dd, *J* = 22.5, 13.1 Hz, 2H), 3.02 (t, *J* = 13.1 Hz, 2H), 2.30 (dd, *J* = 18.5, 4.1 Hz, 1H).
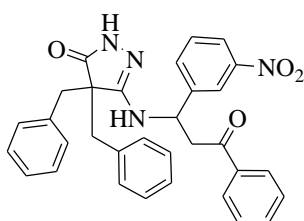
(**220**)   (**221**)   (**222**)

IR spectrum of the compound (**220**) showed -NH stretching 3433 cm⁻¹ and peaks for C=O were obtained at 1686 and 1642 for amide C=O and ketone. The PMR spectrum demonstrated signals for aromatic protons at δ 7.75 – 7.70 (m, 2H), 7.69 – 7.62 (m, 1H), 7.53 (t, *J* = 7.7 Hz, 2H), 7.31 – 7.25 (m, 1H), 7.18 (d, *J* = 8.0 Hz, 2H), 7.13 – 7.06 (m, 6H), 7.01 – 6.91 (m, 2H), 6.91 (dd, *J* = 8.1, 6.5 Hz, 1H), 6.55 (s, 2H), 6.51 (d, *J* = 7.8 Hz, 1H). The signals for aliphatic protons were observed at δ 5.47 (dd, *J* = 8.6, 4.1 Hz, 1H), 3.41 – 3.33 (m,

1H), 3.10 (dd, *J* = 15.6, 13.1 Hz, 2H), 3.00 (dd, *J* = 15.1, 13.2 Hz, 2H), 2.27 (dd, *J* = 18.5, 4.1 Hz, 1H).
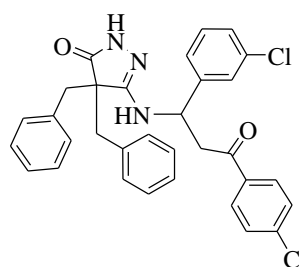
IR spectrum of the compound (**221**) showed -NH stretching 3436 cm^{-1} and peaks for C=O were obtained at 1688 and 1641 for amide C=O and ketone. The PMR spectrum demonstrated signals for aromatic protons at δ 8.03 (dd, *J* = 8.2, 2.4, 1.0 Hz, 1H), 7.80 (dd, *J* = 8.4, 1.4 Hz, 2H), 7.75 – 7.68 (m, 2H), 7.59 (t, *J* = 7.7 Hz, 2H), 7.38 (t, *J* = 8.0 Hz, 1H), 7.27 – 7.22 (m, 2H), 7.17 (t, *J* = 7.7 Hz, 2H), 7.13 (d, *J* = 3.8 Hz, 1H), 7.07 – 7.04 (m, 1H), 7.03 – 7.01 (m, 3H), 6.67 (s, 2H). The signals for aliphatic protons were observed at δ 5.63 (dd, J = 8.1, 4.6 Hz, 1H), 3.49 (dd, J = 18.5, 8.2 Hz, 1H), 3.16 (dd, J = 13.2, 11.2 Hz, 2H), 3.06 (t, J = 12.6 Hz, 2H), 2.61 (dd, J = 18.4, 4.7 Hz, 1H).

IR spectrum of the compound (**222**) showed -NH stretching 3452 cm^{-1} and peaks for C=O were obtained at 1684 and 1640 for amide C=O and ketone. The PMR spectrum demonstrated signals for aromatic protons at δ 7.80 – 7.74 (m, 2H), 7.73 – 7.65 (m, 1H), 7.60 – 7.53 (m, 2H), 7.30 – 7.22 (m, 2H), 7.22 – 7.07 (m, 7H), 6.99 – 6.90 (m, 2H), 6.69 (ddd, *J* = 8.3, 2.6, 0.9 Hz, 1H), 6.53 (s, 2H), 6.42 (t, *J* = 2.1 Hz, 1H), 6.14 – 6.08 (m, 1H). The signals for aliphatic protons were observed at δ 5.55 (dd, J = 8.7, 4.1 Hz, 1H), 3.61 (s, 3H), 3.37 (dd, J = 18.2, 8.7 Hz, 1H), 3.15 (dd, J = 17.0, 13.2 Hz, 2H), 3.06 (dd, J = 23.2, 13.2 Hz, 2H), 2.28 (dd, J = 18.2, 4.1 Hz, 1H). ^{13}C-NMR spectrum of the compound exhibited aromatic signals at δ 196.28, 170.26, 159.39, 158.67, 141.08, 135.81, 135.51, 133.26, 129.70, 129.33, 128.69, 128.60, 127.69, 127.54, 126.31, 119.08, 112.64, 111.40 and aliphatic peaks at 57.93, 54.67, 49.65, 41.41, 40.88, 39.63, 39.14. The mass spectrum showed quasi molecular peak at m/z 518 [M+1]$^{+}$ and an isotope peak at 519 [M+2]$^{+}$.
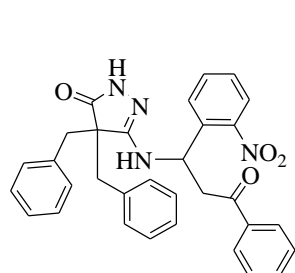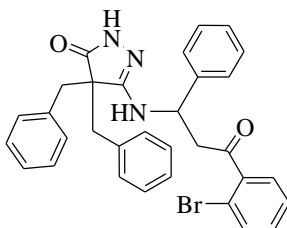
(**223**)   (**224**)   (**225**)
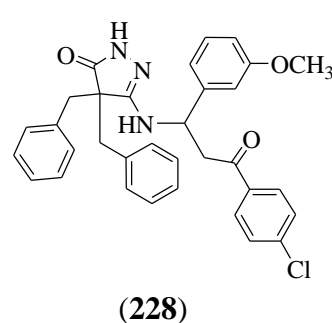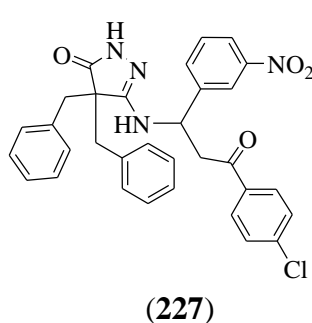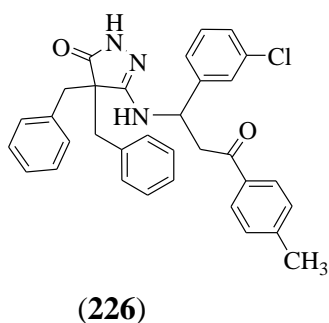
IR spectrum of the compound (**223**) showed -NH stretching 3442 cm^{-1} and peaks for C=O were obtained at 1689 and 1643 for amide C=O and ketone. The PMR spectrum demonstrated signals for aromatic protons at δ 8.03 (dd, *J* = 8.3, 2.3 Hz, 1H), 7.83 – 7.77 (m, 2H), 7.74 – 7.68 (m, 2H), 7.59 (t, *J* = 7.7 Hz, 2H), 7.38 (t, *J* = 8.0 Hz, 1H), 7.27 – 7.22 (m,

2H), 7.20 – 7.10 (m, 4H), 7.09 – 7.00 (m, 5H), 6.67 (s, 2H). The signals for aliphatic protons were observed at δ 5.63 (dd, J = 8.2, 4.7 Hz, 1H), 3.49 (dd, J = 18.5, 8.2 Hz, 1H), 3.16 (dd, *J* = 13.2, 11.3 Hz, 2H), 3.06 (t, J = 12.6 Hz, 2H), 2.61 (dd, J = 18.5, 4.7 Hz, 1H).

IR spectrum of the compound (**224**) showed -NH stretching 3461 cm^{-1} and peaks for C=O were obtained at 1686 and 1640 for amide C=O and ketone. The PMR spectrum demonstrated signals for aromatic protons at δ 7.79 (dd, *J* = 8.4, 1.3 Hz, 2H), 7.76 – 7.69 (m, 1H), 7.59 (dd, *J* = 8.3, 7.3 Hz, 2H), 7.23 (dd, *J* = 7.8, 5.9 Hz, 5H), 7.21 – 7.18 (m, 4H), 7.16 (t, *J* = 7.7 Hz, 2H), 7.02 – 6.95 (m, 1H), 6.62 (s, 2H), 6.51 (d, *J* = 8.5 Hz, 2H). The signals for aliphatic protons were observed at δ 5.54 – 5.48 (m, 1H), 3.39 – 3.29 (m, 1H), 3.18 (dd, *J* = 23.5, 13.1 Hz, 2H), 3.06 (dd, *J* = 13.1, 8.6 Hz, 2H), 2.36 (dd, *J* = 18.5, 4.0 Hz, 1H).

IR spectrum of the compound (**225**) showed -NH stretching 3437 cm^{-1} and peaks for C=O were obtained at 1685 and 1641 for amide C=O and ketone. The PMR spectrum demonstrated signals for aromatic protons at δ 7.70 – 7.65 (m, 2H), 7.37 (d, *J* = 8.0 Hz, 2H), 7.30 – 7.21 (m, 2H), 7.21 – 7.04 (m, 9H), 7.02 – 6.95 (m, 1H), 6.84 (t, *J* = 2.0 Hz, 1H), 6.59 (s, 2H), 6.54 (m, 1H). The signals for aliphatic protons were observed at δ 5.53 (dd, *J* = 8.8, 3.9 Hz, 1H), 3.37 (dd, *J* = 18.3, 8.9 Hz, 1H), 3.16 (dd, *J* = 14.9, 13.1 Hz, 2H), 3.06 (dd, *J* = 14.9, 13.1 Hz, 2H), 2.27 (dd, *J* = 18.3, 4.0 Hz, 1H). ^{13}C-NMR spectrum of the compound exhibited aromatic signals at δ 195.63, 170.31, 159.57, 143.76, 142.01, 135.63, 135.47, 133.21, 132.43, 129.67, 129.50, 129.27, 129.10, 127.88, 127.60, 126.64 – 126.22, 125.42 and aliphatic peaks at 58.04, 49.25, 41.19, 40.69, 40.20, 21.05.

(**226**)   (**227**)   (**228**)

IR spectrum of the compound (**226**) showed -NH stretching 3437 cm^{-1} and peaks for C=O were obtained at 1684 and 1641 for amide C=O and ketone. Peak for -CH$_3$ was obtained at 3199 cm^{-1}. The PMR spectrum demonstrated signals for aromatic protons at δ 7.69 (d, *J* = 8.3 Hz, 2H), 7.42 – 7.34 (m, 2H), 7.27 – 7.23 (m, 2H), 7.21 – 7.12 (m, 8H), 7.09 (t, *J* = 7.9 Hz, 1H), 7.04 – 6.97 (m, 1H), 6.85 (s, 1H), 6.59 (s, 2H), 6.56 – 6.51 (m, 1H). The signals for aliphatic protons were observed at δ 5.53 (dd, *J* = 8.8, 3.9 Hz, 1H), 3.40 (d, *J* = 8.9 Hz, 1H),

3.16 (dd, *J* = 14.8, 13.1 Hz, 2H), 3.06 (dd, *J* = 14.6, 13.2 Hz, 2H), 2.44 (s, 3H), 2.27 (dd, *J* = 18.4, 3.9 Hz, 1H). ^{13}C-NMR spectrum of the compound exhibited aromatic signals at δ 195.63, 170.29, 159.55, 143.77, 142.00, 135.62, 135.46, 133.20, 132.42, 129.66, 129.49, 129.26, 129.10, 127.88, 127.59, 126.64, 125.42 and aliphatic peaks at 58.03, 49.23, 41.17, 40.68, 21.05. The mass spectrum showed quasi molecular peak at m/z 536 [M]$^+$ and an isotope peak at 538 [M+2]$^+$.
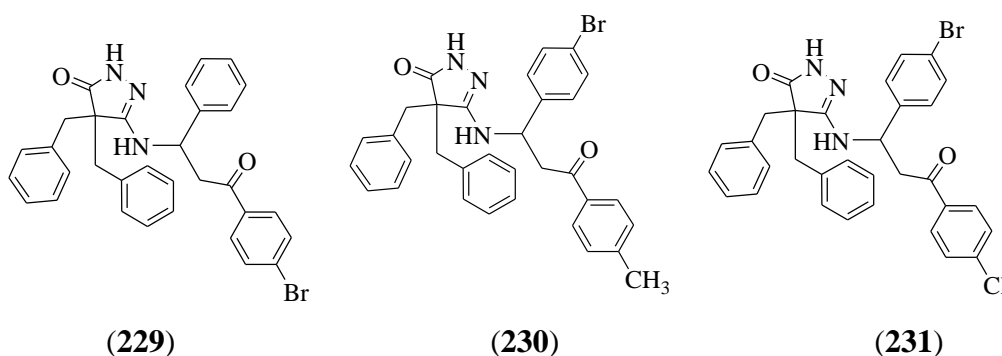
IR spectrum of the compound (**227**) showed -NH stretching 3448 cm^{-1} and peaks for C=O were obtained at 1690 and 1642 for amide C=O and ketone. The PMR spectrum demonstrated signals for aromatic protons at δ 7.85 (d, *J* = 8.8 Hz, 1H), 7.76 (d, *J* = 8.7 Hz, 2H), 7.62 (d, *J* = 8.4 Hz, 2H), 7.25 – 7.07 (m, 10H), 7.04 – 6.93 (m, 1H), 6.78 (d, *J* = 8.7 Hz, 2H), 6.63 (s, 2H). The signals for aliphatic protons were observed at δ 5.57 (dd, J = 7.7, 4.7 Hz, 1H), 3.37 (m, 1H), 3.13 (dd, J = 26.8, 13.1 Hz, 2H), 3.01 (dd, J = 13.0, 2.1 Hz, 2H), 2.50 (d, J = 3.9 Hz, 1H).

IR spectrum of the compound (**228**) showed -NH stretching 3429 cm^{-1} and peaks for C=O were obtained at 1685 and 1642 for amide C=O and ketone. The PMR spectrum demonstrated signals for aromatic protons at δ 7.80 (d, *J* = 8.6 Hz, 2H), 7.65 (d, *J* = 8.6 Hz, 2H), 7.28 – 7.20 (m, 2H), 7.20 – 7.07 (m, 7H), 7.02 – 6.92 (m, 2H), 6.71 (m, 1H), 6.52 (s, 2H), 6.44 (s, 1H), 6.15 – 6.09 (m, 1H). The signals for aliphatic protons were observed at δ 5.52 (dd, *J* = 8.2, 4.5 Hz, 1H), 3.64 (s, 3H), 3.37 – 3.30 (m, 1H), 3.15 (dd, *J* = 18.3, 13.2 Hz, 2H), 3.05 (dd, *J* = 22.6, 13.2 Hz, 2H), 2.35 (dd, *J* = 18.3, 4.5 Hz, 1H).

(**229**)   (**230**)   (**231**)

IR spectrum of the compound (**229**) showed -NH stretching 3422 cm^{-1} and peaks for C=O were obtained at 1686 and 1643 for amide C=O and ketone. The PMR spectrum demonstrated signals for aromatic protons at δ 7.79 – 7.60 (m, 5H), 7.25 – 7.14 (m, 10H), 7.00-7.97 (t, 1H), 6.62 (s, 2H), 6.52-6.50 (d, 2H). The signals for aliphatic protons were observed at δ 5.52 (dd, *J* = 8.3, 4.2 Hz, 1H), 3.39-35 (dd, *J* = 18.4, 8.3 Hz, 1H), 3.21-3.14 (d,

J = 13.4 Hz, 2H), 3.09-3.04 (dd, *J* = 19.0, 13.2 Hz, 2H), 2.38-2.34 (dd, *J* = 18.5, 4.2 Hz, 1H).
^{13}C-NMR spectrum of the compound exhibited aromatic signals at δ 131.65, 129.72, 129.49, 127.77, 127.58, 127.36, 126.29 and aliphatic peaks at δ 58.08, 49.31, 41.61, 40.78, 39.13. The mass spectrum showed quasi molecular peak at m/z 566 [M]$^+$ and an isotope peak at 568 [M+2]$^+$.
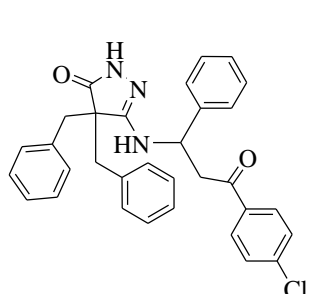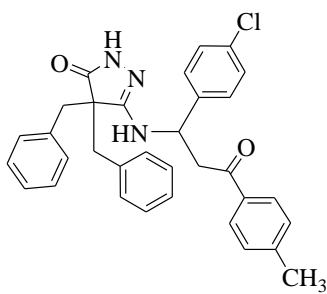
IR spectrum of the compound (**230**) showed -NH stretching 3435 cm^{-1} and peaks for C=O were obtained at 1685 and 1642 for amide C=O and ketone. The PMR spectrum demonstrated signals for aromatic protons at δ 7.69 (d, *J* = 8.2 Hz, 2H), 7.39 (d, *J* = 8.0 Hz, 2H), 7.30 (t, *J* = 7.3 Hz, 1H), 7.27 – 7.20 (m, 5H), 7.20 – 7.14 (m, 5H), 7.04 – 6.98 (m, 1H), 6.59 (s, 2H), 6.51 (d, *J* = 8.5 Hz, 2H). The signals for aliphatic protons were observed at δ 5.50 (dd, *J* = 8.7, 3.8 Hz, 1H), 3.37 – 3.30 (m, 1H), 3.18 (dd, *J* = 21.5, 13.1 Hz, 2H), 3.12 – 3.03 (m, 2H), 2.45 (m, 1H), 2.30 (s, 3H). ^{13}C-NMR spectrum of the compound exhibited aromatic signals at δ 195.65, 170.16, 159.53, 143.78, 138.91, 135.74, 135.49, 133.21, 130.43, 129.65, 129.47, 129.12, 129.01, 128.70, 128.06, 127.81, 127.55, 126.83, 126.34, 119.47 and aliphatic peaks at δ 58.13, 48.93, 41.21, 40.63, 21.05. The mass spectrum showed quasi molecular peak at m/z 579 [M]$^+$ and an isotope peak at 581 [M+2]$^+$.

IR spectrum of the compound (**231**) demonstrated -NH stretching 3441 cm^{-1} and peaks for C=O were obtained at 1684 and 1643 for amide C=O and ketone. The PMR spectrum demonstrated signals for aromatic protons at δ 7.82 – 7.72 (m, 2H), 7.67 (d, *J* = 8.6 Hz, 2H), 7.24 – 7.21 (m, 5H), 7.19 (s, 3H), 7.16 (d, *J* = 7.5 Hz, 2H), 7.03 – 6.96 (m, 1H), 6.61 (s, 2H), 6.55 – 6.49 (m, 2H). The signals for aliphatic protons were observed at δ 5.49 (dd, *J* = 8.1, 4.4 Hz, 1H), 3.36 (dd, *J* = 18.6, 8.2 Hz, 1H), 3.17 (dd, *J* = 25.0, 13.1 Hz, 2H), 3.06 (dd, *J* = 13.1, 8.6 Hz, 2H), 2.41 (dd, *J* = 18.6, 4.4 Hz, 1H). The mass spectrum showed quasi molecular peak at m/z 600 [M]$^+$ and an isotope peak at 602 [M+2]$^+$.

(**232**)   (**233**)   (**234**)
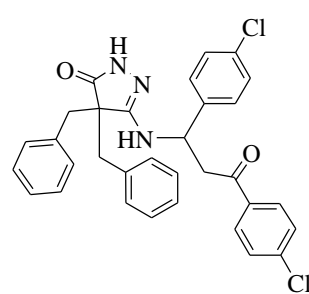
IR spectrum of the compound (**232**) demonstrated -NH stretching 3419 cm^{-1} and peaks for C=O were obtained at 1685 and 1645 for amide C=O and ketone. The PMR spectrum demonstrated signals for aromatic protons at δ 7.75 (d, J = 8.2 Hz, 2H), 7.61 (d, J = 8.2 Hz, 2H), 7.19 (m, 5H), 7.14 – 7.04 (m, 5H), 7.00 (t, J = 7.3 Hz, 2H), 6.94 (t, J = 7.4 Hz, 1H), 6.52 (s, 4H). The signals for aliphatic protons were observed at δ 5.52 (dd, J = 8.3, 4.1 Hz, 1H), 3.34 – 3.28 (m, 1H), 3.14 (dd, J = 26.4, 13.1 Hz, 2H), 3.02 (dd, J = 18.9, 13.1 Hz, 2H), 2.30 (dd, J = 18.5, 4.2 Hz, 1H). ^{13}C-NMR spectrum of the compound exhibited aromatic signals at δ 195.30, 170.22, 159.43, 139.40, 138.19, 135.81, 135.49, 134.43, 129.68, 129.50, 128.70, 127.78, 127.58, 126.30 and aliphatic peaks at 58.09, 49.31, 41.59, 40.78, 40.20. The mass spectrum showed quasi molecular peak at m/z 521 [M+1]$^{+}$ and an isotope peak at 522 [M+2]$^{+}$.

IR spectrum of the compound (**233**) demonstrated -NH stretching 3442 cm^{-1} and peaks for C=O were obtained at 1684 and 1643 for amide C=O and ketone. The PMR spectrum demonstrated signals for aromatic protons at δ 7.68 (d, J = 8.3 Hz, 2H), 7.41 – 7.35 (m, 2H), 7.27 – 7.23 (m, 3H), 7.23 – 7.20 (m, 1H), 7.20 – 7.18 (m, 2H), 7.18 – 7.13 (m, 3H), 7.10 – 7.05 (m, 2H), 7.03 – 6.96 (m, 1H), 6.61 – 6.52 (m, 4H). The signals for aliphatic protons were observed at δ 5.52 (dd, J = 8.8, 3.8 Hz, 1H), 3.34 (dd, J = 18.4, 8.8 Hz, 1H), 3.18 (dd, J = 22.1, 13.1 Hz, 2H), 3.06 (dd, J = 13.1, 9.1 Hz, 2H), 2.43 (s, 3H), 2.29 (dd, J = 18.3, 3.9 Hz, 1H). ^{13}C-NMR spectrum of the compound exhibited aromatic signals at δ 129.66, 129.48, 128.67, 128.33, 127.77, 127.54, 126.34 and aliphatic peaks at 58.16, 48.88, 41.42, 40.62, 39.68. The mass spectrum showed quasi molecular peak at m/z 535 [M]$^{+}$ and an isotope peak at 537 [M+2]$^{+}$.
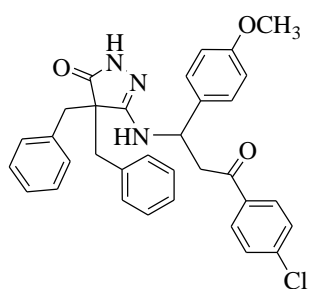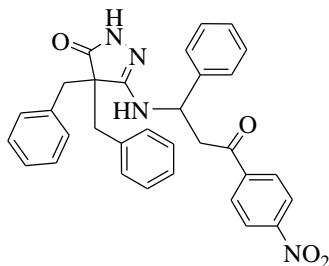
IR spectrum of the compound (**234**) demonstrated -NH stretching 3441 cm^{-1} and peaks for C=O were obtained at 1684 and 1642 for amide C=O and ketone. The PMR spectrum demonstrated signals for aromatic protons at δ 7.78 (d, J = 8.6 Hz, 2H), 7.64 (d, J = 8.6 Hz, 2H), 7.24 – 7.21 (m, 3H), 7.20 (m, 1H), 7.19 – 7.17 (m, 2H), 7.17 – 7.12 (m, 3H), 7.09 – 7.06 (m, 2H), 7.02 – 6.94 (m, 1H), 6.61 – 6.53 (m, 4H). The signals for aliphatic protons were observed at δ 5.51 (dd, J = 8.1, 4.4 Hz, 1H), 3.35 (dd, J = 18.5, 8.1 Hz, 1H), 3.17 (dd, J = 24.9, 13.1 Hz, 2H), 3.05 (dd, J = 13.2, 8.5 Hz, 2H), 2.42 (dd, J = 18.5, 4.4 Hz, 1H). ^{13}C-NMR spectrum of the compound exhibited aromatic signals at δ 129.66, 129.48, 128.67, 128.33, 127.77, 127.54, 126.34 and aliphatic peaks at 58.16, 48.88, 41.42, 40.62, 39.68. The mass spectrum showed quasi molecular peak at m/z 556 [M]$^{+}$ and an isotope peak at 558 [M+2]$^{+}$.

(**235**)   (**236**)   (**237**)

IR spectrum of the compound (**235**) demonstrated -NH stretching 3442 cm^{-1} and peaks for C=O were obtained at 1683 and 1642 for amide C=O and ketone. The PMR spectrum demonstrated signals for aromatic protons at δ 7.80-7.78 (dd, 2H), 7.67-7.65 (dd, 2H), 7.25-7.14 (m, 9H), 7.02-6.99 (t, 1H), 6.61-6.59 (m, 2H), 6.52-6.50 (m, 4H). The signals for aliphatic protons were observed at δ 5.50-5.48 (m, 1H), 3.71 (s, 3H), 3.36-3.31 (m, 1H), 3.19-3.12 (m, 2H), 3.08-3.02 (m, 2H), 2.33-2.28 (dd, 1H). The mass spectrum showed quasi molecular peak at m/z 552 [M]$^{+}$.
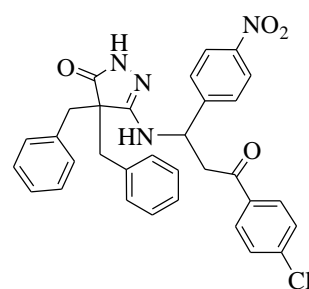
IR spectrum of the compound (**236**) demonstrated -NH stretching 3432 cm^{-1} and peaks for C=O were obtained at 1683 and 1643 for amide C=O and ketone. The PMR spectrum demonstrated signals for aromatic protons at δ 7.91-7.89 (d, 2H), 7.81 (d, 2H), 7.74-7.71 (t, 1H), 7.61-7.58 (t, 2H), 7.25-7.14 (m, 9H), 7.01-6.97 (t, 1H), 6.83-6.81 (d, *J*= 8.8, 2H), 6.68 (s, 2H). The signals for aliphatic protons were observed at δ 5.65-6.62 (m, 1H), 3.48-3.42 (q, 1H), 3.23-3.15 (m, 2H), 3.09-3.06 (m, 2H), 2.54-2.49 (dd, 1H).
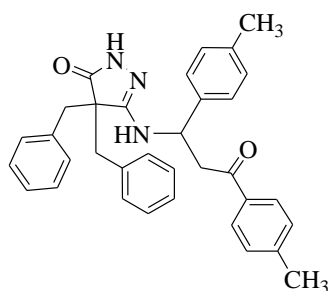
IR spectrum of the compound (**237**) demonstrated -NH stretching 3455 cm^{-1} and peaks for C=O were obtained at 1683 and 1636 for amide C=O and ketone. The PMR spectrum demonstrated signals for aromatic protons at δ 7.86-7.83 (d, 2H), 7.76-7.64 (d, 2H), 7.62-7.61 (d, 2H), 7.19-7.09 (m, 8H), 6.97-6.94 (m, 1H), 6.79-6.77 (d, 2H), 6.62 (s, 2H). The signals for aliphatic protons were observed at δ 5.57-5.55 (m, 1H), 3.40-3.36 (m, 1H), 3.31-3.09 (m, 2H), 3.02-2.99 (m, 2H), 2.4 (m, 1H). The mass spectrum showed quasi molecular peak at m/z 567 [M]$^{+}$ and an isotope peak at 569 [M+2]$^{+}$.
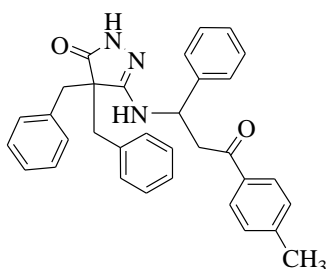

(**238**)   (**239**)   (**240**)

IR spectrum of the compound (**238**) demonstrated -NH stretching 3459 cm^{-1} and peaks for C=O were obtained at 1685 and 1640 for amide C=O and ketone. The PMR spectrum demonstrated signals for aromatic protons at δ 7.85-7.82 (d, 2H), 7.73-7.71 (t, 1H), 7.61-7.58 (m, 2H), 7.15-7.09 (m, 5H), 7.05-7.04 (t, 2H), 7.03-6.99 (dd, 2H), 6.93-6.91 (dd, 2H), 6.58-6.56 (d, 2H), 6.49 (s, 2H) . The signals for aliphatic protons were observed at δ 5.65-5.62 (m, 1H), 3.43-3.39 (t, 1H), 3.15-3.06 (dd, 2H), 3.03-2.97 (m, 2H), 2.37-2.32 (dd, 1H), 2.28 (s, 3H), 1.92 (s, 3H).

IR spectrum of the compound (**239**) demonstrated -NH stretching 3443 cm^{-1} and peaks for C=O were obtained at 1684 and 1642 for amide C=O and ketone. The PMR spectrum demonstrated signals for aromatic protons at δ 7.69-7.67 (d, 2H), 7.39-7.37 (d, 2H), 7.26-7.25 (d, 2H), 7.22-7.14 (m, 7H), 7.10-7.09 (m, 1H), 7.03-6.98 (m, 3H), 6.55-6.52 (m, 4H). The signals for aliphatic protons were observed at δ 5.58-5.55 (m, 1H), 3.36-3.32 (m, 1H), 3.22-3.14 (m, 2H) 3.10-3.03 (m, 2H), 2.43 (s, 3H), 2.22-2.18 (dd, 1H). The mass spectrum showed quasi molecular peak at m/z 502 [M]$^{+}$ and an isotope peak at 503 [M+2]$^{+}$.
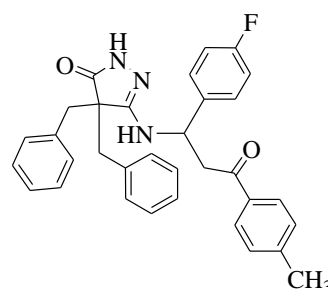
IR spectrum of the compound (**240**) demonstrated -NH stretching 3440 cm^{-1} and peaks for C=O were obtained at 1684 and 1642 for amide C=O and ketone. The PMR spectrum demonstrated signals for aromatic protons at δ 7.88-7.85 (m, 2H), 7.43-7.40 (t, 2H), 7.25-7.14 (m, 9H), 7.01-7.00 (t, 1H), 6.85-6.84 (d, 2H), 6.53 (s, 2H), 6.44-6.43 (d, 2H). The signals for aliphatic protons were observed at δ 5.53-5.50 (m, 1H), 3.36-3.31 (q, 1H), 3.21-3.13 (m, 2H), 3.09-3.02 (m, 2H), 2.28-2.24 (dd, 1H), 2.22 (s, 3H). The mass spectrum showed quasi molecular peak at m/z 520 [M+1]$^{+}$.

(**241**)   (**242**)   (**243**)

IR spectrum of the compound (**241**) demonstrated -NH stretching 3437 cm^{-1} and peaks for C=O were obtained at 1682 and 1642 for amide C=O and ketone. The PMR spectrum demonstrated signals for aromatic protons at δ 7.75-7.73 (d, 2H), 7.62-7.60 (d, 2H), 7.18-7.08 (m, 9H), 6.96-6.92 (t, 1H), 6.82-6.79 (t, 1H), 6.55-6.53 (m, 4H). The signals for

aliphatic protons were observed at δ 5.47-5.45 (m, 1H), 4.16-4.11 (m, 1H), 3.34-3.32 (q, 1H), 3.15-3.07 (dd, 2H), 3.02-2.97 (m, 2H), 2.35-2.30 (dd, 1H).
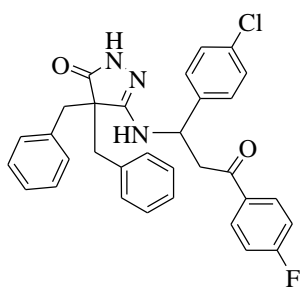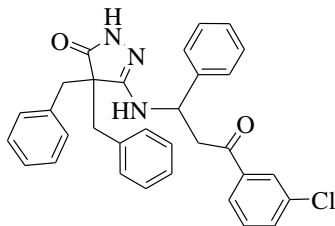
IR spectrum of the compound (**242**) demonstrated -NH stretching 3419 cm^{-1} and peaks for C=O were obtained at 1685 and 1645 for amide C=O and ketone. The PMR spectrum demonstrated signals for aromatic protons at δ 7.75 (d, 2H), 7.62-7.60 (d, 2H), 7.21-7.17 (m, 6H), 7.14-7.05 (m, 5H), 7.06-6.99 (t, 2H), 6.95-6.92 (t, 1H), 6.52-6.51 (d, 4H). The signals for aliphatic protons were observed at δ 5.53-5.51 (m, 1H), 3.33-3.30 (m, 1H), 3.18-3.10 (m, 2H), 3.05-2.99 (m, 2H), 2.32-2.27 (dd, 1H).
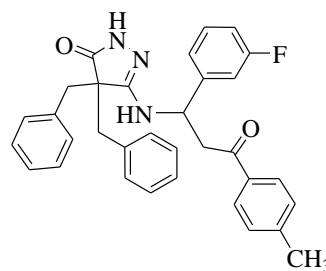
IR spectrum of the compound (**243**) demonstrated -NH stretching 3440 cm^{-1} and peaks for C=O were obtained at 1684 and 1641 for amide C=O and ketone. The PMR spectrum demonstrated signals for aromatic protons at δ 7.89-7.85 (q, 2H), 7.43-7.40 (t, 2H), 7.25-7.14 (m, 9H), 7.01-6.98 (m, 1H), 6.85-6.84 (d, 2H), 6.53 (s, 2H), 6.44-6.43 (d, 2H). The signals for aliphatic protons were observed at δ 5.53-5.50 (m, 1H), 3.38-3.31 (q, 1H), 3.21-3.13 (m, 2H), 3.09-3.02 (m, 2H), 2.28-2.24 (dd, 1H), 2.22 (s, 3H).
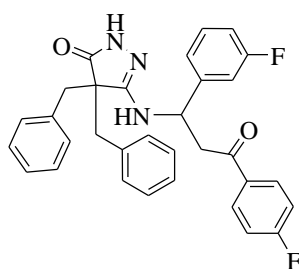

(**244**)

IR spectrum of the compound (**244**) demonstrated -NH stretching 3414 cm^{-1} and peaks for C=O were obtained at 1685 and 1645 for amide C=O and ketone. The PMR spectrum demonstrated signals for aromatic protons at δ 7.43-7.39 (t, 2H), 7.27- 7.19 (m, 7H), 7.17-7.13 (m, 3H), 7.02 – 6.98 (t, 1H), 6.87-6.84 (t, 2H), 6.62– 6.57 (m, 4H). The signals for aliphatic protons were observed at δ 5.54-5.52 (m, 1H), 3.36-3.34 (d, 1H), 3.21-3.13 (dd, 2H), 3.08-3.03 (dd, 2H), 2.41-2.36 (dd, 1H). The mass spectrum showed quasi molecular peak at m/z 524 [M+1]$^{+}$.

(**245**)   (**246**)   (**247**)

IR spectrum of the compound (**245**) showed -NH stretching 3442 cm⁻¹ and peaks for C=O were obtained at 1684 and 1642 for amide C=O and ketone. The PMR spectrum demonstrated signals for aromatic protons at δ 7.85 – 7.79 (m, 2H), 7.76 – 7.68 (m, 1H), 7.63 – 7.56 (m, 2H), 7.11 (dt, *J* = 7.9, 6.0 Hz, 5H), 7.04 (dd, *J* = 8.4, 7.0 Hz, 2H), 6.98 (d, *J* = 7.8 Hz, 2H), 6.92 (d, *J* = 7.7 Hz, 2H), 6.57 (dd, *J* = 7.3, 1.0 Hz, 2H), 6.49 (s, 2H). The signals for aliphatic protons were observed at δ 5.63 (dd, *J* = 8.4, 3.8 Hz, 1H), 3.44 – 3.38 (m, 1H), 3.11 (dd, *J* = 28.8, 13.1 Hz, 2H), 3.00 (dd, *J* = 16.0, 13.1 Hz, 2H), 2.35 (dd, *J* = 18.6, 3.8 Hz, 1H), 2.30 (s, 3H), 1.92 (s, 3H). The mass spectrum showed quasi molecular peak at m/z 516[M+1]⁺.
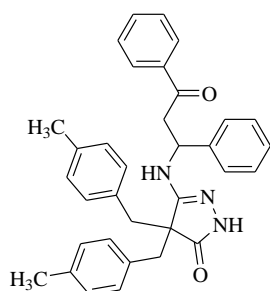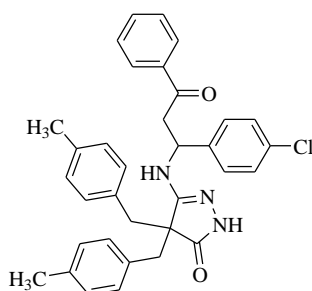
IR spectrum of the compound (**246**) showed -NH stretching 3437 cm⁻¹ and peaks for C=O were obtained at 1685 and 1644 for amide C=O and ketone. The PMR spectrum demonstrated signals for aromatic protons at δ 7.79 – 7.74 (m, 2H), 7.66 (t, *J* = 7.4 Hz, 1H), 7.53 (t, *J* = 7.6 Hz, 2H), 7.08 – 6.99 (m, 6H), 6.88 (dd, *J* = 12.9, 7.7 Hz, 4H), 6.61 (d, *J* = 8.2 Hz, 2H), 6.47 (s, 2H). The signals for aliphatic protons were observed at δ 5.55 (dd, *J* = 8.0, 4.3 Hz, 1H), 3.31 (d, *J* = 8.0 Hz, 1H), 3.05 (dd, *J* = 25.8, 13.1 Hz, 2H), 2.95 (d, *J* = 13.0 Hz, 2H), 2.50 – 2.43 (m, 1H), 2.24 (s, 3H), 1.90 (s, 3H). ¹³C-NMR spectrum of the compound exhibited aromatic signals at δ 195.98, 170.31, 159.64, 138.74, 135.75, 135.28, 135.21, 133.28, 132.67, 132.47, 130.88, 129.44, 129.33, 128.64, 128.43, 128.29, 128.23, 128.11, 127.63, 127.39 and aliphatic peaks at 58.32, 48.66, 41.57, 40.15, 39.13, 20.55, 20.19. The mass spectrum showed quasi molecular peak at m/z 550 [M]⁺ and an isotope peak at 552 [M+2]⁺.
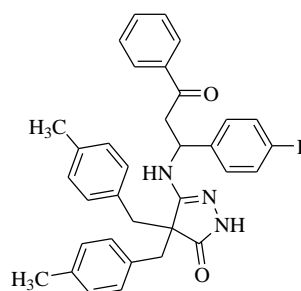
IR spectrum of the compound (**247**) showed -NH stretching 3438 cm⁻¹ and peaks for C=O were obtained at 1689 and 1643 for amide C=O and ketone. The PMR spectrum demonstrated signals for aromatic protons at δ 7.85 – 7.78 (m, 2H), 7.73 – 7.69 (m, 1H), 7.58 (t, *J* = 7.7 Hz, 2H), 7.08 (dd, *J* = 17.7, 7.9 Hz, 4H), 6.93 (dd, *J* = 14.6, 7.9 Hz, 4H), 6.85 (t, *J*

= 8.9 Hz, 2H), 6.67 (dd, *J* = 8.6, 5.6 Hz, 2H), 6.50 (s, 2H). The signals for aliphatic protons were observed at δ 5.60 (dd, J = 8.2, 4.2 Hz, 1H), 3.41 (d, J = 8.3 Hz, 1H), 3.09 (dd, J = 25.2, 13.1 Hz, 2H), 2.99 (dd, J = 13.2, 4.9 Hz, 2H), 2.47 (dd, J = 18.6, 4.2 Hz, 1H), 2.28 (s, 3H), 1.95 (s, 3H). The mass spectrum showed quasi molecular peak at m/z 534[M+1]$^+$.
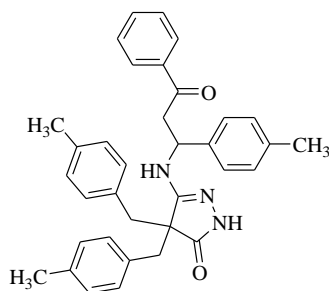

(**248**)   (**249**)

IR spectrum of the compound (**248**) showed -NH stretching 3457 cm^{-1} and peaks for C=O were obtained at 1687 and 1638 for amide C=O and ketone. The PMR spectrum demonstrated signals for aromatic protons at δ 7.84 – 7.78 (m, 2H), 7.74 – 7.68 (m, 1H), 7.59 (t, *J* = 7.7 Hz, 2H), 7.09 (dd, *J* = 10.7, 7.9 Hz, 4H), 6.94 (dd, *J* = 20.6, 7.7 Hz, 4H), 6.84 (d, *J* = 7.9 Hz, 2H), 6.51 – 6.44 (m, 4H). The signals for aliphatic protons were observed at δ 5.59 (dd, *J* = 8.5, 3.8 Hz, 1H), 3.35 (d, *J* = 8.5 Hz, 1H), 3.09 (dd, *J* = 25.9, 13.1 Hz, 2H), 2.99 (dd, *J* = 15.7, 13.1 Hz, 2H), 2.34 (dd, *J* = 18.5, 3.9 Hz, 1H), 2.30 (s, 3H), 2.24 (s, 3H), 1.94 (s, 3H). The mass spectrum showed quasi molecular peak at m/z 530[M+1]$^+$.
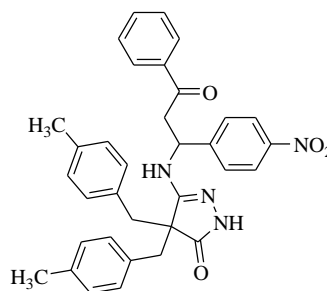
IR spectrum of the compound (**249**) showed -NH stretching 3435 cm^{-1} and peaks for C=O were obtained at 1684 and 1642 for amide C=O and ketone. The PMR spectrum demonstrated signals for aromatic protons at δ 7.90 (d, *J* = 8.9 Hz, 2H), 7.86 – 7.80 (m, 2H), 7.76 – 7.68 (m, 1H), 7.62 – 7.56 (m, 2H), 7.08 (dd, *J* = 10.4, 8.0 Hz, 4H), 6.99 – 6.84 (m, 6H), 6.59 (s, 2H). The signals for aliphatic protons were observed at δ 5.70 (dd, *J* = 7.6, 4.6 Hz, 1H), 3.45 (dd, *J* = 18.8, 7.6 Hz, 1H), 3.11 (dd, *J* = 32.1, 13.2 Hz, 2H), 3.00 (dd, *J* = 13.2, 10.3 Hz, 2H), 2.69 (dd, *J* = 18.8, 4.6 Hz, 1H), 2.27 (s, 3H), 1.97 (s, 3H). The mass spectrum showed quasi molecular peak at m/z 561 [M+1]$^+$.

4.7.2 Synthesis of 3,3-dibenzyl-3,3*a*-dihydro-5,7-diphenylpyrazolo[1,5-*a*]pyrimidin-2(1*H*)-one derivatives (250-261)

3-Amino-4,4-dibenzyl-1*H*-pyrazol-5(4*H*)-one (**129**) was synthesized by using a method discussed in section 4.4.2.1 and 4.4.2.2. Substituted/unsubstituted chalcones were synthesized by reacting different benzaldehyde with various acetophenones in presence of KOH and aqueous ethanol as discussed in section 4.7.1.1.

The desired final compounds (**250-261**) were obtained by condensing substituted chalcones (**CH1-34**) with 3-amino-4,4-dibenzyl-1*H*-pyrazol-5(4*H*)-one (**129**) in presence of potassium hydroxide in *n*-propanol. The reaction proceeds via Michael-aza addition of -NH$_2$ on the double bond of chalcone followed by cyclization reaction to give pyrazolo[1,5-*a*]pyrimidin2(1*H*)-one scaffold.
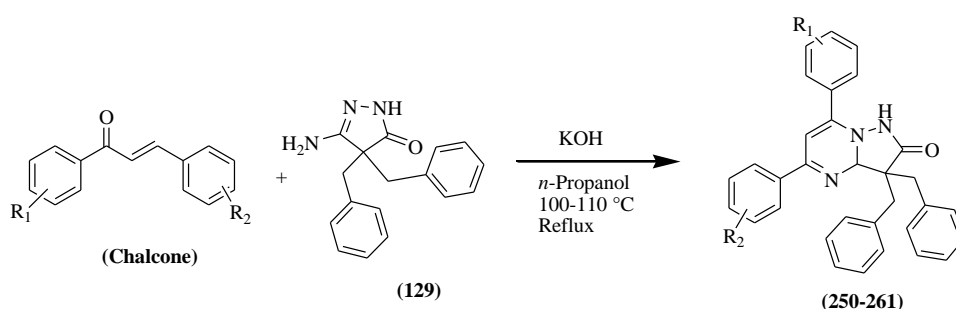
Comp ID	R$_1$	R$_2$	Comp ID	R$_1$	R$_2$
250	-H	-H	**256**	-H	-3F
251	-H	-4Cl	**257**	-4F	-H
252	-H	-4NO$_2$	**258**	-4CH$_3$	-4CH$_3$
253	-H	-4CH$_3$	**259**	-4CH$_3$	-4F
254	-H	-4F	**260**	-4CH$_3$	-H
255	-H	-3Cl	**261**	-4Cl	-H

Scheme 6: Synthesis of final compounds (**250**-**261**)

IR spectrum of compound (**250**) showed peaks at 1728 cm^{-1} for -C=O stretching. The mass spectrum offered quasi molecular ion peak at m/z 468 [M]$^+$. Its PMR spectrum demonstrated a multiplet for two aromatic protons at 8.22 – 8.13(m, 2H), while other seven aromatic protons appeared as multiplet at 7.64 – 7.41 (m, 9H). Ten aromatic protons appeared as multiplet at 7.15 – 7.05 (m, 10H). Four aliphatic protons of -CH$_2$ can be seen at 3.64 – 3.60 (m, 2H), 3.44-3.39 (dd, *J* = 12.9, 6.8 Hz, 2H).
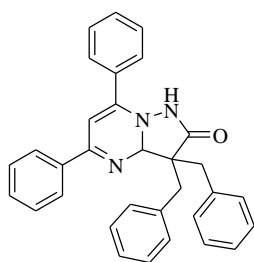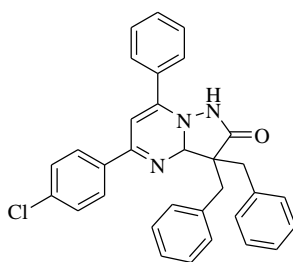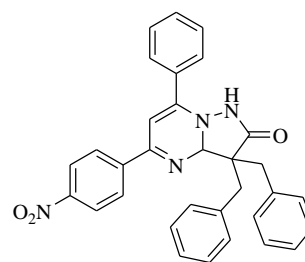
(**250**)   (**251**)   (**252**)

Compound (**251**) showed IR peaks for C=O at 1717 cm^{-1}. The mass spectrum gave peak at m/z 502 [M]$^+$. Its PMR spectrum gave aromatic protons as multiplet at 8.21-8.19 (m, 2H), 7.64-7.63 (m, 3H), 7.50-7.46 (m, 3H). Further two aromatic protons gave doublet at 7.34-7.32 (d, 2H). Aromatic protons appeared as multiplet at 7.13-7.12 (m,4H), 7.08-7.04 (m, 6H). A doublet of doublet was observed for four aliphatic protons at 3.63-3.40 (dd, 4H). The ^{13}C NMR spectrum of compound (**251**) gave aromatic carbons at 182.47, 161.59, 156.25, 144.39, 138.13, 135.02, 134.73, 134.54, 131.99, 130.75, 129.81, 129.74, 129.53, 128.87, 128.40, 127.75, 127.32, 127.05, 126.96, 114.16 while aliphatic carbons as 58.96, 42.69, 41.01.

IR spectrum of compound (**252**) showed at 1636 cm^{-1} for -C=O. Its PMR spectrum gave aromatic protons at δ 8.14 (d, *J* = 8.7 Hz, 1H), 7.60 – 7.58 (m, 2H), 7.50 – 7.32 (m, 2H). Further aromatic peaks were observed at δ 7.16 – 7.10 (m, 4H), 7.06 (dd, *J* = 5.0, 2.1 Hz, 5H). the aliphatic peaks appeared at 3.62 (d, *J* = 12.9 Hz, 2H), 3.40 (d, *J* = 12.9 Hz, 2H).
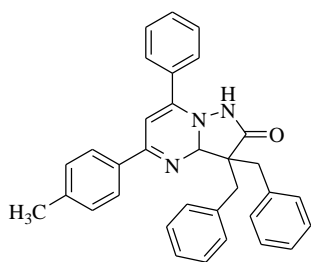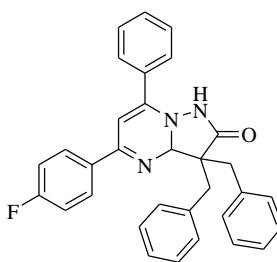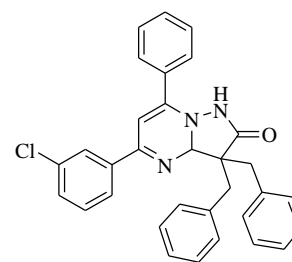
(**253**)   (**254**)   (**255**)

IR spectrum of the compound (**253**) gave C=O peak at 1643 cm^{-1} and -CH$_3$ peak was obtained at 3066 cm^{-1}. Its mass spectrum gave molecular ion peak at m/z 482 [M]$^+$. Its PMR spectrum demonstrated a multiplet for one aromatic proton at 8.21 – 8.20 (m, 1H), while three aromatic protons appeared as multiplet at 7.64 – 7.62 (m, 3H). Further one aromatic proton appeared as singlet 7.52 (s, 1H) and two protons at 7.45-7.43 (d, *J* = 8.3 Hz, 2H). One aromatic proton appeared as doublet at 7.37 (d, *J* = 1.8 Hz, 1H). Remaining aromatic protons

appeared as multiplet at 7.17 – 7.12 (m, 6H) and 7.06-7.04 (m, 5H). The aliphatic -CH$_2$ protons can be seen as doublet at 3.61 (d, *J* = 12.9 Hz, 2H) and 3.40 (d, *J* = 12.9 Hz, 2H) while the methyl protons appeared as singlet at 2.34 (s, 3H).

The C=O peak in the IR spectrum of compound (**254**) appeared at 1669 cm^{-1}. The mass spectrum gave molecular ion peak at m/z 486 [M]$^+$. The PMR spectrum gave pentat peaks for two aromatic protons at 8.21-8.18 (m, 2H) while three protons appeared as triplet at 7.64-7.62 (t, 3H). Two aromatic protons can be seen as multiplet at 7.56-7.53 (m, 2H) while another proton as singlet at 7.78 (s, 1H). Aromatic protons were observed as multiplet at 7.14-7.12 (m, 4H) and 7.08-7.03 (m, 8H). Aliphatic protons of -CH$_2$ appeared at 3.63-3.60 (d, 2H) and 3.43-3.39 (d, 2H).

Compound (**255**) showed IR peaks for C=O at 1642 cm^{-1}. The mass spectrum gave peak at m/z 502 [M]$^+$. Its PMR spectrum gave aromatic protons as triplet at 8.21-8.19 (t, 2H), 7.64-7.63 (t, 3H), 7.50-7.46 (m, 3H). Further, one aromatic proton appeared as singlet at 7.47 (s, 1H). Three aromatic protons gave multiplet at 7.41-7.37 (m, 3H). A doublet can be seen of single aromatic proton at 7.31-7.29 (d, 1H), while a multiplet was observed at 7.24-7.22 (m, 1H). Further aromatic protons appeared at 7.13-7.10 (m, 4H) and 7.07-7.06 (m, 6H). One proton was seen as singlet at 4.28 (s, 1H). The -CH$_2$ protons appeared as doublet of doublet at 3.64-3.61 (dd, 2H) and 3.43-3.40 (dd, 2H).
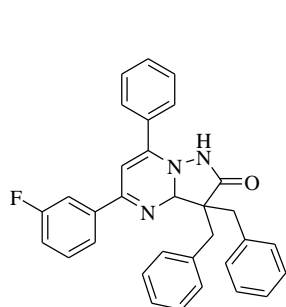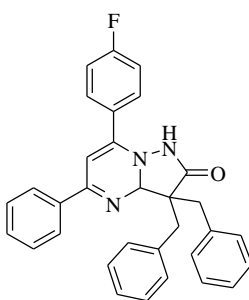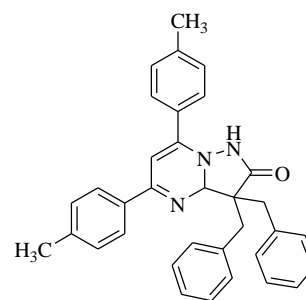
(**256**)   (**257**)   (**258**)

The C=O peak in the IR spectrum of compound (**256**) appeared at 1652 cm^{-1}. The PMR spectrum gave pentat peaks for two aromatic protons at 8.21-8.18 (m, 2H) while three protons appeared as triplet at 7.64-7.62 (t, 3H). Two aromatic protons can be seen as multiplet at 7.56-7.53 (m, 2H) while another proton as singlet at 7.78 (s, 1H). Aromatic protons were observed as multiplet at 7.14-7.12 (m, 4H) and 7.08-7.03 (m, 8H). Aliphatic protons of -CH$_2$ appeared at 3.63-3.60 (d, 2H) and 3.43-3.39 (d, 2H).

The C=O peak in the IR spectrum of compound (**257**) appeared at 1643 cm^{-1}. The mass spectrum gave quasi molecular ion peak at m/z 486 [M]$^+$. The PMR spectrum gave multiplet peaks for two aromatic protons at 8.21-8.18 (m, 2H) while two protons appeared as multiplet at 7.50-7.48 (m, 2H). Single aromatic protons can be seen at 7.48 (s, 1H) and 7.46-7.41 (d, 1H). Two aromatic protons can be seen as multiplet at 7.38-7.36 (d, 2H), while another two protons as triplet at 7.34-7.28 (t, 2H). Aromatic protons were observed as multiplet at 7.14-7.11 (m, 4H) and 7.08-7.04 (m, 6H). Aliphatic protons of -CH$_2$ appeared as dd at 3.63-3.60 (dd, 2H) and 3.41-3.38 (dd, 2H).
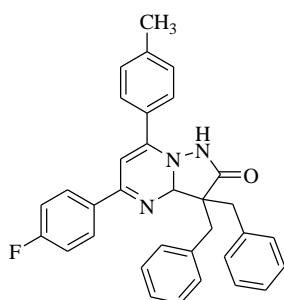
The C=O peak in the IR spectrum of compound (**258**) appeared at 1646 cm^{-1} whereas -CH$_3$ peak appeared at 3029 cm^{-1}. The mass spectrum gave quasi molecular ion peak at m/z 496 [M]$^+$. The PMR spectrum gave doublet for two aromatic protons at 8.11-8.09 (d, *J*= 8.4, 2H). A singlet can be seen at 7.47 (s, 1H), while a triplet was observed at 7.45-7.41 (t, *J*=8.4 and *J*=7.2, 4H) for four protons. Aromatic protons appeared at 7.17 (s, 1H) 7.15-7.12 (m, 5H), 7.06-7.02 (6H). Aliphatic protons for -CH$_2$ appeared as dd at 3.62-3.59 (dd, *J*=12.8, 2H) and 3.41-3.38 (dd, *J*=12.8, 2H) while methyl protons appeared a singlets at 2.50 (s, 3H), 2.34 (s, 3H).
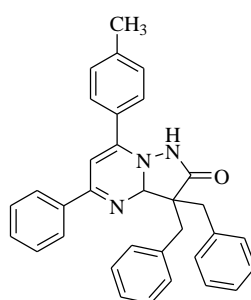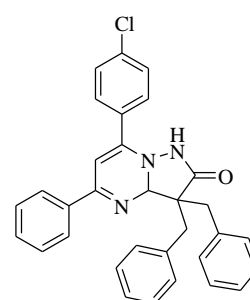
| (**259**) | (**260**) | (**261**) |

The C=O peak in the IR spectrum of compound (**259**) appeared at 1683 cm^{-1}. The mass spectrum gave quasi molecular ion peak at m/z 500 [M]$^+$. The PMR spectrum gave doublet for one aromatic proton at 8.11 (d, *J* = 8.2 Hz, 1H) while dd for another aromatic proton at 7.53 (dd, *J* = 8.8, 5.0 Hz, 1H). Other aromatic protons appeared at 7.48 – 7.40 (m, 1H), 7.22 (d, *J* = 9.4 Hz, 1H), 7.13 (dd, *J* = 6.9, 2.8 Hz, 2H), 7.09 – 7.01 (m, 3H). Aliphatic protons for -CH$_2$ appeared as doublet at 3.23 (d, *J* = 13.5 Hz, 2H), 2.97 (d, *J* = 13.5 Hz, 2H), 2.55 (s, 3H).

The IR spectrum of compound (**260**) gave peak at 1638 cm^{-1} for carbonyl. Its mass spectrum gave molecular ion peak at m/z 482 [M]$^+$. Its PMR spectrum gave peaks at in the

range of 8.11 to 2.50. A doublet was observed for two aromatic protons at 8.11-8.09 (d, J=8.0, 2H) while three aromatic protons gave multiplet at 7.49-7.47 (m, 3H) and 7.42-7.40 (m, 3H). Further multiplets were obtained by aromatic protons at 7.37-7.33 (m, 2H), 7.14-7.12 (m, 4H), 7.07-7.03 (m, 6H). Aliphatic protons for -CH$_2$ were can be seen as doublet at 3.62-3.59 (d, J=12.8, 2H), 3.41-3.38 (d, J=12.8, 2H) while methyl protons appeared at 2.50 (s, 3H).

The IR spectrum of the compound (**261**) gave C=O peak at 1685 cm^{-1}. Its mass spectrum gave molecular ion peak at m/z 502 [M]$^+$. Its PMR spectrum gave aromatic protons in the range of 8.15-7.05. A multiplet was observed for two protons at 8.15-8.12 (m, 2H). Another multiplet for aromatic protons appeared at 7.60-7.58 (m, 2H) and 7.49-7.47 (m, 3H), 7.43-7.41 (m, 1H), 7.37-7.34 (m, 2H), 7.13-7.11 (m, 4H), 7.07-7.05 (m, 6H). Aliphatic protons for -CH$_2$ were can be seen as dd at 3.63-3.60 (dd, J=12.8, 2H), 3.41-3.38 (dd, J=12.8, 2H).

4.8 Biological screening of synthesized compounds as anti-TB agents by MABA assay

The prepared compounds were evaluated for their percentage inhibition against *Mycobacterium bovis* (BCG). Overall, four compounds (**213, 214, 216** and **220**) out of 51 compounds exhibited inhibition of the bacteria. It was found that compound **213** and **220** was exhibiting 91% and 93% inhibition, comparable to that of standard drugs. Compounds **214** and **220** having fluorine and bromine respectively in their structure, are showing inhibition, thus it can be agreed that presence of halogen atom is favorable for inhibitory activity. The results are shown in **Table 4.11** and **Figure 4.16**. Compound (**216**) exhibited MIC value of 1.5 µg/mL.

Table 4.11: Anti-tubercular activity of the synthesized compounds (**211-39** and **250-261**)

Comp ID	% Inhibition	Comp ID	% Inhibition	Comp ID	% Inhibition
211	NI	**228**	NI	**245**	NI
212	NI	**229**	NI	**246**	NI
213	91	**230**	NI	**247**	NI
214	79	**231**	NI	**248**	NI
215	NI	**232**	NI	**249**	NI
216	89	**233**	NI	**250**	NI
217	NI	**234**	NI	**251**	NI

218	NI	235	NI	252	NI
219	NI	**236**	NI	**253**	NI
220	93	**237**	NI	**254**	NI
221	NI	**238**	NI	**255**	NI
222	NI	**239**	NI	**256**	NI
223	NI	**240**	NI	**257**	NI
224	NI	**241**	NI	**258**	NI
225	NI	**242**	NI	**259**	NI
226	NI	**243**	NI	**260**	NI
227	NI	**244**	NI	**261**	NI
Isoniazid	93.46	**Rifampicin**	96.09	**Blank**	0.06

NI: No inhibition at 10 µg/mL; isoniazid: 0.04 µg/mL; rifampicin: 0.08 µg/mL
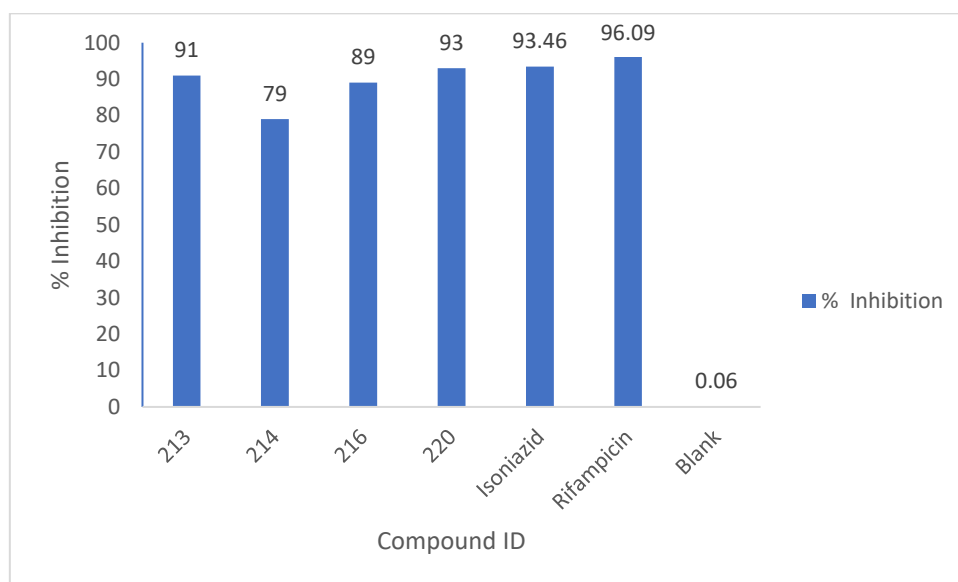
Figure 4.16: Percentage inhibition of *Mycobacterium bovis* (BCG) by the synthesized compounds using MABA assay.

4.9 Molecular docking, ADMET studies of the synthesized compounds

4.9.1 Computational studies of compounds (211-249 and 250-261)

Docking of all the compounds were performed with DprE1 enzyme to assess the plausible binding and binding interactions between the compound and active site. The binding affinity of the compounds are given in the **Table 4.12**.

Table 4.12: Binding affinity of the compounds (**211-39** and **250-261**)

Comp ID	Binding affinity (Kcal/mol)	Comp ID	Binding affinity (Kcal/mol)	Comp ID	Binding affinity (Kcal/mol)
211	-9.6	**228**	-10.6	**245**	-10.1
212	-9.4	**229**	-9.6	**246**	-10.6
213	-9.6	**230**	-9.9	**247**	-10.4
214	-9.9	**231**	-9.8	**248**	-10.9
215	-9.5	**232**	-9.4	**249**	-10.3
216	-9.4	**233**	-10.7	**250**	-11.2
217	-10	**234**	-9.7	**251**	-10.8
218	-10	**235**	-9.1	**252**	-10.9
219	-9.6	**236**	-10	**253**	-10.8
220	-9.2	**237**	-10.1	**254**	-11.2
221	-9.7	**238**	-10.2	**255**	-11.6
222	-9.2	**239**	-9.7	**256**	-11.4
223	-9.7	**240**	-10.1	**257**	-11.3
224	-9.8	**241**	-10.7	**258**	-10.9
225	-9.7	**242**	-10.1	**259**	-10.9
226	-10	**243**	-10.3	**260**	-10.7
227	-10.6	**244**	-9.9	**261**	-10.6
QN118 **(Standard)**	-9.5				
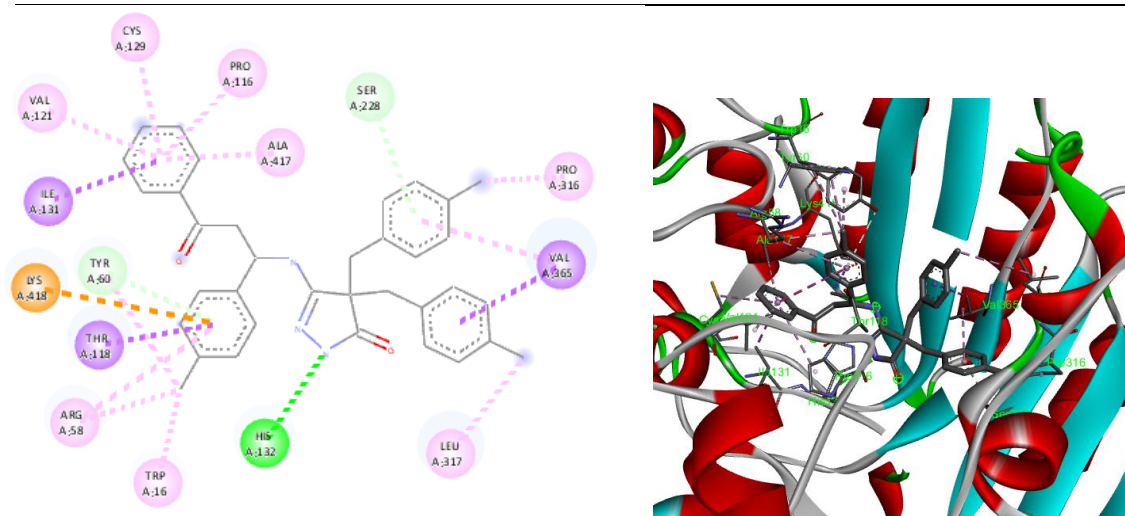
Figure 4.17: 2D and 3D interactions compound (**248**) with DprE1.

Docking of the compounds within the active site of the enzyme DprE1 helped in understanding the type of interactions between the enzyme and the enzyme. Compound (**248**) demonstrated highest binding affinity of -10.9 Kcal/mol. Compound (**248**) was found to have interactions with pi-alkyl interactions with CYS 129, Val 121, PRO 316 and TRP 16 (**Figure 4.17**). It is also forming pi-sigma interactions with LYS 418. The compound is interacting with the enzyme via Vander Waals interactions. All these interactions indicate towards the high docking score of the compound (**248**).
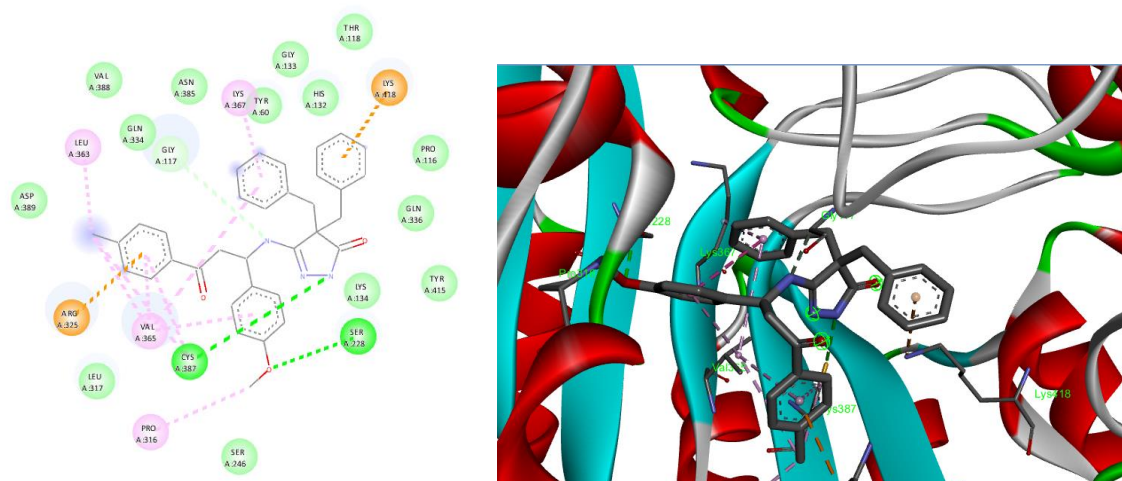
Figure 4.18: 2D and 3D interactions compound (**235**) with DprE1.

Compound (**235**) was found to have lowest binding affinity of -9.1 Kcal/mol. Although, the compound (**235**) is seen to have various type of interaction within the active site of the ligand such as Vander Waals interactions, pi-alkyl interactions (**Figure 4.18**). But it is evident that too many Vander Waals interactions are reducing the binding affinity of the compounds with the enzyme.
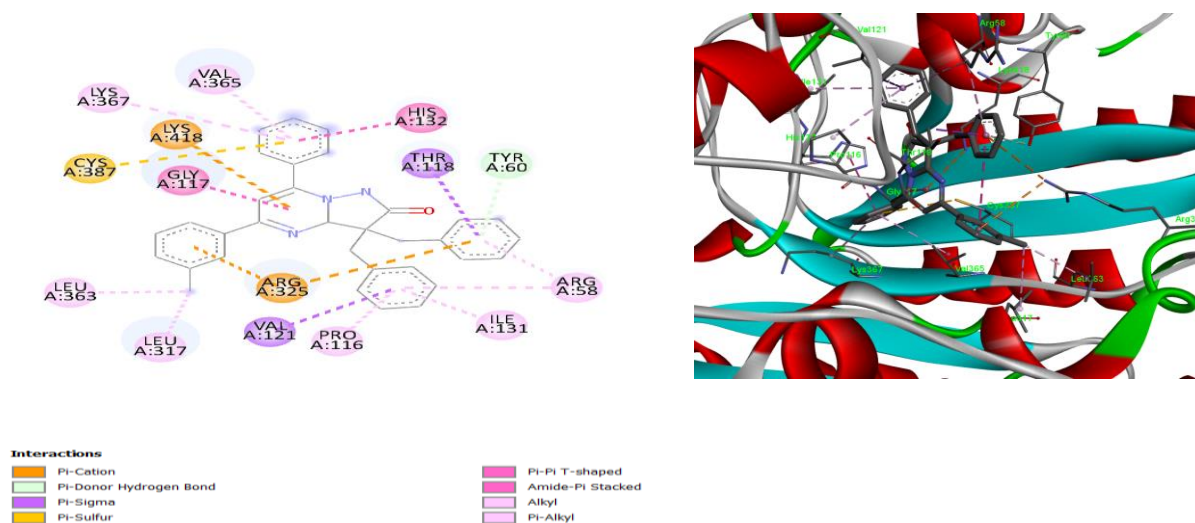
Figure 4.19: 2D and 3D interactions of compound (**255**) with DprE1

Compound (**255**) having 3-chloro substitution was found to have highest binding affinity of -11.6 Kcal/mol. The aromatic rings of compound (**255**) were found to exert pi-carbon interactions with CYS 387, LYS 418 and ARG 325 amino acid residue. Also, pi-sigma interactions were formed between the dibenzyl ring and VAL 121 AND THR 118 amino acid residue. One of the dibenzyl ring was found to interact with TYR 60 via pi-donor hydrogen bond. The compound (**255**) was found to have alkyl interactions with LYS 367, VAL 365 and ARG 58 amino acid residues (**Figure 4.19**).
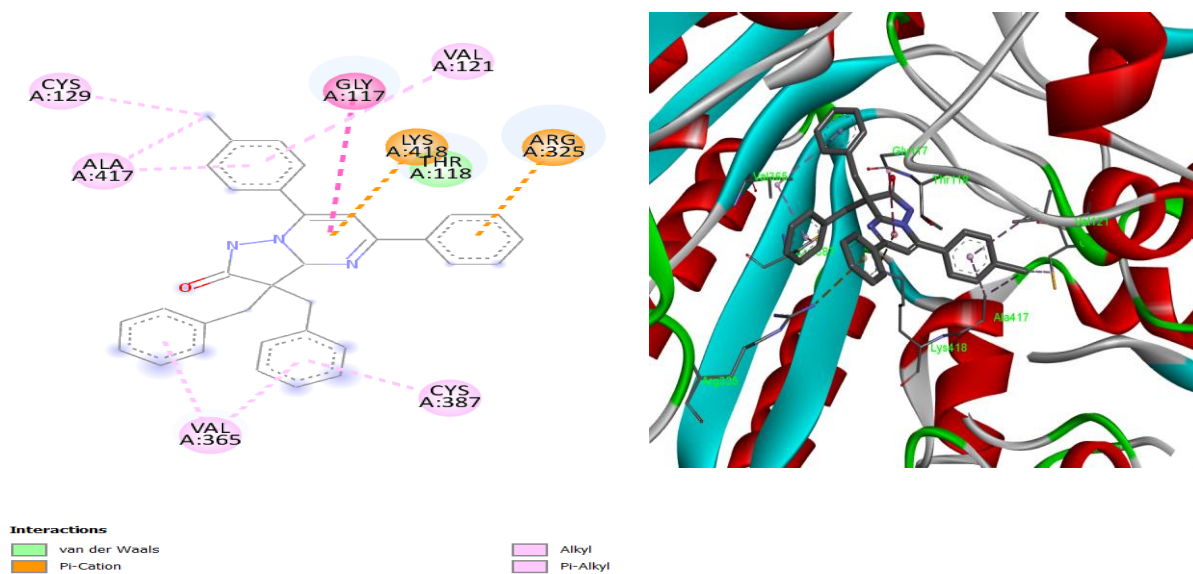
Figure 4.19: 2D and 3D interactions of compound (**261**) with DprE1

Compound (**261**) having 4-chloro substitution was found to have highest binding affinity of -10.6 Kcal/mol. It is evident that compounds (**261**) is having lesser interactions within the active site of the enzyme. The compound (**261**) was exhibiting van der Waals interactions with THR 118 amino acid residue. The dibenzyl aromatic rings were found to form alkyl interactions with CYS 387 and VAL 365 amino acid residue. The pyrimidine ring was found to have amide-pi stacked interactions with GLY 117 amino acid residue (**Figure 4.19**).

4.9.2 ADMET predictions of the compounds (211-249 and 250-261)

ADMET predictions gave an insight into the physiological properties of the designed compounds. The results for compounds (**211-249**) are given in the **Table 4.13**. The molecular weight of the designed compounds was found to be in range of 487-600 g/mol. Hydrogen bond acceptors were in range of 5-3 whereas hydrogen bond donors for all the designed

compounds were found to be 2-3. The TPSA of all the compounds was found in the range of 70.56-116.38. The lipophilicity of compounds in terms of iLOGP was found to be in range of 2.48-4.20 indicating good lipophilicity. But the compounds were predicted to have low aqueous solubility having Log S value in the range of -6.50 to -7.78. Additionally, all the compounds were predicted to exhibit high gastro intestinal absorption. Most of the compounds were predicted not to cross blood brain barrier (BBB) except compound (**211, 213** and **239)**. All the compounds were predicted to interact with either one or more of the Cyt P450 enzyme such as CYP2C9, CYP3A4 etc.

Table 4.13: ADMET predictions of the compounds (**211-261**)

Comp ID	MW	HBA	HBD	TPSA	iLogp	Clogp	Log S	GIA	BBB	LP
211	487	3	2	70.56	3.31	5.10	-6.58	High	Yes	1
212	**522**	3	2	70.56	3.75	5.66	-7.18	High	No	No
213	**501**	3	2	70.56	3.80	5.48	-6.89	High	Yes	No
214	505	4	2	70.56	3.46	5.42	-6.74	High	No	No
215	566	3	2	70.56	3.85	5.75	-7.50	High	No	No
216	532	5	2	116.3	2.48	4.27	-6.65	High	No	Yes
217	517	4	2	79.79	3.78	5.14	-6.67	High	No	2
218	522	3	2	70.56	3.85	5.69	-7.18	High	No	No
219	505	4	2	70.56	3.74	5.48	-6.74	High	No	No
220	566	3	2	70.56	3.56	5.69	-7.50	High	No	No
221	532	5	2	116.3	3.03	4.39	-6.65	High	No	Yes
222	517	4	2	79.79	3.68	5.12	-6.67	High	No	No
223	532	5	2	116.3	2.64	4.30	-6.65	High	No	Yes
224	566	3	2	70.56	3.14	5.60	-7.50	High	No	No
225	556	3	3	70.56	3.80	6.15	-7.78	High	No	No
226	536	3	2	70.56	3.99	5.99	-7.49	High	No	No
227	567	5	2	116.3	3.21	4.89	-7.25	Low	No	No
228	552	4	2	79.79	4.06	5.67	-7.26	High	No	No
229	566	3	2	70.56	4.09	5.80	-7.50	High	No	No
230	580	3	2	70.56	4.20	6.09	-7.80	High	No	No
231	600	3	2	70.56	3.83	6.22	-8.09	High	No	No

	MW	HBA	HBD	TPSA	iLOGP	ClogP	Log S	GIA	BBB	LP
232	522	3	2	70.56	3.81	5.68	-7.18	High	No	No
233	536	3	2	70.56	3.91	5.98	-7.49	High	No	No
234	556	3	2	70.56	3.42	6.07	-7.78	High	No	No
235	552	4	2	79.79	4.01	5.66	-7.26	High	No	No
236	532	5	2	116.3	2.96	4.36	-6.65	High	No	Yes
237	567	5	2	116.3	3.28	4.91	-7.25	Low	No	No
238	515	3	2	70.56	3.79	5.75	-7.19	High	No	No
239	501	3	2	70.56	3.65	5.45	-6.89	High	Yes	No
240	519	4	2	70.56	3.86	5.78	-7.05	High	No	No
241	536	3	2	70.56	3.91	5.98	-7.49	High	No	No
243	519	4	2	70.56	3.85	5.78	-7.05	High	No	No
245	515	3	2	70.56	3.87	5.77	-7.19	High	No	No
246	550	3	2	70.56	3.94	6.26	-7.79	High	No	No
247	533	4	2	70.56	3.77	6.04	-7.36	High	No	No
248	529	3	2	70.56	3.65	6.01	-7.50	High	No	No
249	560	5	2	116.3	3.37	5.01	-7.27	Low	No	No
250	469	2	1	44.7	4.02	5.36	-6.94	High	Yes	1
251	504	2	1	44.7	4.16	5.86	-7.53	High	Yes	2
252	514	4	1	90.52	3.57	4.59	-7.01	High	No	2
253	483	2	1	44.7	4.13	5.66	-7.24	High	Yes	1
254	487	3	1	44.7	4.02	5.64	-7.1	High	Yes	1
255	504	2	1	44.7	4.16	5.86	-7.53	High	Yes	2
256	487	3	1	44.7	4.18	5.68	-7.1	High	Yes	1
257	487	3	1	44.7	3.94	5.63	-7.1	High	Yes	1
258	497	2	1	44.7	4.49	6.01	-7.55	High	Yes	1
259	501	3	1	44.7	4.34	5.98	-7.41	High	Yes	2
260	483	2	1	44.7	4.13	5.66	-7.24	High	Yes	1
261	504	2	1	44.7	4.16	5.86	-7.53	High	Yes	2

MW: Molecular weight (g/mol); HBA: H-bond acceptors; HBD: H-bond donors; TPSA: Topological polar surface area; iLOGP; Lipophilicity (Log $P_{o/w}$); ClogP Lipophilicity (Consensus Log $P_{o/w}$); Log S: Water solubility (ESOL); GIA: Gastrointestinal absorption; BBB: Blood-brain-barrier permeation; CYP: Cytochrome P450 enzyme inhibition; LP: Lipinski violation

The results for compounds (**250-261**) are given in the **Table 4.13**. The molecular weight of the designed compounds was found to be in range of 469-514 g/mol. Hydrogen bond acceptors were in range of 4-2 whereas hydrogen bond donors for all the designed compounds were found to be one. The TPSA of all the compounds was found to be 44.7 except for compound (**252**) which has TPSA of 90.52. The lipophilicity of compounds in terms of iLOGP was found to be in range of 3.57-7.49 indicating good lipophilicity. But the compounds were predicted to have low aqueous solubility having Log S value in the range of -6.94 to -7.55. Additionally, all the compounds were predicted to exhibit high gastro intestinal absorption. Most of the compounds except (**252**) were predicted to cross blood brain barrier. All the compounds were predicted to interact with CYP2C9.

Table 4.14: Toxicity prediction of compounds (**211-261**)

Comp ID	Prediction by Dereck	Prediction by Sarah	Comp ID	Prediction by Dereck	Prediction by Sarah
211	Inactive	Negative	**237**	**Plausible**	**Positive**
212	Inactive	**Equivocal**	**238**	Inactive	Negative
213	Inactive	Negative	**239**	Inactive	Negative
214	Inactive	Negative	**240**	Inactive	Negative
215	Inactive	**Equivocal**	**241**	Inactive	Negative
216	**Plausible**	**Positive**	**242**	Inactive	Negative
217	Inactive	Negative	**243**	Inactive	Negative
218	Inactive	Negative	**244**	Inactive	Negative
219	Inactive	**Equivocal**	**245**	Inactive	Negative
220	Inactive	**Equivocal**	**246**	Inactive	Negative
221	**Plausible**	**Positive**	**247**	Inactive	Negative
222	Inactive	Negative	**248**	Inactive	Negative
223	**Plausible**	Negative	**249**	**Plausible**	**Positive**
224	Inactive	Negative	**250**	Inactive	Out of domain
225	Inactive	Negative	**251**	Inactive	Out of domain
226	Inactive	Negative	**252**	**Plausible**	Out of domain
227	**Plausible**	**Positive**	**253**	Inactive	Out of domain
228	Inactive	Negative	**254**	Inactive	Out of domain
229	Inactive	Negative	**255**	Inactive	Out of domain

230	Inactive	Negative	256	Inactive	Out of domain
231	Inactive	Negative	257	Inactive	Out of domain
232	Inactive	Negative	258	Inactive	Out of domain
233	Inactive	Negative	259	Inactive	Out of domain
234	Inactive	Negative	260	Inactive	Out of domain
235	Inactive	Negative	261	Inactive	Out of domain
236	**Plausible**	**Positive**			

Genotoxic profile of the compounds was predicted by Nexus software[11] which helps in determining if any particular motif of the compound structure is causing mutagenicity. The Derek results indicating "Inactive" implies that the compounds are predicted to be non-mutagenic. Plausible results indicate that there is a possibility of compounds being mutagenic and the weight of evidence supports the proposition.

Sarah results indicating "positive" implies the compound is predicted to be positive in a bacterial reverse mutation assay (Ames test). Whereas, negative results indicate that the compounds are predicted to be negative in a bacterial reverse mutation assay (Ames test). Equivocal results imply that a strong argument cannot be made based on the training set for either activity or inactivity in Ames test. Out of domain results indicate that the prediction is not possible because at least one atom present in a fragment of the compounds is not represented in the training set used to build the model.

It is noteworthy that compounds having chlorine atom (**227** and **237**) and nitro group in their structure (**227**, **236, 237** and **249**) are predicted to be mutagenic.

4.10 References:

(1)   Makarov, V.; Manina, G.; Mikusova, K. *et al.* Benzothiazinones Kill Mycobacterium Tuberculosis by Blocking Arabinan Synthesis. **2011**, *324* (5928), 801–804. https://doi.org/10.1126/science.1171583.Benzothiazinones.

(2)   Makarov, V.; Neres, J.; Hartkoorn, R. C. *et al.* The 8-Pyrrole-Benzothiazinones Are Noncovalent Inhibitors of DprE1 from Mycobacterium Tuberculosis. *Antimicrob. Agents Chemother.* **2015**, *59* (8), 4446–4452. https://doi.org/10.1128/AAC.00778-15.

(3)   Landge, S.; Mullick, A. B.; Nagalapur, K. *et al.* Discovery of Benzothiazoles as Antimycobacterial Agents: Synthesis, Structure-Activity Relationships and Binding Studies with Mycobacterium Tuberculosis Decaprenylphosphoryl-β-d-Ribose 2′-Oxidase. *Bioorganic Med. Chem.* **2015**, *23* (24), 7694–7710. https://doi.org/10.1016/j.bmc.2015.11.017.

(4)   Shirude, P. S.; Shandil, R. K.; Manjunatha, M. R. *et al.* Lead Optimization of 1,4-Azaindoles as Antimycobacterial Agents. **2014**. https://doi.org/10.1021/jm500571f.

(5)   Shirude, P. S.; Shandil, R.; Sadler, C. *et al.* Azaindoles: Noncovalent DprE1 Inhibitors from Scaffold Morphing Efforts, Kill Mycobacterium Tuberculosis and Are Efficacious in Vivo. **2013**. https://doi.org/10.1021/jm401382v.

(6)   Naik, M.; Humnabadkar, V.; Tantry, S. J. *et al.* 4-Aminoquinolone Piperidine Amides: Noncovalent Inhibitors of DprE1 with Long Residence Time and Potent Antimycobacterial Activity. *J. Med. Chem.* **2014,** 57 (12), 5419-34. https://doi.org/10.1021/jm5005978.

(7)   Neres, J. O.; Hartkoorn, R. C.; Chiarelli, L. R. *et al.* 2-Carboxyquinoxalines Kill Mycobacterium Tuberculosis through Noncovalent Inhibition of DprE1. *ACS Chem. Biol.* **2015**, 10(3), 705-14. https://doi.org/10.1021/cb5007163.

(8)   Stanley, S. A.; Schmidt Grant, S.; Kawate, T. *et al.* Identification of Novel Inhibitors of M. Tuberculosis Growth Using Whole Cell Based High-Throughput Screening. *ACS Chem. Biol* **2012**, *7*, 2022. https://doi.org/10.1021/cb300151m.

(9)   Karabanovich, G.; Dušek, J.; Savková, K. *et al.* Development of 3,5-Dinitrophenyl-Containing 1,2,4-Triazoles and Their Trifluoromethyl Analogues as Highly Efficient Antitubercular Agents Inhibiting Decaprenylphosphoryl-β- d -Ribofuranose 2′-

Oxidase. *J. Med. Chem.* **2019**, *62* (17), 8115–8139.
https://doi.org/10.1021/acs.jmedchem.9b00912.

(10)   Hayes, R. N. Spectrometry of 2-Chloro-s-Triazines. *Biomed. Environ. Mass Spectro.*
1990, *19*, 273–279.

(11)   Greene, N.; Judson, P. N.; Langowski, J. J.; Marchant, C. A. Knowledge-Based Expert
Systems for Toxicity and Metabolism Prediction: DEREK, StAR and METEOR. *SAR
QSAR Environ. Res.* **1999**, *10* (2–3), 299–314.
https://doi.org/10.1080/10629369908039182.